Evaluation of Climate Change Impact on Upper Blue Nile Basin Reservoirs

(Case Study on Gilgel Abay Reservoir, Ethiopia)

Habtom Mulugeta Bekele

August, 2009

Evaluation of Climate Change Impact on Upper Blue Nile Basin Reservoir

(Case Study on Gilgel Abay Reservoir, Ethiopia)

By

Habtom Mulugeta Bekele

A Thesis Submitted in Partial Fulfillment of the Requirements for the Degree of Masters of Science in Hydraulics and Hydropower Engineering of Arba-Minch University.

Arba Minch University
School of Post Graduate Studies

August, 2009

Certification

The undersigned certify that he has read the Thesis entitled**: Evaluation of Climate Change Impact on Upper Blue Nile Basin Reservoir** and hereby recommend for acceptance by the Arba-Minch University in partial fulfillment of the requirements for the degree of Master of Science (Engineering).

_____	_____
Dr. Ing Seleshi Bekele	Dr. Kassa Tadele
(Supervisor)	(Co-Supervisor)
_____	_____
Date	Date

Dedicated to the Almighty of God,
The Alpha and Omega,
The beginning and the end,
The first and the last

Abstract

Nowadays the sign of climate change and its impact is revealing on different natural and man made systems, in one or other ways. Accordingly, this impact is significant on the water resource system. This study mainly deals with evaluation of the climate change impact on the Gilgel Abay reservoir which is found in Upper Blue Nile Basin, using the reliability, resilience and vulnerability indices (RRV-criteria). Projection of the future climate variables is done by using General Circulation Model (GCM) which is considered as the most advanced tool for estimating the future climatic condition. Statistical Down Scaling Method (SDSM) is applied in order to downscale the climate variables at catchment level. A hydrological model, HBV was utilized to simulate the water balance. The performance of the model was assessed through calibration and validation process and resulted R^2=0.82 during calibration and R^2=0.8 during validation. The projected future climate variable shows an increasing trend for both maximum and minimum temperature however, for the case precipitation it doesn't manifest a systematic increase or decreasing trend in the next century. The evaporation from the open water surface of reservoir reveals an average annual increase by 2.1 % when the projected average annual temperature and precipitation increases from the baseline period by an amount of 0.53^{o}C and 0.82 % respectively in 2020s under the A2a emission scenario, when the average annual temperature is rise by 1.15 ^{o}C and the precipitation increase by 0.85 % in 2050s with A2a emission scenario, the reservoir open water evaporation will expected to increase by 6 %, while in the time horizon of 2080s, the precipitation shows an increase amount by 1.6 % and the temperature raise 1.97 ^{o}C consequently the open water evaporation is expected to rise by 22 % for the same A2a emission scenario.

On average for both A2a and B2a emission scenarios the time based reliability (the probability of the reservoir to meet the target demand) of Gilgel Abay reservoir shows a value of above 80 %, i.e. 80% of the time the target demand is fully supplied and the resilience (the speed of recovery of the reservoir, form failure) shows value above 60%, a value of 100% resilience shows the reservoir needs very short time to recover itself from failing to meet the demand and the dimensionless vulnerability (the average volumetric severity of failure during failure period divides by the target demand) of the Gilgel Abay reservoir falls in range (25%-30%).The sensitivity analysis of the reservoir with a hypothetical climate change scenario indicates that the reliability and resilience of the reservoir is sensitive to precipitation change than change in

temperature on contrary dimensionless vulnerability of the reservoir doesn't show remarkable difference for both the change in precipitation and temperature

Key words: Climate Change, GCM, SDSM, Reservoir, Reliability, Resilience, Vulnerability, Blue Nile, Gilgel Abay.

Acknowledgements

Above all I thank the almighty of GOD for his mercy and grace upon me during all my works and in all my life.

I would like to express my sincere gratitude to my employer Arba-Minch University (AMU) for providing me to learn my MSc. Program. I am also grateful to International Water Management Institute (IWMI) for their financial support and their hospitality in all my works.

Very special thanks to my supervisor, Dr. Ing. Seleshi Bekele, for giving me valuable guidance and for his friendly approach through out my research. I am also indebted to my co-supervisor Dr. Kassa Tadele, for his support, encouragement and priceless comments in my thesis. With out them, this work wouldn't have been realized.

I would also like to express my appreciation to Arba-Mnich University School of Graduate Studies staff members and libraries for their provision of the necessary reference books and assistance for my study.

I would like to thank also National Metrological Agency, Ministry of Water Resource and Water Works Design and Supervision Enterprise office, especially Ato Getachew Yared for providing me the necessary data.

Last but the bests, I would like to thank my wonderful family, for their ultimate support through out my life.

Habtom Mulugeta

habtomhydro@gmail.com

Table of content

List of Figures

List of tables

1. Introduction

1.1 Background

The impact of climate change on water resources are the most crucial research agenda in world wide level (IPCC, 2007). This change in climate causes a significant impact on the water resource by disturbing the normal hydrological processes. Future change in overall flow magnitude, variability and timing of the main flow event are among the most frequently cited hydrological issues (Fredrick, 2002: Wurbs et al., 2005).

The IPCC finding indicates that developing countries, such as Ethiopia will be more vulnerable to climate change. Because of the less flexibility to adjust the economical structure and being largely dependent on agriculture, the impact of climate change has far reach implication in Ethiopia.

Blue Nile Basin is one of the largest basins in the country with high population pressure, degradation of land and highly dependent on agricultural economy (Tsegay, 2006). The increase in population growth, economical development and climate change have been proven by IPCC, 2007 to cause rise in water demand, necessity of improving flood protection system and drought (water scarcity).

The Blue Nile Basin is generally divided in to 14 Sub-basins according to their configuration in topology, among them Tana Sub-basin is the major basin which include the main source of water for the whole Blue Nile i.e. Lake Tana and with some proposed and existing infrastructures.

The Gilgel Abay [1] reservoir is one of the proposed projects in Upper Blue Nile Basin which is included in Tana Sub-basin. The implementation of this reservoir will expected to minimize the food scarcity from the surrounding area by irrigating 13,500 ha area. Generally, the introduction

[1] In this study unless it is stated the name "Gilgel Abay" and "Upper Gilgel Abay" are used interchangeably to represent the area upstream of the Gilgel Abay gauging stations.

of irrigation will make farmers feel more secure about their basic food supply and enable them to diversify their crops based on local market demand and export opportunities.

Even though there is huge uncertainty related to climate change in Ethiopia, there are few or no studies conducted on the existing and upcoming reservoirs related to this climate variability. Although the Gilgel Abay reservoir is on going to be implemented, its performance under future climatic condition is not investigated yet. Therefore, understanding the performance of the Gilgel Abay reservoir using different climate and hydrological model is more urgent than ever. For that reason, this study mainly deals with evaluating of the impact of climate change on the Gilgel Abay reservoir performance. The performance evaluation is carried out by using reliability, resilience and vulnerability indices which considered as the preeminent method to ensure consistent assessment of reservoir system performance (Thomas et. al, 2004). This thesis is done as a part of the big project which is currently carried by the collaboration of International Water Management Institute and Arba-Minch University (IWMI-AMU) under a broad project title of "Re-thinking Water Storage for Climate Change Adaptation in Sub-Saharan Africa".

1.2 Research Objectives

The general objective of this study is to evaluate the impact of climate change on the Gilgel Abay reservoir. The specific objectives are

- To downscale the climate variables for upstream Gilgel Abay catchment.
- To evaluate the rate of change in open water evaporation from Gilgel Abay reservoir with the future climate change.
- To examine the reservoir capability to meet the target demand in the future climate condition under its regulation policy.
- To examine how fast the reservoir can recover itself from the unsatisfactory condition (i.e. from failure to meet the target demand) under future climatic change.
- To examine the over all sensitivity of the reservoir by using a hypothetical climate scenario.

In order to meet the above objectives, the key question addressed in the study is that, what are the general trends of the future climate compared to the present condition and how can this affect the Gilgel Abay reservoir and reservoir management parameters or/and sustainability indices ?

The major significant of this study is, it allows the planners, decision makers and any concerned persons to understand the consequences of climate change on hydrological variables and the impacts these have on reservoirs water resource planning management and accordingly device decision and management support tools.

1.3 Conceptual frame works for the Study

The over all procedure adopted for this can be described by the following flow chart.

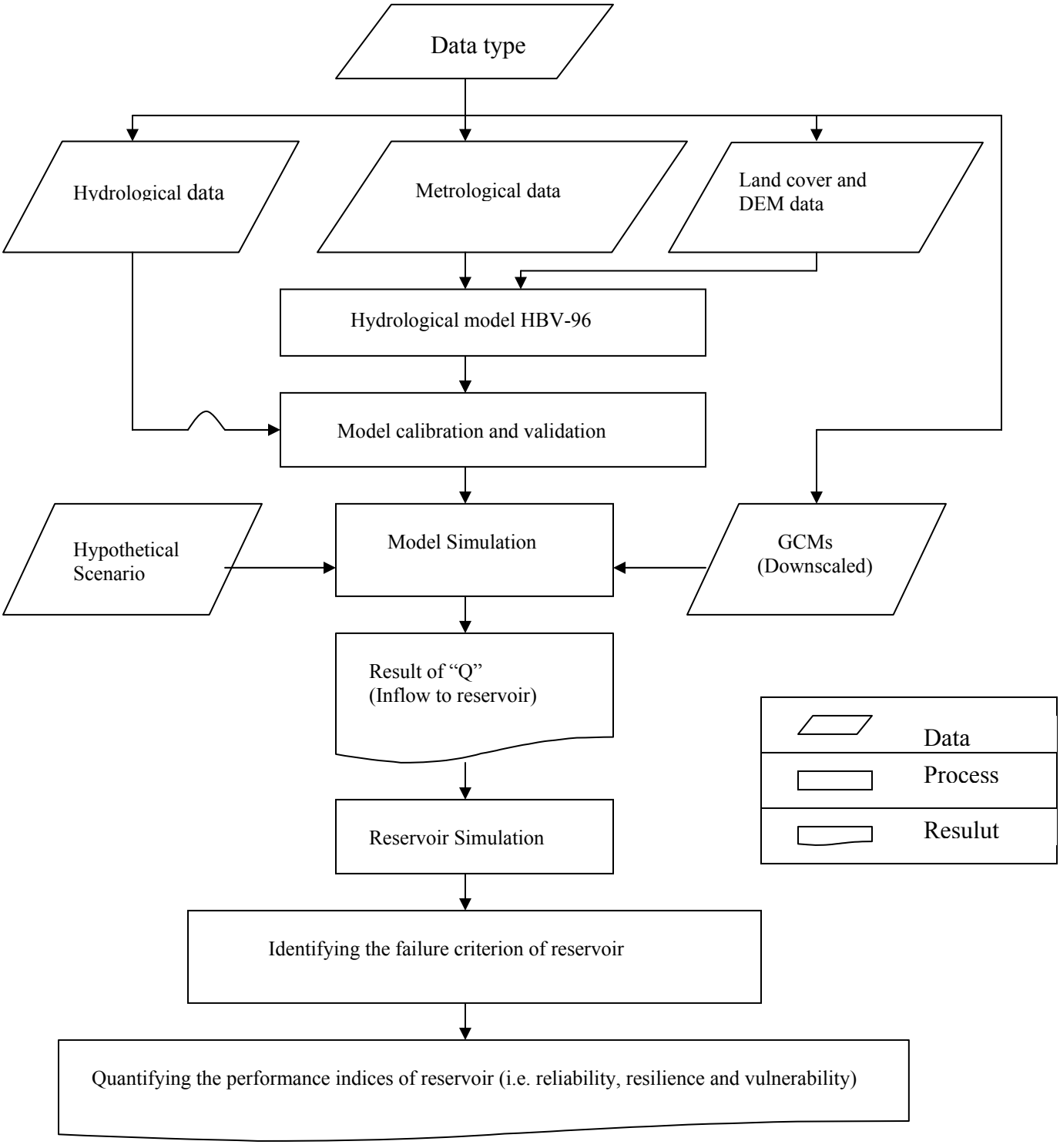

Figure1.1 Conceptual frame works for the study

1.4 Limitation of the study

In this study the impact of climate change was assessed by using one GCM model and by assuming the land cover will remain the same. The study also doesn't consider the sediment inflow to the reservoir at future time horizons. However, in real world the land cover change and sediment inflow will occur due to natural and human influences.

1.5 Thesis outline

This thesis contains eight chapters organized as follows. Chapter one gives a general introduction to the study with its objective, relevance and research questions. Chapter two gives a brief description of the study area. Chapter three describes the reviewed literature related to the study. Chapter four deals with the material and methodology adopted for the study. Chapter five concerned with the data screening part. Chapter six describes how the models are setup and data are analyzed Chapter seven discussed the result of the study and lastly chapter eight ends with the conclusions and recommendations by the study

2. Study Area

2.1 Catchment description

Gilgel Abay catchment is the largest of the four main sub-basins of Lake Tana Basin. It drains the southern part of Lake Tana basin to perennially feed Gilgel Abay River which empties itself in Lake Tana. Being the main tributary of Lake Tana, Gilgel Abay River originates from springs, considered as sacred water by the local people, located at an elevation 2750 m a.m.s.l near Mt. Gish. The catchment area upstream of Lake Tana is around 5000 km2. The catchment has two gauged sub catchments, Upper Gilgel Abay and Koga that have size of 1655 km^2 and 307 km^2, respectively (as extracted from SRTM).

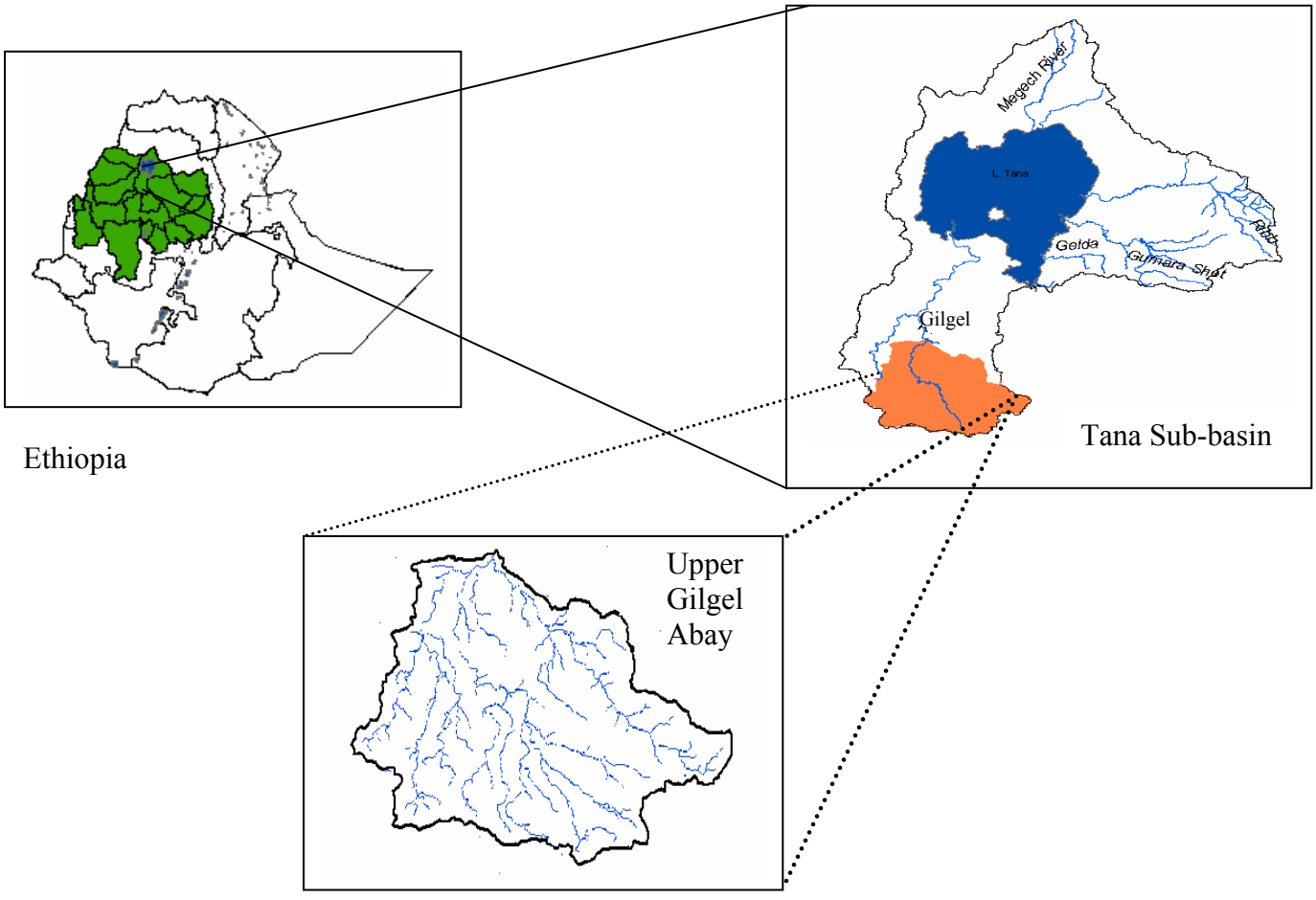

Figure 2. 1 Location of Upper Gilgel Abay Catchment

2.1.1 Location

Geographic location of Gilgel Abay catchment extends from 10 °56' to 11° 51' N latitude and 36° 44' to 37° 23' E longitude.

2.1.2 Topography and slope

Gilgel Abay catchment is located south of Lake Tana. Rugged mountainous topography characterizes the southern part of the catchment and along its periphery in the west and southeast. The remaining portion of the catchment is typically low laying plateau. The elevation ranges from 1932 m to 2917 m a.m.s.l. The excessive slope area of the watershed lies in the south and decrease northwards.

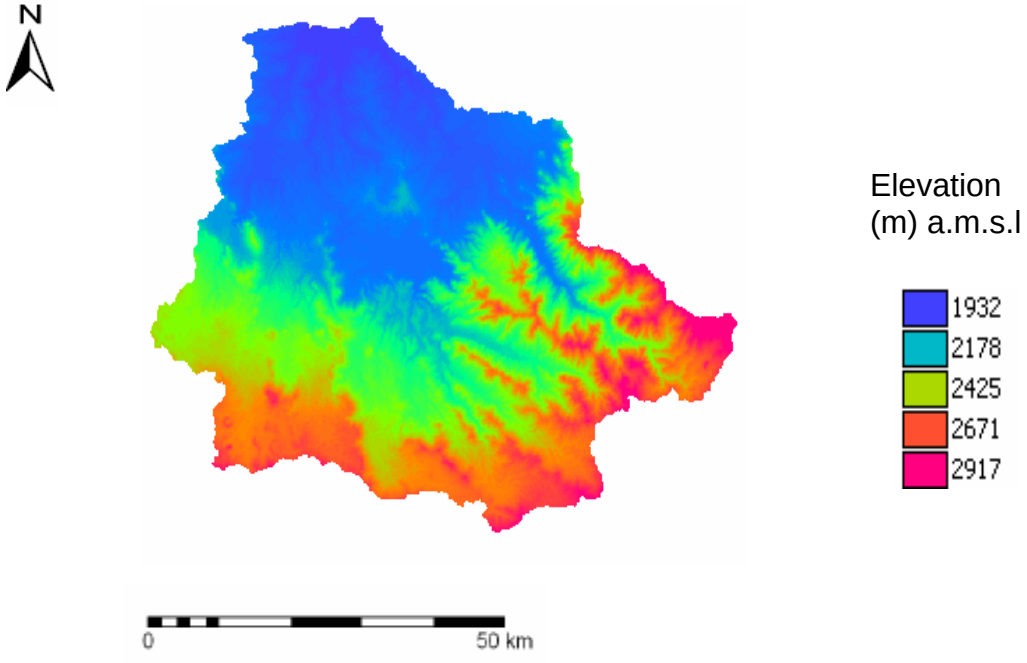

Figure 2. 2 DEM of Upper Gilgel Abay.

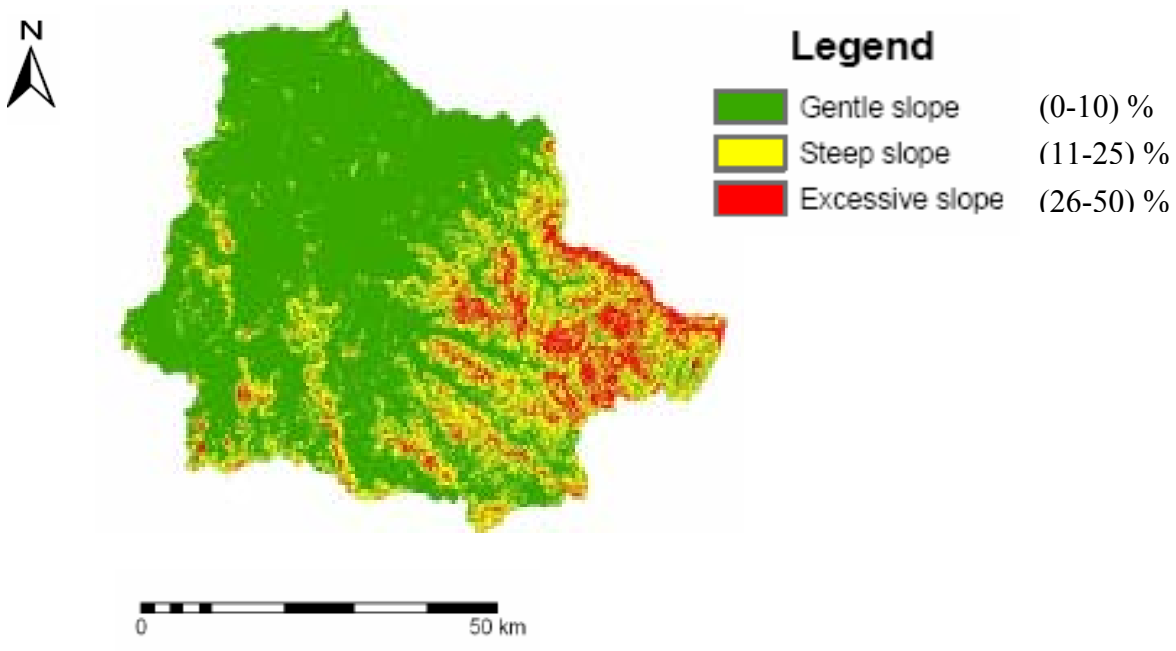

Figure 2. 3 Slope classification for upper Gilgel Abay catchment

2.1.3 Climate

The climate of Ethiopia is mainly controlled by the seasonal migration of the Inter-tropical Convergence Zone (ITCZ) and associated atmospheric circulation as well as by the complex topography of the country. It has a diversified climate ranging from semi arid desert type in the low lands to humid and temperate type in the southwest.

Rainfall in the Upper Gilgel Abay catchment originates from moist air coming from Atlantic and Indian oceans following the north-south movement of the ITCZ. Different studies conducted on Lake Tana Basin and Blue Nile Basin (Conway, 2000; Kebede et al., 2006; Sutcliffe & Parks, 1999; Tarekegn and Tadege, 2005) indicated that hydrological year of the study area is characterized by one main rainy season between June to September, in which 70% to 90 % of the annual total rainfall occurs. Observation of rainfall data of surrounding meteorological stations indicates variation of rainfall amount in the area with a decreasing trend from south to north; for example, long term mean annual rainfall at Sekela (station at the south most of the catchment) and Abay Sheleko (Northern to upper Gilgle Abbay catchment) stations are 1870 mm and 1020 mm, respectively.

According to Conway (1999) the climate of the high elevation areas can be considered as a temperate and that of the low elevation areas as tropical. The local climate classification in Ethiopia is based on elevation and temperature. In other words, depending on elevation for any area there is associated mean annual temperature range. This enables identifying traditional climate zone of a given area. The three traditional climate zones of Ethiopia are: Kola (elevation less than 1800 m a.m.s.l and mean annual temperature 20 – 28 ^{o}C), Woina Dega (elevation between 1800 m and 2400 m a.m.s.l and mean annual temperature 16 – 20 ^{o}C), and Dega (elevation between greater than 2400 m a.m.s.l and mean annual temperature 6 – 16 ^{o}C).

2.2 Gilgel Abay Dam/Reservoir

2.2.1 Location, Geography and Access

The Gilgel Abbay River has a mean annual discharge of 67.22 m³/s and mean annual yield of 2,120 MCM. The catchment area at the dam site is 2044 km^2. The dam is located on the Gilgel Abbay River, on the southern side of Lake Tana Sub Basin; West Gojam Zone of Amhara National Regional State .The Upstream Watershed covers West Gojam and Awi Administrative Zones of the Amhara National Regional which include the two proposed upstream reservoirs (Koga and Jemma) (figure 2.4) [source:-Feasibility study of Lake Tana Sub-Basin Dam Project, 2009].

The dam axis is located in between the geographic grid ref.UTM E 282262, N 1267718 and E 283466, N 1267460. Both the left and right abutments rise to an elevation higher than 1899 m. The location of the river bed at the center of the dam axis (in UTM) is E = 282810 m and N= 1267613 m with a riverbed elevation of 1832 m. The dam has Full supply level (NWL –spillway crest) of 1891.8 m m.a.s.l, with reservoir volume of 360 Mm^3.

Access to the dam axis is possible from Bahi-dar town using the prevailing asphalt high way for the first 45 km and turning left or South East at Wottet Abbay town using the dry weather road. From Wottet Abbay up to Durbete 12km and from Durbete to dam site 17km

The purpose of this dam/reservoir is to develop 13,500Ha of irrigated agriculture, thereby generating a demand for agricultural support services, as well as infrastructure development and this will enable farmers to fully benefit from more reliable access to sources of water [source:- Feasibility study of Lake Tana Sub-Basin Dam Project, 2009].

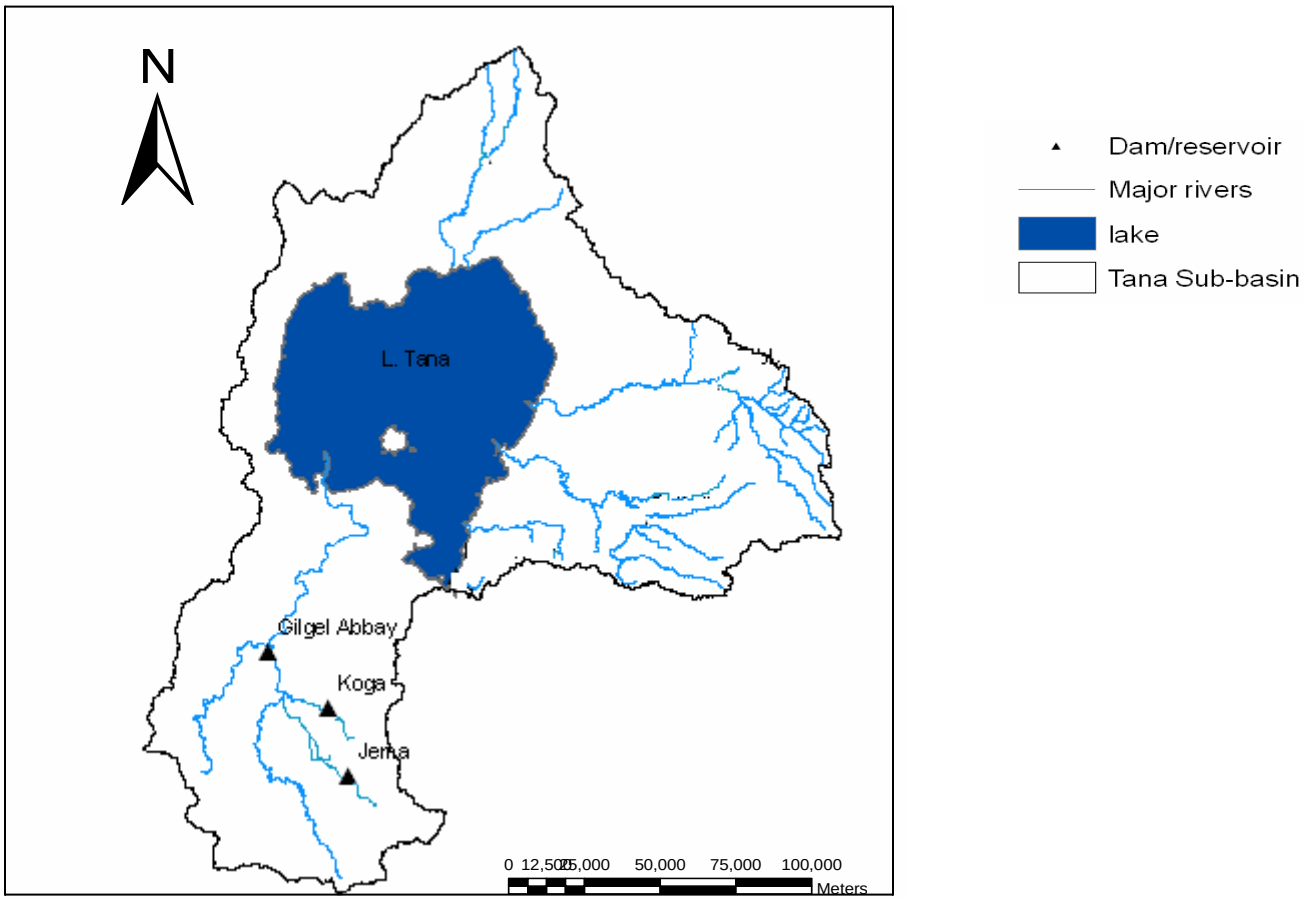

Figure 2. 4 Gilgel Abay and Upstream reservoirs in the Tan-basin.

3. Literature review

Climate change can simply defined as the change in the climatic elements or variables through time (USAID, 2007).

3.1 Over view of climate change

Climate change is the sever problem that the whole world facing today. It is now widely accepted that climate change is already happening and further change is inevitable; over the last century (between 1906 and 2005), the average global temperature rose by about 0.74 ^{o}C. This has occurred in two phases, from 1910s to 1940s and more strongly from the 1970s to the present (IPCC, 2007a).

Many studies into the detection and attribution of climate change have found that most of the increase in average global surface temperature over the last 50 years is attributable to human activities (IPCC, 2001a).

It is estimated that, for the 20th Century, the total global mean sea level has risen 12-22 cm, this rise has been caused by the melting of snow cover and mountain glaciers (both of which have decline on average in both hemispheres)(IPCC, 2007a). The IPCC also notes that observations over the past century shows, changes are occurring in the amount, intensity, frequency and types of precipitation globally (IPCC, 2007a).

At this point it is worth mentioning the role and remit of the Intergovernmental Panel on Climate Change (IPCC). The IPCC was established in 1988 by the World Meteorological Organization and the United Nations Environment Programme, and its role is to "assess on a comprehensive, objective, open and transparent basis the scientific, technical and socio-economic information relevant to understanding the scientific basis of risk of human-induced climate change, its potential impacts and options for adaptation and mitigation". Among the different assessment that are carried out by the IPCC, the most recent which published in 2007, states the projected global surface warming lies within the range 0.6 to 4.0^{o}C, whilst the projected see level rise lies with in the range 0.18 to 0.59 m at the end of next century (IPCC, 2007a).

3.2 Modeling Climate Change

In order to estimate the impacts of anthropogenic emissions on climate, a mathematical model called a Global Circulation Model (GCM) has to be constructed of the complete climate system, which must include the atmosphere, oceans, land and cryosphere (glaciers and ice sheets). This model is a mathematical description of the earth's climate system, firstly broken down into layers (both above and below sea level) and then each grid is broken down into boxes or 'cells'.

A number of research centers around the world have developed their own versions of GCMs, but all predictions contain uncertainties. For example, because future emissions of greenhouse gases are unknown, numerous emissions scenarios have been developed; therefore, different scenarios will obviously produce different results. However, the largest uncertainty arises from the models themselves. Even if each of the different GCMs uses the same emissions scenario, they will give quite different predictions due to the different ways they represent aspects of the climate system (Robert K and Colin H, 2007).

3.3 Climate scenario and their purpose

Future greenhouse gas (GHG) emissions are the product of very complex dynamic systems, determined by driving forces such as demographic development, socio-economic development, and technological change. Their future evolution is highly uncertain. Scenarios are alternative images of how the future might unfold and are an appropriate tool with which to analyze how driving forces may influence future emission outcomes and to assess the associated uncertainties. They assist in climate change analysis, including climate modeling and the assessment of impacts, adaptation, and mitigation. The possibility that any single emissions path will occur as described in scenarios is highly uncertain (IPCC, 2007 working group III)

3.4 The SRES emissions scenarios

There are four narrative storylines defined by special report on emission scenario (SRES) team to describe the relationship between the driving force of green house gas and aerosols emission and

their evolution in the next century, labeled as A1, B1, A2 and B2. The storylines can be summarized as follows;

- A1 scenario family: - reflects the world as very rapid economic growth, global population peaks in the mid-century and decline thereafter, and rapid introduction of new and more efficient technologies.

- B1 scenario family: - reflects the world as a convergent world with the same global population as in the A1 storyline but with rapid changes in economic structures toward a service and information economy, with reductions in materials intensity, and the introduction of clean an resource efficient technologies.

- A2 scenario family: - reflects the world as continuously increasing global population and regionally oriented economic growth that is more fragmented and slower than in other storylines.

- B2 scenario family: - reflects the world in such a way that the world emphasis goes to local solutions to economic, social, and environmental sustainability, with continuously increasing population (lower than A2) and intermediate economic development.

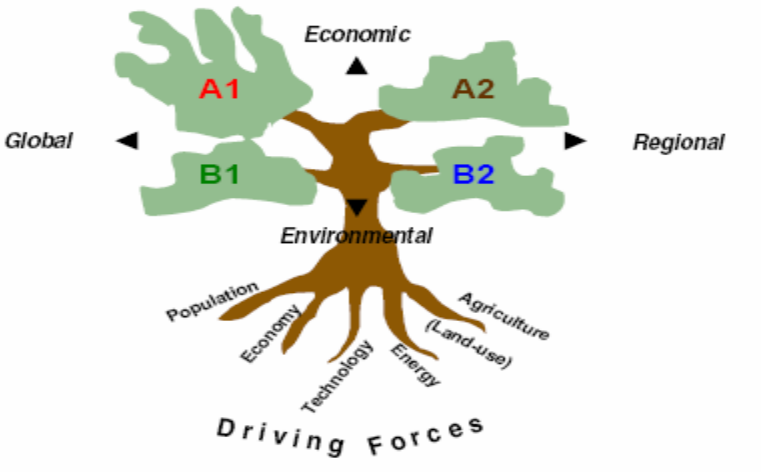

Figure 3. 1 the four IPCC SRES scenario storylines (IPCC-TGICA, 2007)

3.5 Impacts of Climate Change on Water Resource and Reservoir

Findings of the IPCC 2001, strongly suggests that water resource respond to global warning in ways that will negatively impacted the water availability and water supplies. The climate change has also the potential to deteriorate the surface water quality due to increased evapo-transpiration, lower flows and rivers becoming warmer, making the management of water treatment works (and subsequent compliance with the drinking water quality regulations) more challenging. The reduction in the runoff volume will lead to the decrease in the inflow to the reservoirs consequently; longer period might be required to fill the reservoir. As result of the increase in temperature the rate of evaporation from the reservoir open water surface may increase and this may create the reservoir to fail to supply at least the required amount of demand because of its depletion or decrease in the active storage volume and/or water level.

3.6 Modeling Hydrological Responses to Climate Change

When GCMs comes to quantifying the potential impacts of climate change on water resources, more problems arise. GCMs generally operate at coarse resolutions across the continents, but much smaller scales (in both time and space) are required for catchment hydrological modeling (Bergkamp et al. 2003).

Generally coarse spatial resolution of GCMs also presents a significant problem when rainfall is being considered. GCMs usually generate an estimate of the average rainfall over a large grid square for the GCM time step, but they fail to take into account localized temporal and spatial variations in rainfall which, on a smaller scale, can produce highly significant results (Calder, 2005). The situation is further complicated because of the exceptional diversity demonstrated across the Upper Blue Nile Basin in terms of its topography, geology, land use and pattern of water use, all of which directly influence regional and more local hydrological responses to climate variability. Even though, GCMs has the above main limitations, currently it has been recognized to be able to represent reasonably well the main futures of global distribution of the basic climate parameters (Gates et al., 1999; Lambert and Boer, 2001). In order to decrease the

uncertainty related to coarse resolution of GCMs, usually, most climate impact assessment researches use different downscaling methods such as dynamic downscaling method and/or statistical downscaling method.

Downscaling is the term given to the process of deriving finer resolution data (e.g., for a particular site) from coarser resolution GCM data. It may be possible to define a relationship, or relationships, between site climate and large-scale (i.e., GCM grid box scale) climate which can then be used to derive more realistic values of the future climate at the site scale.

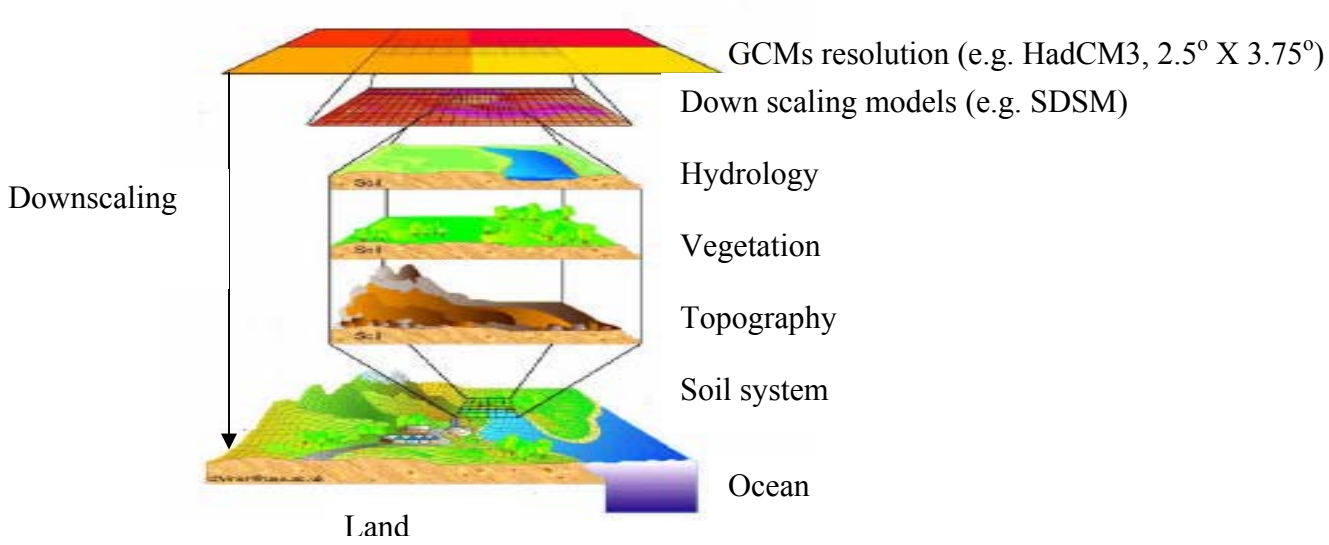

Figure 3. 2 Schematic illustrating of the general approach for downscaling

3.7 Climate change in Ethiopia

According to the Ethiopian National Meteorological Services Agency (NMSA, 2001) study for 42 meteorological stations, the country has experienced both dry and wet years over the last 50 years. Trend analysis of the annual rainfall show that there was a declining trend in the northern half of the country and southern Ethiopia while there is an increasing trend in the central part of the country. However, the overall trend in the entire country is more or less constant. Figure 3.3 shows the year to year variation of rainfall over the country expressed in terms of normalized rainfall anomaly averaged over 42 stations.

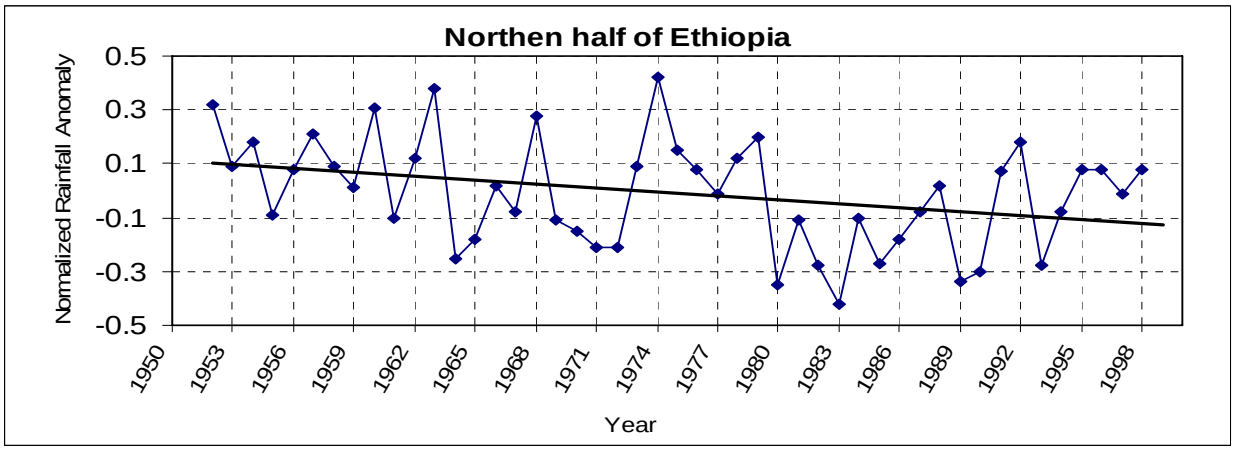

(a)

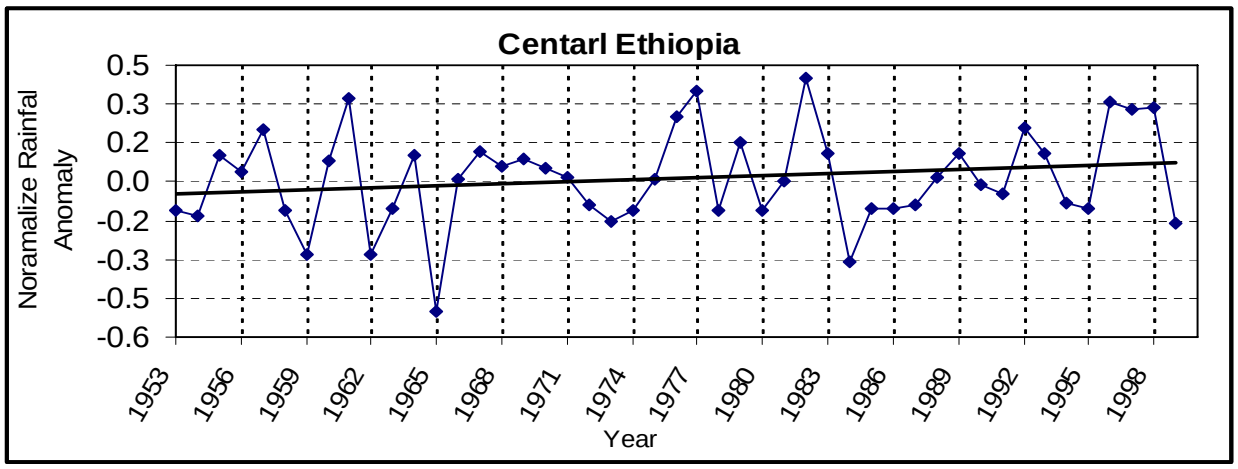

(b)

Figure 3. 3 (a) Annual variability of rainfall over Northern half; and, (b) Central Ethiopia expressed in normalized deviation (NMSA , 2001).

The study of NMSA at the same year for 40 stations showed that there have been very warm and very cold years. However, the general trend showed there was an increase in temperature over the last 50 years. The study also noted that the minimum temperature is increasing at a higher rate than the maximum temperature. Figure 3.4 shows the year to year variation of annual maximum and minimum temperatures expressed in terms of normalized temperature anomalies averaged over 40 stations.

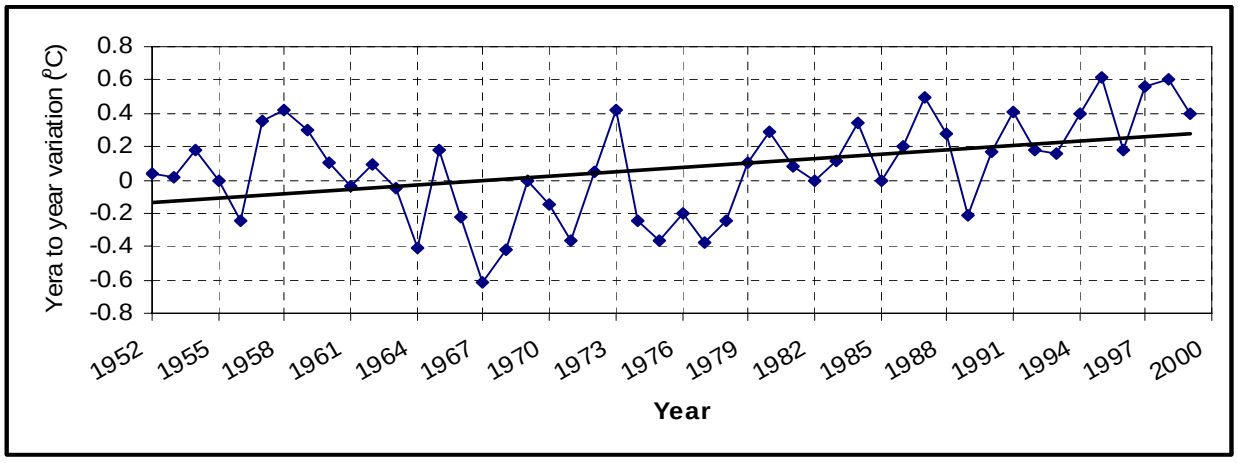

(a)

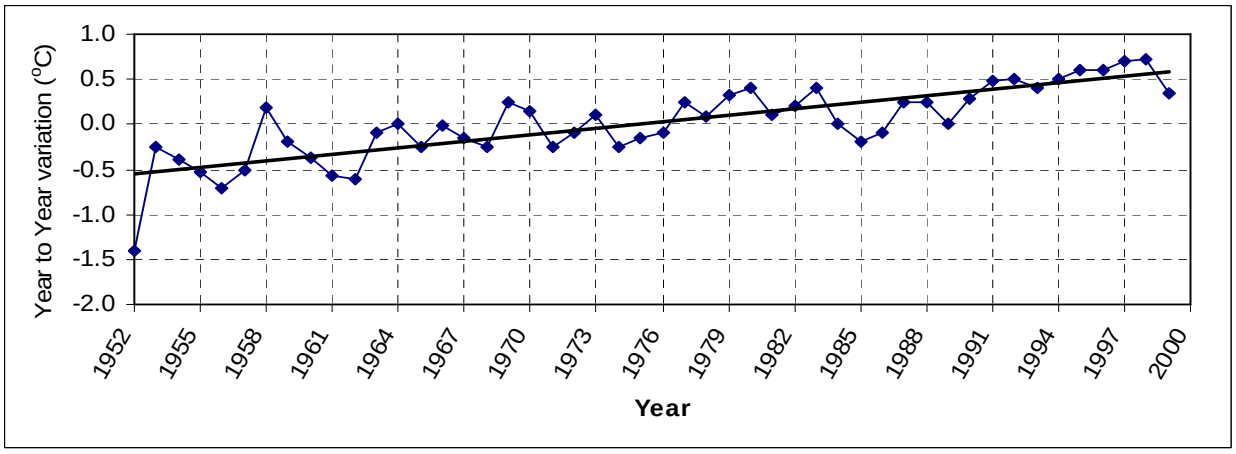

(b)

Figure 3. 4 (a) Annual mean maximum and (b) minimum temperatures variability and trend over Ethiopia (NMSA, 2001)

Associated with rainfall and temperature change and variability, there was a recurrent draught and flood events in the country. There was also observation of water level rise and dry up of lakes in some parts of the country depending on the general trend of the temperature and rainfall pattern of the regions.

3.8 Performance criteria

Some assessment of climate change impact on the water resource and related infrastructures (reservoirs) were evaluated by using different performance criteria in the previous studies or researches which are conducted in various place of the world.

Performance criteria provide a measure of just how well a plan or management policy performs. The performances criteria of the water resource system can be derived, once the hydrological inputs are simulated and produces what one believes could occur in the future (Loucks, 1997). These time series value themselves can be measured by the major and most commonly used statistical performance criteria; these are reliability, resilience and vulnerability. The relative sustainability of the system with respect to each of these criteria is higher when there is greater reliability and resilience, and smaller vulnerability.

Generally, reliability measures the probability that the system will remain in non failure state and resilience describes the ability of a system to return to non-failure state after a failure occurred while vulnerability measures the likely damages of failure events.

3.9 Hydrologic Modeling

Hydrologic models are simplified, conceptual representations of a part of the hydrologic cycle. They are primarily used for hydrologic prediction and for understanding hydrologic processes. Without going into too much detail, deterministic hydrologic models can be classified into three main categories (Juraj M, 2003)

1. **Lumped models**. Parameters of lumped hydrologic models do not vary spatially within the basin and thus, basin response is evaluated only at the outlet, without explicitly accounting for the response of individual sub-basins. Parameters of lumped models often do not represent physical features of hydrologic processes and usually involve certain degree of empiricism. The impact of spatial variability of model parameters is evaluated by using certain procedures for calculating effective values for the entire basin. The most commonly employed procedure is an area-weighted average (Haan et al., 1982). Lumped models are not usually applicable to event-scale processes. If the interest is primarily in the discharge prediction only, then these models can provide just as good simulations as complex physically based models (Beven, 2000).

2. **Semi-distributed models**. Parameters of semi-distributed (simplified distributed) models are partially allowed to vary in space by dividing the basin into a number of smaller sub-basins.

There are two main types of semi-distributed models: 1) kinematic wave theory models (KW models, such as HEC-HMS), and 2) probability distributed models (PD models, such as TOPMODEL). The KW models are simplified versions of the surface and/or subsurface flow equations of physically based hydrologic models (Beven, 2000). In the PD models spatial resolution is accounted for by using probability distributions of input parameters across the basin.

3. **Distributed models**. Parameters of distributed models are fully allowed to vary in space at a resolution usually chosen by the user. Distributed modeling approach attempts to incorporate data concerning the spatial distribution of parameter variations together with computational algorithms to evaluate the influence of this distribution on simulated precipitation-runoff behavior. Distributed models generally require large amounts of (often unavailable) data for parameterization in each grid cell. However, the governing physical processes are modeled in detail, and if properly applied, they can provide the highest degree of accuracy.

3.9.1 Introduction to HBV rainfall-runoff model

The Hydrologiska Byrans Vattenbalansavdelning (HBV) model was developed at Swedish Metrological and Hydrological Institute (SMHI) during the early 1970's. The HBV is a semi – distributed conceptual rainfall-runoff model for continuous simulation of catchment runoff and out flow from reservoirs, the model consistence of subroutines for precipitation and snow accumulation, soil moisture accounting, actual evaporation and uses simple transformation functions routine procedures. Soil moisture accounting is governed by two simple relations that are parameterized by *FC*, which is the maximum soil moisture storage (mm) in the model, and LP that is the limit for potential evapo-transpiration and Beta control the contribution of the soil moisture storage, SM, to the response function ΔQ/ΔP.

$$\Delta Q / \Delta P = \left[SM / FC \right]^{Beta} \quad \text{.....3.1}$$

Q denotes the discharge and P denotes the precipitation while $\Delta Q / \Delta P$ is to be interpreted as runoff coefficient. Actual evapo-transpiration, Ea, which is controlled by the soil moisture routine, is linearly related to the potential evapo-transpiration, Ep, and reads;

$$Ea = Ep * \min\left\{\left(SM / (lp * Fc)\right), 1\right\} \text{.....} 3.2$$

In HBV-IHMS the runoff routine comprises two reservoirs that distribute generated runoff over time to obtain quick and slow part of catchments runoff hydrograph. Runoff generated from the upper reservoir represents quick runoff discharges while runoff from the lower reservoir represents ground water discharges.

$$Q_0 = K * UZ^{(1+alfa)} \text{.....} 3.3$$

Where Q_0 is the direct runoff from upper reservoir the parameters UZ and KHQ are the upper reservoir storage and the quick flow recession coefficient while Alfa is a measure for the non-linearity of the flow. The lower reservoir is a simple linear reservoir that simulates base flow contributions by percolation from upper reservoir.

$$Q_1 = K_4 * LZ \text{.....} 3.4$$

Q_1 denotes the outflow from lower reservoir; LZ is the lower reservoir storage while K_4 is the recession coefficient. Obviously, the combination of the parameters control runoff contribution over time that affects the shape of hydrograph.

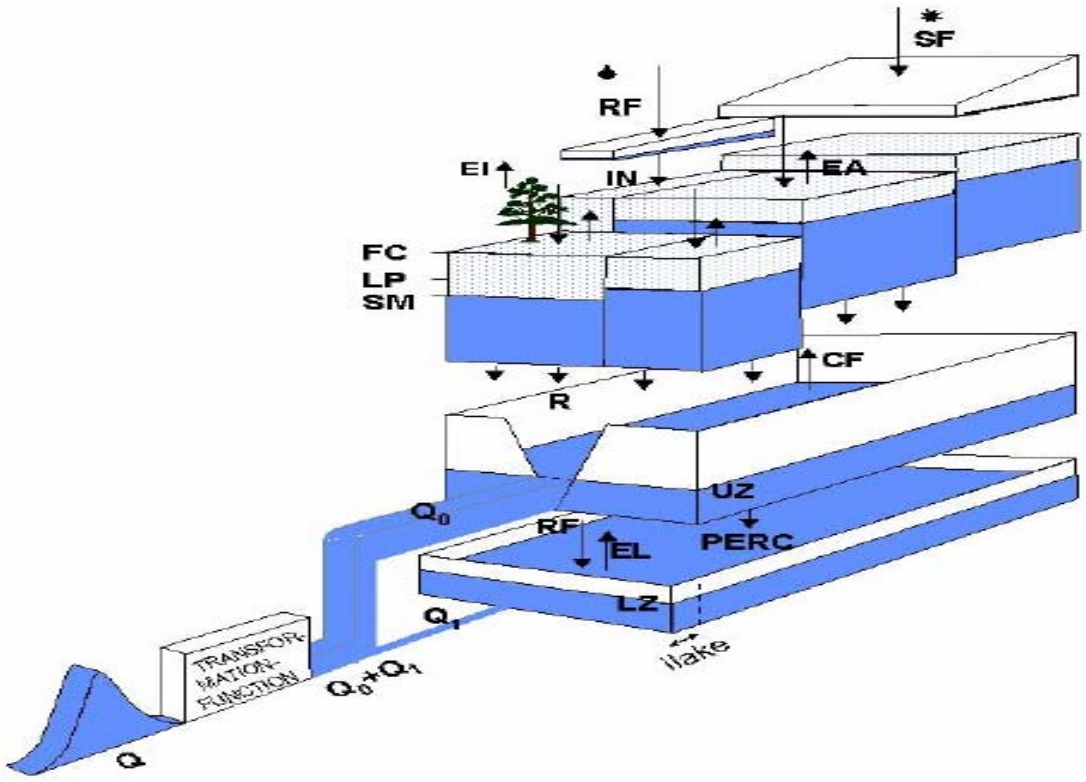

Figure 3. 5 Schematic representations of HBV model for one basin

Where,

SF: snowfall, RF: rainfall, EI: evapo-transpiration, IN: infiltration, EA: actual evaporation, FC: Maximum soil moisture storage, SM: compound soil moisture routine, CF: capillary rise, R: seepage, UZ; upper zone reservoir, Q_o; direct runoff from upper reservoir, EL; lake evaporation, PERC; percolation capacity, LZ: lower zone reservoir and Q1: base flow lower reservoir.

The general water balance of HBV-model can be described as follows;

$$P - E - Q = \frac{d}{dt}\left[SP + SM + UZ + LZ + lake(reservoir)\right] \quad \text{.....3.5}$$

Where,

P**:** Precipitation, Q: Runoff, SP: Snow pack, SM :Soil moisture, UZ :Upper groundwater zone, LZ :Lower groundwater zone, and $lake(\text{Re}servoir)$:Lake (reservoir volume)

3.10 Previous Studies on the Potential Impact of Climate Change on the Water Resources of Upper Blue Nile Basin

Because of the problems associated with climate change modeling and hydrological modeling, limited research into the effects of climate change on water resources has been undertaken in Upper Blue Nile Basin.

3.10.1 Research on Climate Change Impact on Hydrology and Water Resources of the Upper Blue Nile River Basin, Ethiopia (IWMI RR-126)

The study divides the basin in to six sub-basins and develops six different climate scenarios from global circulation models (GCMs). The research uses simple two hydrological models to simulate the runoff. The main findings of the study can be summarized as follows;

- The climate in most of the Upper Blue Nile River Basin is likely to become wetter and warmer in the 2050s.
- Low flow may become higher and sever mid-to long term drought are likely to become less frequent throughout the basin; and
- The potential future dam operation are unlikely to significantly affect the water availability to Sudan and Egypt based on predicted outflow from six GCMs and many dam operational policies.

3.10.2 Study on the water availability of the Blue Nile Basin catchment under climate Change

In this study the assessment was done on selected 10 catchments of the basin. The water availability of the selected catchment were evaluated by developing a hypothetical scenario within the range of (-30 to +30 percent change) for both precipitation and potential evapo-transpiration have been investigated. And a general climate change sensitivity map for the basin is developed (Bimrew M., 2008).

3.10.3 Study on Tana Sub-Basin

The impact of climate change on water resource of Lake Tana sub-basin was assessed on the basis of CCCM and GFCD3 UK89 climate change prediction. The CCCM and GFCD3 GCMs predict a reduction of annual runoff by 18.2% and 12.6% respectively , while UKMo GCM predicts wetter condition and as result of an increase in 2.5% in annual runoff (Tarekegn and Tadege, 2006).

4. Materials and Method

For any research, identifying clear and efficient methodology is a crucial for the effectiveness of the study not only from time budget point of view, but also from the quality of the research result.

General Methodology

Basically, the general methodology for the study can be described by the following flow chart;

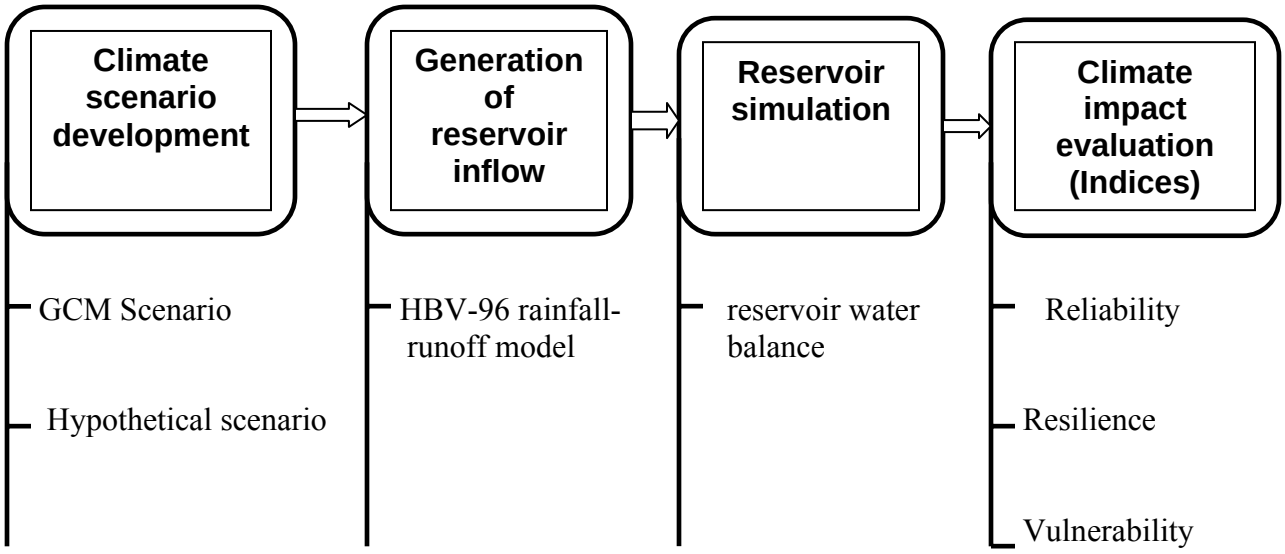

Figure 4. 1 General methodology flow chart used in the study

4.1. Climate Scenario

4.1.1 GCMs and Emission scenario

Use of all available GCMs and emission scenario will result in a better understanding of climate change. However, due to the limited amount time available to complete the study, this research deals with the out put from HadCM3 model for A2 and B2 scenarios. HadCM3 is a coupled atmospheric-ocean GCM developed at Hadley Center for Climate Prediction and Research, UK. HadCM3 is applied in this study because the model is widely applied in many climate change

studies and it provides large scale daily predictor variables which can be used for Statistical Downscaling Model (SDSM).

4.1.2 Statistical Down Scaling Methods (SDSM)

SDSM which is designed to downscale climate information from coarse-resolution of GCMs to local or site level is applied here to downscale the precipitation, maximum and minimum temperatures for the study area. SDSM uses linear regression techniques between predictor and pridictand to produce multiple realizations (ensembles) of synthetic daily weather sequences. The predictor variables provide daily information about large scale atmosphere condition, while the pridictand described the condition at the site level.

It is appropriate to use this software when the impact assessments is require at small-scale or regional level, provided that quality observational data and large scale daily GCMs climate variables are available. Additionally, the mode can also produces a range of statistical parameters such as variances, frequencies of extremes and spell lengths for the downscaled climatic parameters (R.L. Wilby and C.W.Dawson, 2007).

SDSM software is published in different version at various times, among them the latest version is adopted for this particular study (i.e. version 4.2.2 SDSM software coded in Visual Basic 6.0).

The main reasons to apply the SDSM model for the study are;

- It is widely applied in many regions of the world over a range of different climatic condition.
- It can be runs on PC-based systems and has been tested on Windows 98/NT/2000/XP.
- The availability of the software (i.e. new users can register and download freely the software package at https://co-public.lboor.ac.uk/cocwd/SDSM/)
- Compared to other downscaling methods, the knowledge of atmospheric chemistry required by the SDSM is less.
- The required time for simulating the surface weather parameter is low.
- The ability of the model to permit risk/uncertainty analyses by using the generated ensembles.

Drawbacks related SDSM

The limitation related to SDSM model can be summarized as follows;

- The relationship between the predictor and predictand is achieved by only considering the data statistical condition, i.e. the model does not take in to consideration the physical nature of the catchments (major drawback).
- It requires high quality data for model calibration;
- The model is highly sensitive to the choice of predictor variables and empirical transfer scheme.

Structure and operations of SDSM

The structure and operations of SDSM can be best described with respect to seven tasks as indicated in ***bold box*** in the following figure (R.L. Wilby and C.W.Dawson, 2007).

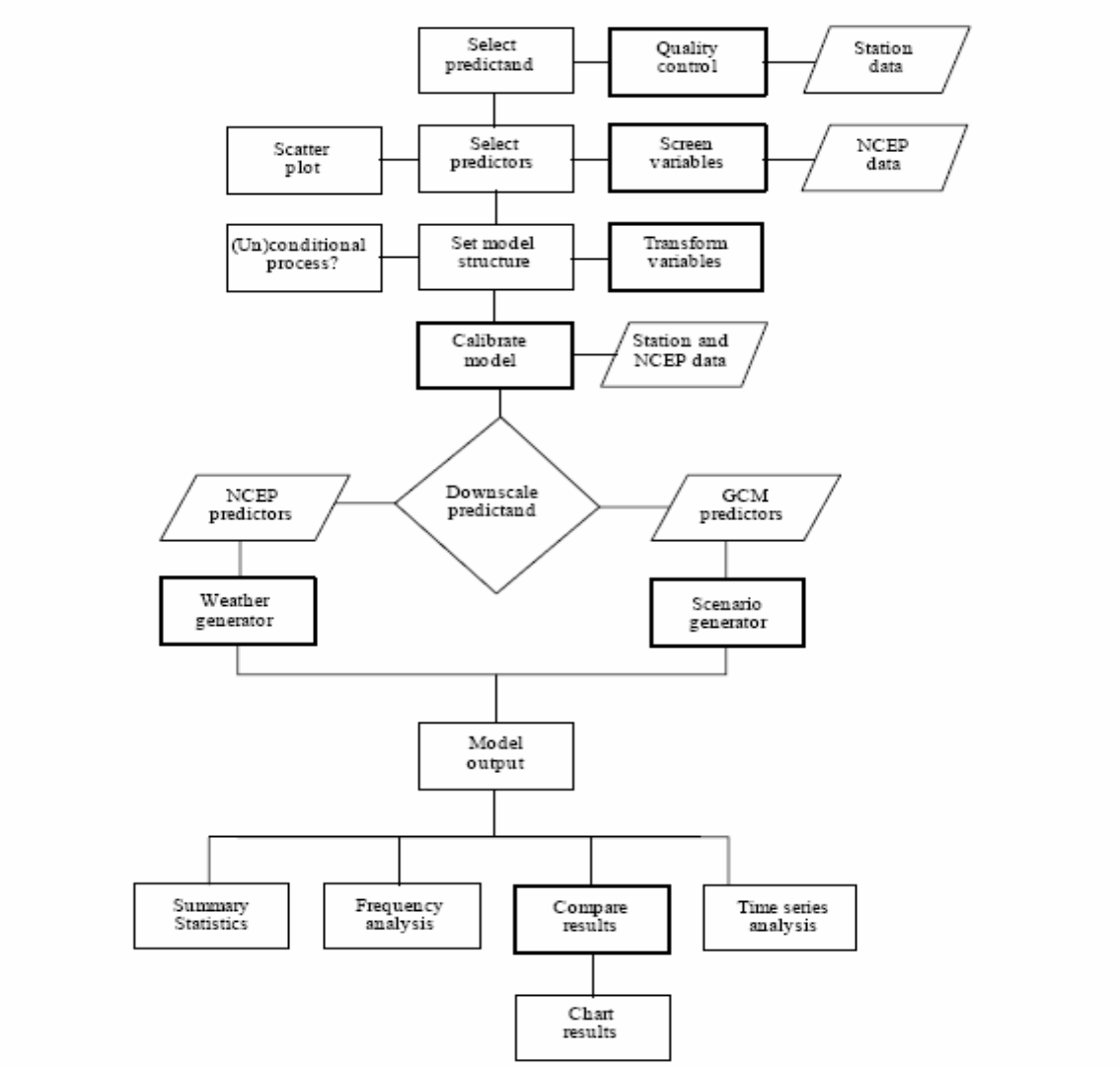

Figure 4. 2 SDSM (version 4.2) Climate scenario generations

Quality control and data transformation: - The quality control in SDSM used to identify the gross data error, specification of missing data code and outliers prior to model calibration. In many instances it may be appropriate to transform predictors and/or the predictand prior to model calibration. The transform facility takes chosen data files and applies selected transformations (e.g., logarithm, power, inverse, lag, binomial, etc).

Screening of downscaling predictor variables: - Identifying empirical relationships between gird predictors (such as mean sea level pressure) and single site predictands (such as station precipitation) is central to all statistical downscaling methods. The main purpose of the screen variables operation is to assist the user in the selection of appropriate downscaling predictor variables.

Model calibration: - The calibrate model operation takes the specified predictand along with a set of predictor variables, and computes the parameters of multiple regression equations via an optimization algorithm (either dual simplex of ordinary least squares). Then specification of the model structure: whether monthly, seasonal or annual sub–models are required; whether the process is unconditional or conditional. In unconditional models a direct link is assumed between the predictors and predictand but in conditional models, there is an intermediate process between regional forcing and local weather.

Weather generator: - The weather generator operation generates ensembles of synthetic daily weather series for a given observed (or NCEP re–analysis) atmospheric predictor variables. The procedure enables the verification of calibrated models (using independent data) and the synthesis of artificial time series for present climate conditions.

Data analysis: -SDSM provides means of interrogating both downscaled scenarios and observed climate data with the summary statistics and frequency analysis screens. For model output, the ensemble member or mean must also be specified. In return, SDSM displays a suite of diagnostics including monthly/ seasonal/ annual means, measures of dispersion, serial correlation and extreme.

Graphical model out puts or graphical analysis:-Three options for graphical analysis are provided by SDSM 4.2 through the Frequency Analysis, Compare Results, and the Time Series Analysis screens.

Scenario generation:-Finally, the scenario generator operation produces ensembles of synthetic daily weather series for the potential atmospheric predictor variables supplied by a climate model (either for present or future climate experiments), rather than observed predictors.

4.1.3 Hypothetical Scenario

Hypothetical or synthetic scenarios which develops by changing the particular climate element in plausible and arbitrary amount (e.g. $+2^oC$, $+4^oC$ change from the baseline temperature and $\pm 5\%$, $\pm 10\%$, $\pm 20\%$ change form the baseline precipitation) (IPCC, 2001) are adopted for this study in order to exploring the sensitivity of reservoir system.

4.2 Reservoir inflow

Once the HBV-96 rainfall-runoff model generates the flow at the Gilgel Abay gauging station for different time horizons i.e. 2020s (2011-2040), 2050s (2041-2070) and 2080s (2071-2099), the inflow to the Gilgel Abay reservoir for both current (1996-2005) and future time is found by transferring the runoff from the gauging station to the dam site by using the area ratio method, between upstream of the dam site and upstream of Gilgel Abay station, under the assumption that the catchments characteristics and areal rainfall over the two area are the same (see from figure 7.15 to7.18).

4.3 Hydrological Model Selection Criteria

There are numerous criteria which can be used for choosing the "right" hydrologic model. These criteria are always project-dependent, since every project has its own specific requirements and needs. Further, some criteria are also user-depended (and therefore subjective). Among the various project-depended selection criteria, there are four common, fundamental ones that must be always answered (Juraj M, 2003):

1. Required model outputs important to the project and therefore to be estimated by the model (Does the model predict the variables required by the project such as peak flow, event volume and hydrograph, long-term sequence of flows, …?),

2. Hydrologic processes that need to be modeled to estimate the desired outputs adequately (Is the model capable of simulating regulated reservoir operation?),

3. Availability of input data (Can all the inputs required by the model be provided within the time and cost constraints of the project?),

4. Price (Does the investment appear to be worthwhile for the objectives of the project?).

Reasons for selecting HBV-96 model

The reasons behind for selecting HBV-96 model for this study are;

- The model was applied for climate change impact assessment in different countries (Bergstrom, 1992)
- The model simulated the major hydrological process in the catchments.
- Because of its semi-distributed nature its structure is more physically-based than the structure of lumped model, and it is less demanding on input data than fully distributed model.
- It simulates the outflow from the reservoir according to the rating-table or the reservoir regulation policy.
- Its input climatic parameters are in day (or shorter) time scale (which found from the generated SDSM).
- The setup time and expertise required is medium.
- Availability of the model.

The main drawback related to HBV model is that, the model parameters usually calibrated (optimized) manually by trial and error method (Bergstrom, 1992) which sometimes leads to subjective judgment for model parameters and its has also limited information regarding the simplified soil moisture dynamics. In order to reduce the subjective judgment, crosschecking of the optimized model parameters with recommended range is carried out. (See table. 7.4)

4.3.1 Description of HBV-96 model

The HBV model is a semi-distributed conceptual hydrologic model developed by the Swedish Metrological and Hydrologic Institute (SHMI) in 1970s. The HBV model is a standard forecasting tool in nearly 200 basins throughout Scandinavia, and has applied in more than 40 countries including Ethiopia. The model is design to run in on a daily time step (shorter time steps are available as option) and to simulate river runoff in river basins of various sizes. The basin can be disaggregated in to sub-basin, elevation zone, and land cover types. Input data includes precipitation, air temperature, long term average monthly estimates of evapo-transpiration, runoff (for calibration) and basin geographical information. The model consistence of subroutine for snow accumulation and melt, a soil moisture accounting procedure, routines for runoff generation and a simple routine procedure. The treatment of snow accumulation and melt in HBV is based on a simple accounting (degree-day) algorithm (SHMI, 2003). A simple model based on bucket theory is used to represent soil moisture dynamics (Lindström et al, 1997). There is a provision for channel routing of runoff from tributary basins, using a modified Muskingum method. It also simulates the out flow from reservoirs or lakes by specifying the stage-discharge rating curve or providing reservoir regulation policy. The reservoir regulation policy has priority than stage-discharge curve for calculating the out flow from reservoir.

4.3.1.1 HBV-96 model structure

Precipitation and snow accumulation: - Precipitation calculations are made separately for each elevation/vegetation zone with in the basin. To separate between snow and rainfall a threshold temperature is used. There are also separate rainfall and snowfall correction factor to correct the observational errors. The lapse rate parameter for precipitation, *pcalt*, is used to adjust the change precipitation with variation in altitude.

Soil routine:-The soil moisture accounting routine is the main part of controlling runoff formation. This routine is based on the three parameter, β, *lp* and *fc*, as shown in figure 4.3. β controls the contributions the response function ($\Delta Q/\Delta P$) or the increase in soil moisture storage($1- \Delta Q/\Delta P$) from each millimeter of rainfall or snow melt. $\Delta Q/\Delta P$ can also be expressed

as R/IN (using the symbol in figure 3.5). *lp* is a soil moisture value above which evapo-transpiration reaches its potential value, and *fc* is the maximum soil moisture storage (in mm) in the model. The parameter *lp* is given as a fraction of *fc*.

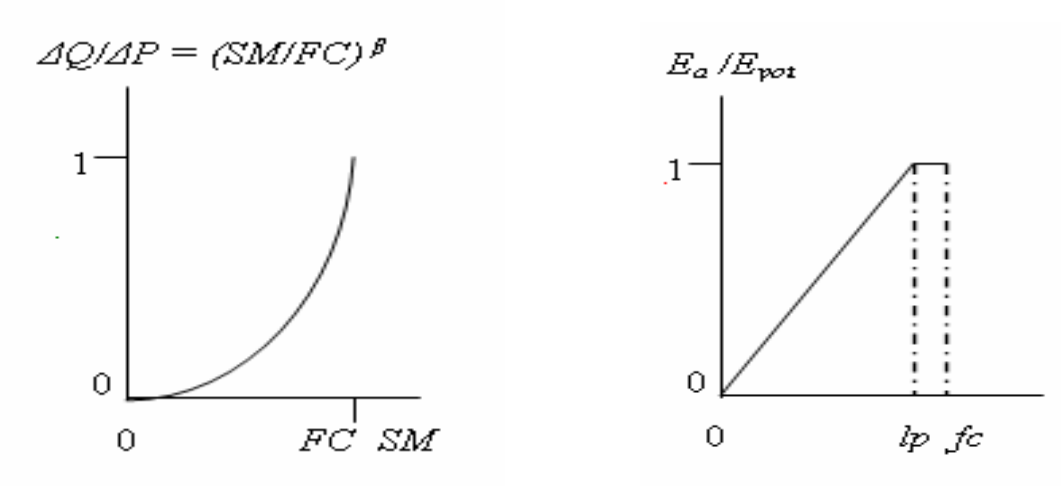

Figure 4. 3 The soil moisture routine for HBV model

Where,

SM: computed soil moisture, ΔP: Contribution from rainfall, ΔQ: Contribution to the response function, FC: Maximum soil moisture storage, β: Empirical coefficient, E_{pot}: Potential evapo-transpiration, Ea: Computed actual evapo-transpiration and Lp: Limit for evapo-transpiration.

Response routines: - The runoff generation routine is the response function which transforms excess water from the soil moisture zone to runoff. It also includes the effect of direct precipitation and evaporation on a part of the reservoir. The function consists of one upper and one lower, linear reservoir (see. equation 3.3 and 3.4)

The yield from the soil moisture zone, i.e., the effective precipitation, will be added to the storage in the upper reservoir. As long as there is water in the upper reservoir, water will percolate to the lower reservoir according to the parameter '*perc'*.

Precipitation and evaporation from reservoir: - Precipitation on reservoir will be the same as for a non-forested zone at the same altitude and will be added to the reservoir water regardless of ice conditions in the same way for both rain and snow. Evaporation from lakes will equal the potential evaporation but can be modified by the parameter *cevpl*.

4.4 Model performance

The performance of the model must be evaluated for the extent of its accuracy (Goswami et al., 2005). Hence, for this study, the model performance in simulating observed discharge was evaluated during calibration and validation by; Inspecting simulated and observed runoff graphs visually (see figure 7.14), by calculating Nash and Sutcliffe efficiency criteria R^2 (commonly used in hydrological modeling) and by calculate the Relative Volume Error (RV_E).

The Nash and Sutcliffe coefficient (R^2) is a measure of efficiency that relates the goodness-of-fit of the model to the variance of measured data (see, equation 4.1). R^2 can range from - ∞ to 1 and an efficiency of 1 indicates a perfect match between observed and simulated discharges. R^2 value between 0.9 and 1 indicate that the model performs very well while values between 0.6 and 0.8 indicate the model performs well (Wale A., 2007). The largest disadvantage of this efficiency criterion is that larger value in a time series are strongly overestimated where as lower values are of minor importance. For the quantification of runoff prediction this leads to an overestimation of model performance during peak flows and underestimation during low flow conditions.

$$R^2 = 1 - \frac{\sum_{i=1}^{n}\left(Q_{sim(i)} - Q_{obs(i)}\right)^2}{\sum_{i=1}^{n}\left(Q_{sim(i)} - \overline{Q_{obs(i)}}\right)^2} \quad \text{.....4.1}$$

Where,

Q_{obs} : Observed flow, Q_{sim} : Simulated flow and $\overline{Q_{obs}}$:Average of observed flow.

The RV_E can vary between ∞ and - ∞ but it performs best when a value of 0 (zero) is generated. Since an accumulated difference between simulated, $Q_{sim\ (i)}$ and $Q_{obs\ (i)}$ observed, discharge is zero. A relative volume error between +5% or -5% indicates that a model performs well while relative volume errors between +5% and +10% and -5% and -10% indicates a model with reasonable performance (Wale A, 2007).

$$RV_E = \left[\frac{\sum_{i=1}^{n} Q_{obs(i)} - \sum_{i=1}^{n} Q_{sim(i)}}{\sum_{i}^{n} Q_{obs(i)}} \right] * 100 \quad \ldots\ldots\ldots\ldots\ldots\ldots\ldots\ldots\ldots\ldots\ldots\ldots\ldots\ldots\ldots\ldots 4.2$$

4.5 Climate impact assessment

The analysis of potential climate change impact on the reservoir system requires simulation of the reservoir water balance under different climate scenarios. An important aspect of planning reservoir systems is to be able to assess their future performance under a wide range of conditions expected during their operating life (Thomas et al, 2004). There are different measures for assessing the reservoir system performance yet they have not been subjected to comparative interpretation over a range of different climate condition. Hence, this specific study select three performance indices (metrics) that are used to evaluate the climate change impact on Gilgel Abay reservoir comparatively, these are; *reliability* (time-based reliability(monthly) and volumetric reliability), *resilience* and *vulnerability* indices.

In order to have a more divergent understanding on the impact of climate change the above performance indices were also analyzed for no reservoir existing conditions using excel-spreadsheet.

The performance metrics have different definitions depending on their applicability condition for this context the following definitions were adopted.

4.5.1 Reliability:-

Reliability can be described as the probability that a reservoir will be able to meet, within the simulation period, the target demand in any given interval of time (often a year or a month). There are several measures of reliability, which are defined as follows.

- Time-based reliability considers the proportion of intervals during the simulation period that reservoir can meet the target demand. A general expression for estimating this metric is:

$$R_t = \frac{N_s}{N}; \qquad 0 < R_t \le 1 \ldots\ldots\ldots\ldots\ldots\ldots\ldots\ldots\ldots\ldots\ldots\ldots\ldots\ldots\ldots\ldots\ldots\ldots 4.3$$

Where,

$R_t =$ Time based reliability.

$N_s =$ The numbers of interval that the target demand is fully meet.

$N =$ The total number of intervals covering the simulation analysis period,

- Volumetric reliability is defined as the volume of water supplied to the demand center divides by the total target demand during the entire simulation period, i.e.

$$R_V = 1 - \frac{\sum_{i}^{N}\left(D_i - D_i^{'}\right)}{\sum_{i}^{N} D_i} = 1 - \frac{Total \quad shortfall}{Total \quad t\arg et \quad demand}; \qquad 0 < R_V \le 1 \ldots\ldots\ldots\ldots\ldots 4.4$$

Where,

$R_V =$ Volumetric reliability

$D_i =$ The target demand during the i^{th} period

$D_i^{'} =$ The volume of water actually supplied or available in the reservoir during the i^{th} period

$N =$ The number of time interval in simulation period.

4.5.2 Resilience:-

Resilience is a metric defining how quickly a reservoir will recover from a failure. The method used in this study is the widely used definition of Hashimoto et al. (1982). According to Hashimoto et al. (1982) the resilience is the probability of a year of success following a year of failure.

$$\varphi = \frac{f_s}{f_d}, \qquad f_d \neq 0 \ldots\ldots\ldots\ldots\ldots\ldots\ldots\ldots\ldots\ldots\ldots\ldots\ldots\ldots\ldots\ldots\ldots\ldots\ldots\ldots\ldots\ldots\ldots\ldots 4.5$$

Where,

$\varphi =$ is the resilience

f_s = is the number of individual continuous sequences of failure periods and

f_d = the total duration of the failure

4.5.3 Vulnerability

- Vulnerability by volume:-

Vulnerability measures the average volumetric severity of failure during a period and is defined by Hashimoto et al. (1982) as follows;

$$\eta' = \frac{\sum_{j=1}^{fs} \max(s_j)}{fs} \quad \text{.....4.6}$$

Where,

η' = Vulnerability

s_j = the volumetric shortfall during the j^{th} continuous failure sequence

f_s = the number of continuous sequence of failure

Because equation 4.6, averages out the maximum shortfall over all the continuous failure periods, then a reduction in f_s will cause η' to increase when the numerator in equation 4.6, remains unchanged. One way to avoid this anomaly is to remove the averaging in equation 4.6.Another point to note about equation 4.7 is that η' is in volumetric units; a more useful expression of vulnerability is its dimensionless form (Thomas et al, 2004) given by:

$$\eta = \frac{\eta'}{Df} \quad 0 < \eta \leq 1 \text{ ……..……4.7}$$

Where,

η = Dimensionless vulnerability

Df = is the constant or average of all demand

The three –tier system of assessment i.e. reliability, resilience and vulnerability could ensure a consistent assessment of reservoir system performance (Thomas et al, 2004).

5. Hydro-meteorological Data Screening

Engineering studies of water resources development and management depend heavily on hydrological data. These data should be stationary, consistent, and homogeneous when they are used for to simulate a hydrological system.

5.1 Meteorological data screening

A time series of hydrological data is strictly stationary if its statistical properties (e.g. its mean, variance, and higher-order moments) are unaffected by the choice of time origin. (By 'unaffected', means that estimates of these properties agree within the range of expected statistical variability). The basic data-screening procedure used here is based upon split-record tests for stability of the variance (F-test) and stability of mean (t-test) of such a time series.

A time series of hydrological data may exhibit jumps and trends owing to what Yevjevich and Jeng (1969) call inconsistency and non-homogeneity. Inconsistency is a change in the amount of systematic error associated with the recording of data. It can arise from the use of different instruments and methods of observation. Non-homogeneity is a change in the statistical properties of the time series. Its causes can be either natural or man-made. These include alterations to land use, relocation of the observation station, and implementation of flow diversions.

The data screening procedure passed through the following principal steps in order to check the *absolute* and *relative* consistency, homogeneity and sationarity of the data, for the selected stations.

1. Rough screening of the data and compute or verify the totals for the hydrological year or season;
2. Plot these totals according to the chosen time step (yearly for this study) and note any trends or discontinuities (visual examination);
3. Test the time series for absence of trend with Spearman's rank-correlation method;

4. Apply the F-test for stability of variance and the t-test for stability of mean to the split, non-overlapping, sub-sets of the time series at the 5-percent level of significance;
5. Test the time series for absence of persistence by computing the first serial-correlation coefficient (used only for flow data);
6. Test the time series for relative consistency and homogeneity with double-mass analysis.

Eight hydro- metrological stations for the study area which are absolutely consistence and homogenous are selected.

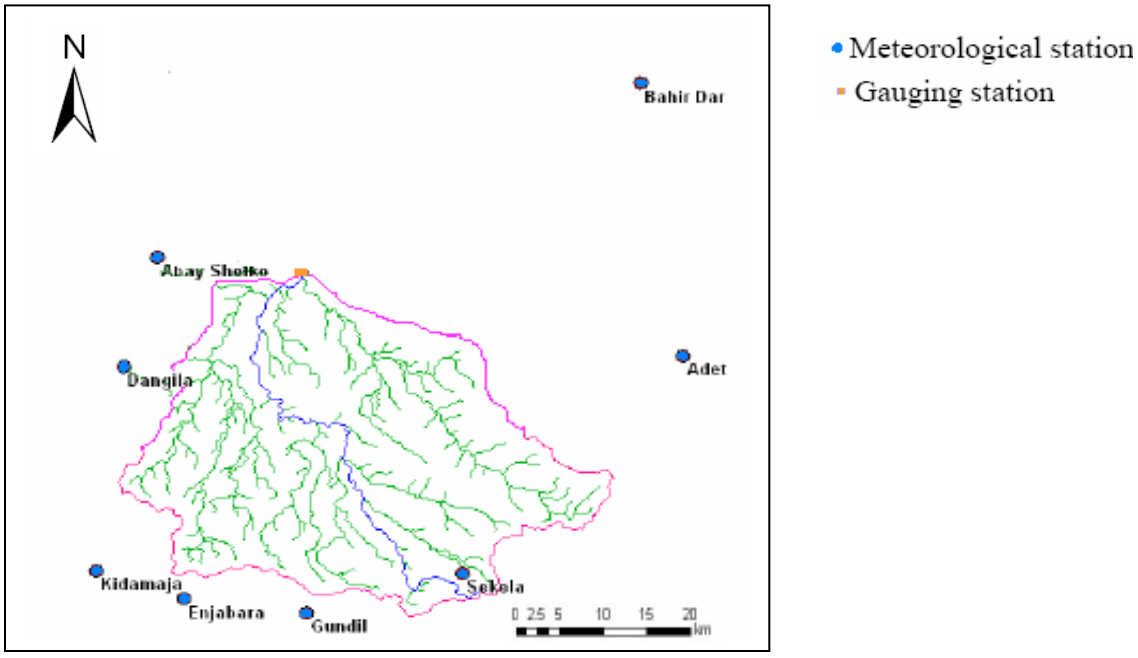

Figure 5. 1 Selected Hydro-Metrological stations

In addition to the above steps the selected rainfall stations was non-dimentionaised and plotted together (see, figure 5.2) to analyze their homogeneity.

The non-dimensionalzing of the month's value is carried out as;

$$Pi = 100\% * \frac{(\bar{P}i)}{\bar{P}} \quad \text{.....5.1}$$

Where,

Pi : Non-dimensional value of rainfall for month i, $\overline{Pi}$: Over year-averaged monthly rainfall at the station i and $\overline{P}$: The over year – average yearly rainfall of the station.

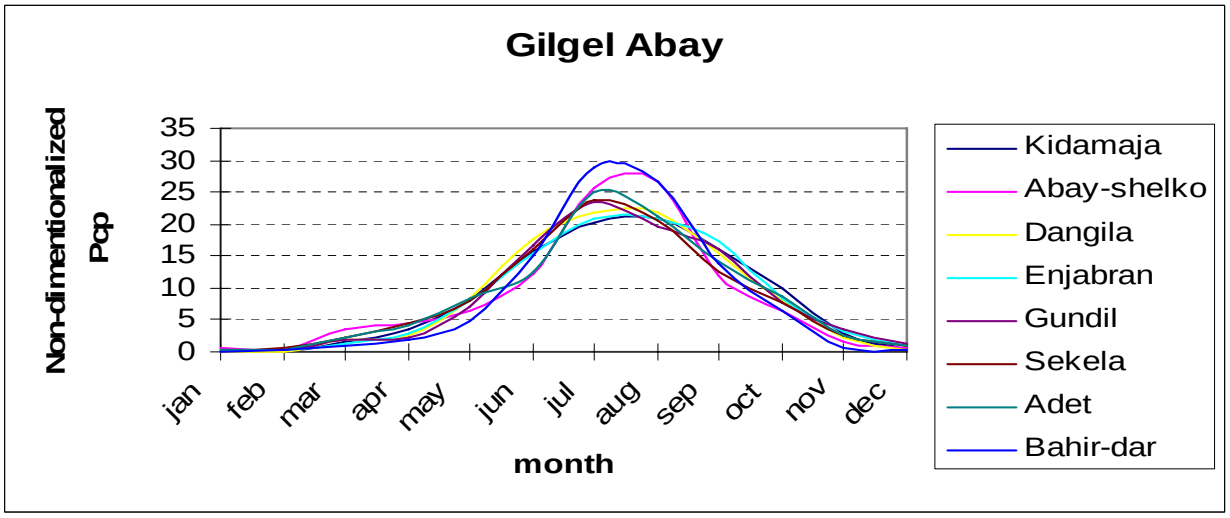

Figure 5. 2 Non- dimensionalzed stations for Upper Gilglel Abay cachment

As shown in the above figure, one can see the homogeneous nature of the stations in study region because they have one distinct climatic and rainfall pattern and in almost all stations, the maximum rain fall falls between June to September.

Graphical comparison and visual examination of the rainfall data was done by plotting the time series monthly rainfall data .The selected stations show similar periodic pattern of records (figure 5.3). Comparison of data of one station with the other stations using tabular and graphical approach didn't show other suspicious values.

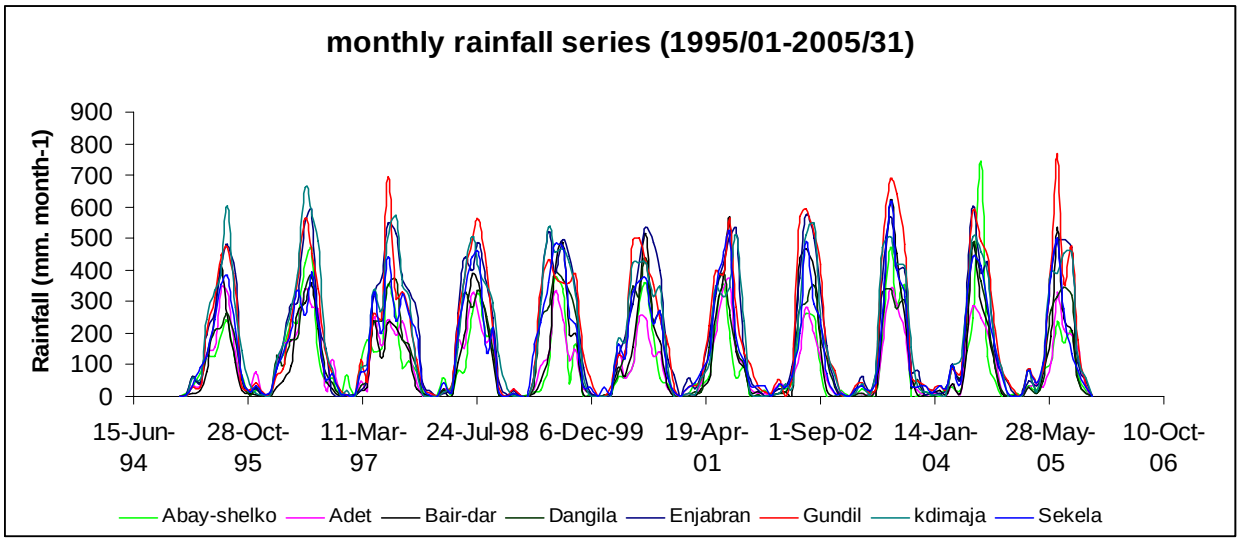

Figure 5. 3 monthly rainfalls of selected stations [mm/month]

A time series observational data is relatively consistent and homogeneous if the periodic data are proportional to an appropriate simultaneous period. This proportionality can be tested by double mass analysis in which accumulated rainfall/hydrological data is plotted against the mean value of all neighborhood stations.

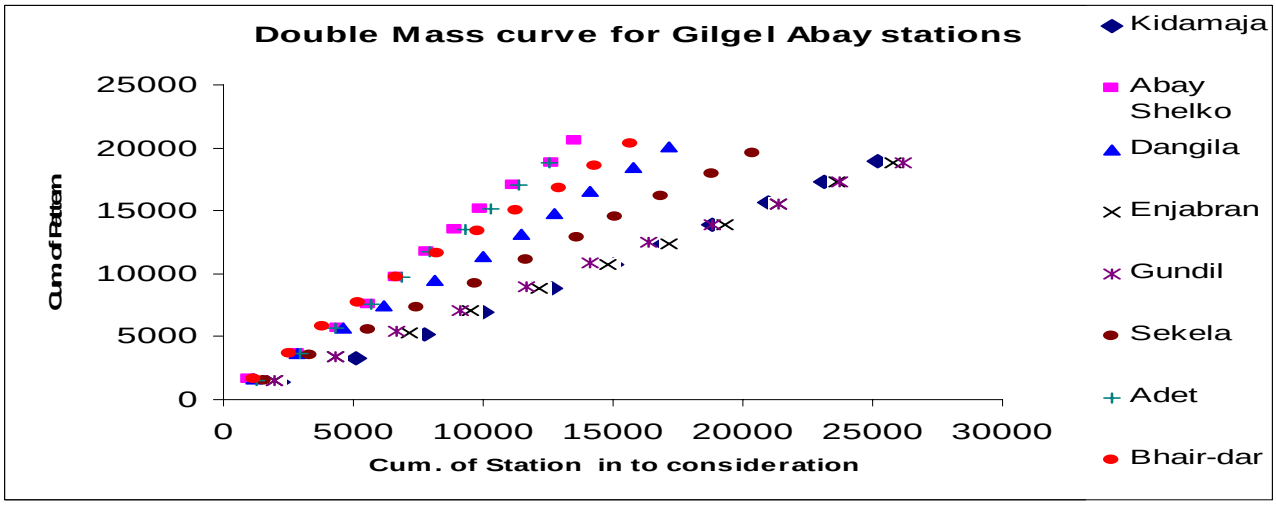

Figure 5. 4 Double mass curve for the selected Metrological stations

5.1.1 Filling of missing data

Stations with missing data were filled by simple linear interpolation and normal ratio method. Normal ratio method are expressed by the following relationship

$$Px = \frac{Nx}{n}\left(\frac{P1}{N1} + \frac{P2}{N2} + ... + \frac{Pn}{Nn}\right) \quad \text{.....5.2}$$

Where,

Px = Missing value of precipitation to be computed.

Nx = Average value of rainfall for the station in question for recording period.

$N1$ = Average value of rainfall for the neighboring station.

$P1....Pn$ = Rainfall of neighboring station during missing period

n = Number of stations used in the computation.

5.2 River discharge data screening

The initial step taken during the river discharge data screening as suggested by Gordon et al. (1992) was quick visual scan of the data time series to detect gross errors such as erroneous peak flow, missed recordings, and flows of constant rate. It helped to detect the year with magnitude change in the data, long periods of missing records, and short-term missing data.

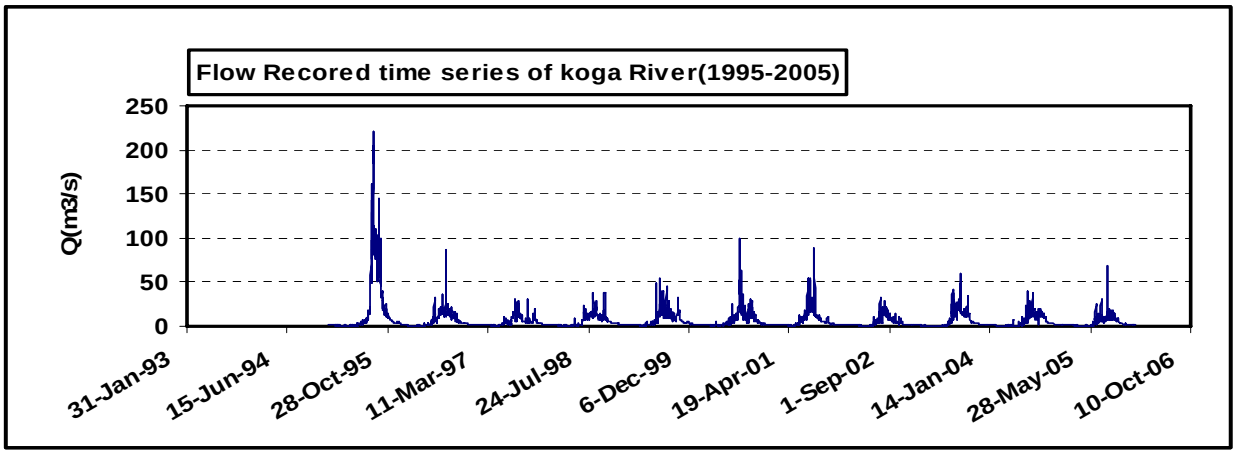

Figure 5. 5 Observed river flow in Koga gauging station

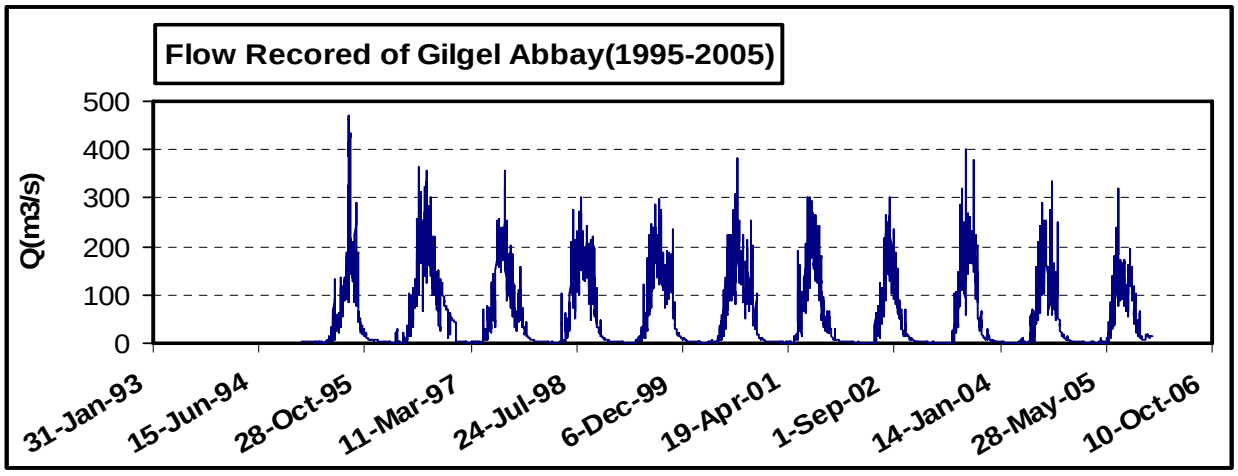

Figure 5. 6 Observed river flow in Gilgel Abay gauging station

Plotting of river flow time series with the respective precipitation and close observation is quite useful in order to point out suspicious records of river flow. As shown the figure 5.7, the Gilgel Abay gauging station exhibit unrealistic record during 1996/97 when it compared to the areal rainfall. Before using this unrealistic data for model calibration and validation, it was treated in such a way that by removing this data from the series and fill the gap by developing regression equation between Gilgel Abby and Koga river flow for the year 1/1/1996 to 12/31/1997. Computation of correlation coefficient between daily records of Gilgel Abay and Koga Rivers for the period between 1/1/1998 to 12/31/2005 by excluding the suspected records gave a value of 0.799.

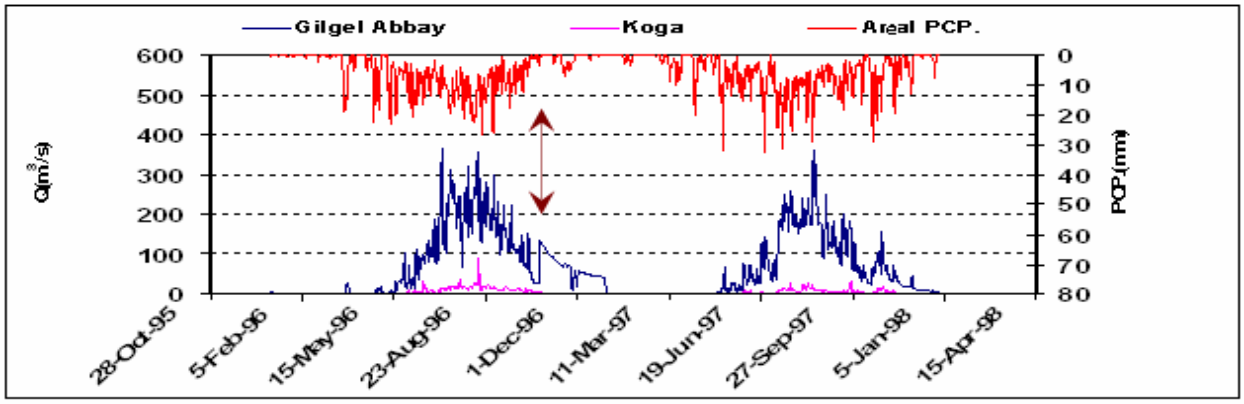

Figure 5. 7 *Selected suspicious year for Gilgel Abay gauging*

$$Q_G = 0.15 + 6.18 * Q_K \quad \text{.....5.3}$$

Where,

Q_G = River discharge for Gilgel Abay gauging station (m^3/s).

Q_K = River discharge for Koga gauging station (m^3/s).

The correlation coefficient for equation 5.3 gives a value of 0.79.

5.3 Other Metrological data screening

Maximum and minimum temperature of 10 year daily record length were collected from NMSA and analyzed over the study area. The lists of available stream and metrological stations name, location and metrological variable have been given in the Appendix D and E respectively.

6. Model setup and data analysis

6.1 Field visit

A field visit to the study area was conducted for duration of five days. The big advantage of the field visit was sought during hydrological modeling because it makes us to be familiar with the landscape and its dominant land-use and land cover of the study area which result to have better feeling of its hydrology.

(a) Gilgel Abay Hydrometric Station

(b) Gilgel Abay dam site

(c) Mild Slope Plateau portion of Gilge Abay Catchments

(d) Erosions affected area in Gilgel Abay Catchments.

(e) Mixed forest around Wetet Abay

(f) Forest and Grass at Mt. Gish.

Figure 6. 1 Selected area of landscape, land cover, and dam site phothos.

6.2 Station Selection for Statistical Down Scaling Method

Since, SDSM is Windows-based decision support tools that used for the rapid development of single-site ensemble and scenarios generation under different regional climate forcing, the correlation coefficient between the selected stations is carried out in order to find a single station for downscaling purpose which has high correlation with most of the other neighboring stations. In additional to the correlation coefficient the quality and the available length of period of record also take into consideration during selection of stations for downscaling.

Table 6. 1 Precipitation Correlation coefficient of eight metrological stations (1996-2005) based on daily data.

	Abay-Sheleko	Bahir-dar	Dangila	Gundil	Kidamaja	Sekela	Adet	Enjabran
Abay-Sheleko	1.00							
Bahir-dar	0.30	1.00						
Dangila	0.40	0.50	1.00					
Gundil	0.30	0.45	0.50	1.00				
Kidamaja	0.30	0.42	0.50	0.40	1.00			
Sekela	0.30	0.50	0.30	0.50	0.40	1.00		
Adet	0.70	0.60	0.50	0.40	0.40	0.40	1.00	
Enjabran	0.34	0.50	0.86	0.40	0.11	0.72	0.40	1.00

As per the above mentioned criteria Bhair-dar stations are chosen for downscaling the climate parameters for Gilgel Abay catchment. For this study because of the limited time available and difficulties related to downscaling of all climate parameters, only the daily precipitation and daily maximum and minimum temperature are downscaled for the study area.

According to World Metrological Organization (WMO), for any climate impact assessment, a 30 year non-overlapping climatological base line period is recommended. The current normal recommended period by WMO is (1961-1990).

6.3 Model Setup

6.3.1 Predictor files

The large scale predictors which are used for SDSM model input can be downloaded from the website of Canadian Institute for climate studies for model output of HadCM3 (http://www.cics.uvic.ca/scenarios/sdsm/select.cgi). The predictors are found in grid basis for different regions in the world, so after selecting the African window the predictors that include the Gilgel Abay catchment is downloaded. This predictor is found in zip file format. When the zip file is opened the following climatic parameters are found;

NCEP_1961-2001: this directory contains 41 years of daily observed predictors' data, derived from the NCEP reanalysis, and normalized (with respect to the mean and standard deviation) over the complete 1961-1990 period. These data are interpolated to the same grid as HadCM3 (2.5^o latitude x 3.75^o longitude) before the normalization is carried out.

H3A2a_1961-2099[2]**:** this directory contains 139 years of daily GCM predictors data, derived from the HadCM3 A2a experiment, and normalized over the 1961-1990 period.

H3B2a_1961-2099[2]: this directory contains 139 year of daily GCM predictor data, derived from the HadCM3 B2a experiment, and normalized over the 1961-1990 period.

NCEP data which are re-analysis sets from the National Center for Environmental Prediction was re-girded to match with the grid system of HadCM3. These data are used for model calibration. Both NCEP and HadCM3 data have daily predictors. There exist 26 predictors variables in both NCEP and HadCM3 which used for analysis (see Appendix C)

When SDSM is applied to downscale the climate variables for study area, the variance inflation which controls the magnitude of variance inflation in downscaled daily weather variables is fixed to a value of 11. The default value (12) produces approximately normal variance inflation. Additionally, the bias correction which used to compensates the tendency to over– or under–estimate the mean precipitation by the downscaling model is fixed to a value of 0.975. The default value (1) indicates no bias correction is taken. The above parameters are fixed in such a way that by comparing the observed and simulated climate variable graphically and adjust these parameter by trial and error method until the simulated variable is much approach to that of the observed climate variable.

6.3.2 Screening of Potential Downscaling Variables

Screening of the potential predictors for the selected pridctand (i.e. observed precipitation, minimum and maximum temperature) is the most crucial and decisive part in statistical downscaling model. Identifying an appropriate large scale girded predictor result in good

[2] For each scenario there are three ensemble members (a, b and c). To take into account the natural variability of the climate and the influence of the choice of which point along the control run increasing greenhouse gas concentrations are introduced, the perturbation of the climate is initiated at three different points along the control run. In the case of the medium-low emissions scenario, only the "a" member was available for analysis.

correlation between observed and downscaled climate variables during model calibration and scenario generation. The recommended methods for screening the potential predictors is starting the processes by selecting seven or eight predictor at a time and analyze their explained variance, then select those predictor which has higher explained variance and drop the rest. For the selected predictor analyze or calculate their correlation matrix with the observed predictand, this statistics identify the amount of explanatory power of the predictor to explain the pedictand and finally the scatter plot is carried out in order identify the nature of the association (linear, non–linear, etc.), whether or not data transformation(s) may be needed, and the importance of outliers. This procedure is repeated by holding those predictors which passé the above criteria and add new predictors from the reset of available predictors.

Because precipitation is conditional process i.e. there is an intermediate processes between regional forcing and local weather, downscaling of precipitation at site level is more challenging than downscaling of maximum and minimum temperature.

The screened potential predictors for Gilgel Abay catchment are shown the following table.

Table 6. 2 Potential predictor for Gilgel Abay

Predictand	Predictor	Symbol
Minimum Temperature	Mean temperature at 2m	nceptemp
	Surface specific humidity	ncepshum
	Surface meridional velocity	ncepp_v
	500 hpa geopotential height	ncepp500
Maximum Temperature	Surface Zonal Velocity	ncepp_u
	Surface divergences	ncepp_zh
	Mean Temperature at 2m	nceptemp
Precipitation	Surface meridional velocity	ncepp_v
	Surface divergence	ncepp_zh
	Relative humidity at 500 hpa	ncepr500

6.4 SDSM Model Calibration, validation and Scenario generation

The model calibration operation takes a selected predictand along with a set of predictor variables, and computes the parameters of multiple regression equations via an optimization algorithm (either dual simplex of ordinary least squares). There are options in SDSM model structure to perform calibration process either monthly, seasonally or annual time scale. Selecting one of these model type decide how the regression parameters are developed (for example if a model type monthly is selected, then the model develops one regression equation for the whole months and if annul model type is selected again one regression equation is develop for the whole one year and so on). For this particular study among the total period length of 1961-1990, 20 years of daily data is used for model calibration and the rest 10 years daily data is used for model validation using a monthly model type.

The Weather Generator operation generates ensembles (up to a maximum of 100) of synthetic daily weather series given observed (or NCEP re–analysis) atmospheric predictor variables. The procedure enables the verification of calibrated models (using independent data) and the synthesis of artificial time series for present climate conditions.

The Scenario Generator operation produces ensembles of synthetic daily weather series from the starting of the baseline period to the end of the next century (1961-2100) for a given daily atmospheric predictor variables supplied by a GCM (either under present or future greenhouse gas forcing). This function is identical to that of the Weather Generator operation in all respects except that it may be necessary to specify a different convention for model dates and source directory for predictor variables.

6.5 HBV-model and Model Inputs

The conceptual semi-distributed HBV model computes runoff from observed daily rainfall, daily temperature, long-term monthly potential evapo-transpiration and runoff data for calibration.

6.5.1. Areal rainfall

The Thiessen polygon method which is one way of calculating areal precipitation is used for this study. This method gives weight to station data in proportion to the space between the stations (IHMS, 2006). The daily areal rainfall is calculated from the daily point measurement of rainfall in and around the catchments by Thiessen polygon method.

$$\overline{p} = \frac{1}{A}\sum_{s=1}^{s=n}(A_s * P_s) \quad \text{.....6.1}$$

Where, $\overline{P}$: Areal average rainfall, P_s: Rainfall measured at sub-region, A_s: Area of sub-region and A: total area of sub regions.

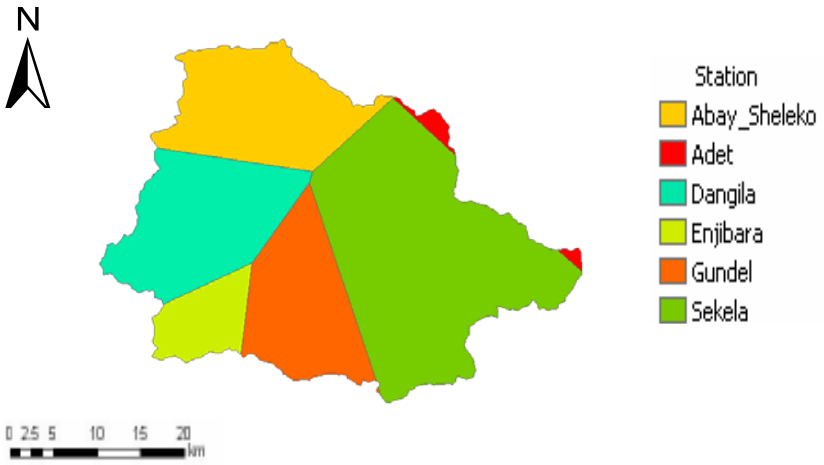

Figure 6. 2 Thiessen polygon for Gilgel Abay Catchment

6.5.2 Catchment data

Due to its semi-distributed nature, HBV model needs sub-division of the basin in to different elevation. Each elevation zone is also divided in to different vegetation cover (forested and non-forested areas, IHMS, 2006). The Gilgel Abay cathment also processed and divided in to different elevations and vegetation zone using DEM hydro-processing from Shuttle Radar Topography Mission (SRTM) with a resolution of 90 m X 90 m and from the land cover data of the study area.

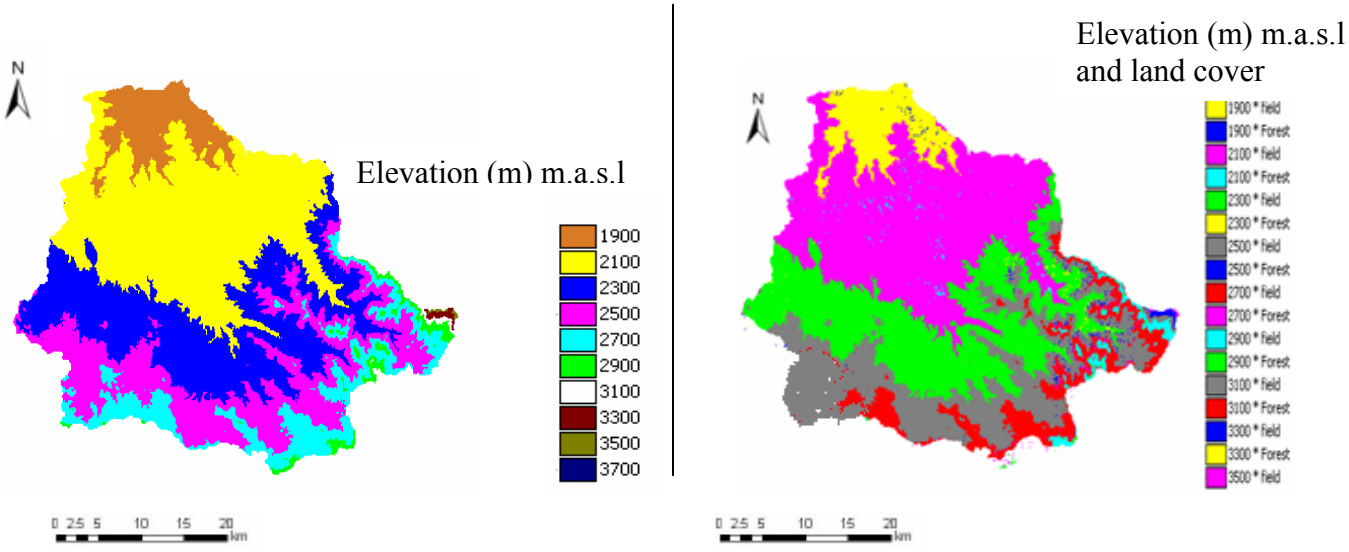

Figure 6. 3 (a) Gilgle Abay catchment sliced at different elevation zone
(b) Gilgel Abay catchment vegetation covers for the different elevation zones.

6.5.3 Potential evapo-transpiration for model calibration and validation

Long-term mean values are used as estimates of potential of evapo-transpiration at a certain time of the year. It is thus assumed that the inter-annual variation in actual evapo-transpiration is much more dependent on the soil moisture conditions than on the inter-annual variation in potential evaporation (IHMS, 2006). For this specific study Penman-Monteith method is adopted to calculate the daily potential evaporation during model calibration and validation. The average potential evapo-transpiration from Bhair-dar and Dangila station is used for model input.

$$ET_0 = \frac{0.408\Delta(R_n - G) + \gamma \frac{900}{T+273} U_2 (e_s - e_a)}{\Delta + \gamma(1 + 0.34U_2)} \quad \text{.....6.2}$$

Where,

ET_o	Reference evapo-transpiration [mm day-1],
R_n	Net radiation at the crop surface [MJ m-2 day-1],
G	Soil heat flux density [MJ m-2 day-1],
T	Mean daily air temperature at 2 m height [°C],
U_2	Wind speed at 2 m height [m s-1],
e_s	Saturation vapour pressure [kPa],
e_a	Actual vapour pressure [kPa],
e_s-e_a	Saturation vapour pressure deficit [kPa],
Δ	Slope vapour pressure curve [kPa °C-1],
γ	Psychrometric constant [kPa °C-1].

In equation 6.2 the value 0.408 converts the net radiation Rn expressed in MJ/m^2.day to equivalent evaporation expressed in mm/day.

Table 6. 3 Long term average monthly potential evapo-transpiration from Bhair-dar and Dangila stations (1996- 2005)

Months	Jan	Feb	Mar	Apr	May	Jun	Jul	Aug	Sep	Oct	Nov	Dec
ETo (mm/month)	106.3	111.7	126.2	133.2	124	97.8	87.1	97.1	103.5	105.7	101.7	95.5

6.5.4 Potential evapo-transpiration for future runoff generation

The potential evapo -transpiration will have different value for the three time horizons (i.e. 2020s, 2050s and 2080s) compared to the present potential evaporation that is calculated using equation 6.2. And since the existing data are the downscaled precipitation and minimum and maximum temperature, the potential evapo-transpiration for future time horizon is calculated by using Hargreaves method (see. equation 6.3). To be compatible with the method adopted during model calibration and validation, a regression equation is developed to estimate the Penman potential evaporation from Hargreves potential evapo-transpiration table (6.4)

$$PET_{HG} = 0.023 * Ra * (T_{maen} + 17.8) * \sqrt{(T_{\max} - T_{\min})} \quad \text{.....6.3}$$

Where,

PET_{HG} Hargreves potential evapo-transpiration;

Ra Extraterrestrial radiation (calculated from latitude and time of year);

T_{mean} Mean temperature;

$T_{\min}$ Minimum temperature; and

$T_{\max}$ Maximum temperature

Table 6. 4 Monthly Conversion equations from PET (Hargreves) to PET (Penman Monteith)

Equation	r^2
$ET_{0\_pen} = 0.827 * ET_{o\_HG} - 0.086$	**0.95**

Table 6. 5 Projected PET at different time horizon in mm/month for HadCM3 A2a

Month	Jan	Feb	Mar	Apr	May	Jun	Jul	Aug	Sep	Oct	Nov	Dec
2020s	107.9	117.4	120.3	118.8	134.1	109.1	110.2	106.9	98.0	88.2	102.8	106.9
2050s	109.7	104.3	107.9	96.8	100.8	108.2	119.1	132.1	135.4	129.5	119.4	114.7
2080s	100.7	100.9	105.4	129.5	138.6	131.6	129.2	121.1	114.8	98.6	85.3	79.7

Table 6. 6 Projected PET at different time horizon in mm/month for HadCM3 B2a

Month	Jan	Feb	Mar	Apr	May	Jun	Jul	Aug	Sep	Oct	Nov	Dec
2020s	112.2	118.2	136.4	132.6	143.1	125.0	121.0	112.0	91.6	90.1	94.0	99.3
2050s	111.4	102.9	105.4	99.2	98.8	106.8	123.0	133.3	134.5	132.1	119.7	111.5
2080s	97.8	108.6	126.4	140.1	141.6	134.6	133.0	126.4	118.1	95.4	81.8	77.1

6.6 Reservoir data analysis

The monthly flow at the Gilgel Abay dam site is calculated by using the area ratio method. The delineated dam site area using Arc GIS software, from the 90 x 90 digital elevation model reveals that the area covers 2,044 km^2 and that of the area upstream of the Gilgel Abay gauging station covers 1655 km^2, hence by assuming the two areas have similar cachment characteristics and climatic condition, the dam site inflow is found by multiplying runoff at the gauging station by their area ratio of 1.235.

The Gilgle Abay reservoir is proposed to irrigate 13,500Ha, and to meet relatively small amount for domestic purpose. The reservoir also expected to release certain amount to the downstream for environmental and ecosystem (riparian) safety. The following table describes the monthly water demand and riparian release that the Gilegel Abay reservoir expected to meet.

Table 6. 7 *Monthly Water Demands and the Riparian Water Releases (source:-Feasibility study of Lake Tana Sub-Basin Dam Project, 2009].*

Water Demand	Jan	Feb	Mar	Apr	May	Jun	Jul	Aug	Sep	Oct	Nov	Dec
Domestic (MCM)	2.34	2.34	2.66	2.66	2.66	2.34	2.34	2.34	2.34	2.34	2.34	2.34
Irrigation (mm/ha)	235	246	219	33	33	82	27	12	12	13	47	170
Riparian (MCM)	14.7	9.1	8.1	7.0	16.6	36.3	247.0	382.3	258.4	62.7	20.6	10.8

6.6.1 The Gilgel Abay inflow series as affected by the Koga and Jemma reservoirs

The two proposed upstream reservoirs (Koga and Jemma) constitute about 29% of the whole Gilgel Abay catchment. When the two dam projects are implemented, the monthly flows at the dam site will be affected. Therefore the monthly flow at the dam site is corrected based up on the following assumptions [Feasibility study of Lake Tana Sub-Basin Dam Project, 2009].

- The stream flows entering the Jemma and Koga reservoirs do not reach the Gilgel Abay reservoir.
- Spills from the two upstream reservoirs were not considered as inflows of Gilgel Abay reservoir because future irrigation plans will reduce the spill volumes as a minimum.
- The riparian releases from Jemma and Koga reservoirs were included in Gilgel Abay reservoir inflows.

Table 6. 8 the monthly average riparian release from Jemma and Koga reservoirs in MCM

	Jan	Feb.	Mar	Apr	May	Jun	Jul	Aug	Sep	Oct	Nov	Dec
Jemma	2.10	2.00	2.30	2.10	1.80	1.00	3.10	13.90	18.90	11.50	2.90	1.90
Koga	1.60	1.50	1.80	1.60	1.30	0.70	2.30	10.50	14.30	8.70	2.20	1.40

The effect of Jemma and Koga reservoirs will be significant only during the dry period of November-May when the demand will exceed the expected supply. However, during July-October wet season the inflow will be much greater than the demand.

The flow at Gilgel Abay gauging station is adjusted in such a way that the riparian release from Koga and Jemma are included only on the Gilgel Abay future runoff (i.e. 2020s, 2050s and 2080s). But the current flow appears to include the full inflow of Koga and Jemma.

6.6.3 Reservoir Operation

The investigation of statistical properties of reliability, resilience and vulnerability (RRV) are based on the time series of monthly runoff or inflow to the reservoir. The times serious of Gilgel Abay monthly inflow are routed through the reservoir with the specified 360 Mm^3 storage (S_t) and the threshold demand (D_t) using (equation 6.4). The Gilgel Abay reservoir operates according to the standard operating policy i.e. the draft or target demand is fully supplied whenever sufficient water exists; otherwise all the available water is put into supply and the reservoir is left empty (source-Feasibility study of lake tan sub-basin dam project). The Gilgel Abay reservoir operation policy is also defined by (figure 6.4)

$$\begin{aligned} &S(t+1) = S(t) + Q(t) - D(t) \\ &S(t+1) < 0 \Rightarrow S(t+1) = 0 \\ &S(t+1) > S_{\max} \Rightarrow S(t+1) = S_{\max} \end{aligned} \qquad \text{…… ……..……6.4}$$

Where $S(t)$ is the reservoir storage at the beginning of the time step t, $S(t) = 0$ for the analysis start with empty level and $S(t) = S_{\max}$ for analysis start with full supply level, $Q(t)$ is inflow to

the reservoir in time step t, $D(t)$ is the target demand from the reservoir in time step t and S_{max} is the reservoir storage capacity i.e. 360Mm^3. The reservoir-area-volume relationships that used during reservoir operation on different time horizon is shown in (figure 6.4)

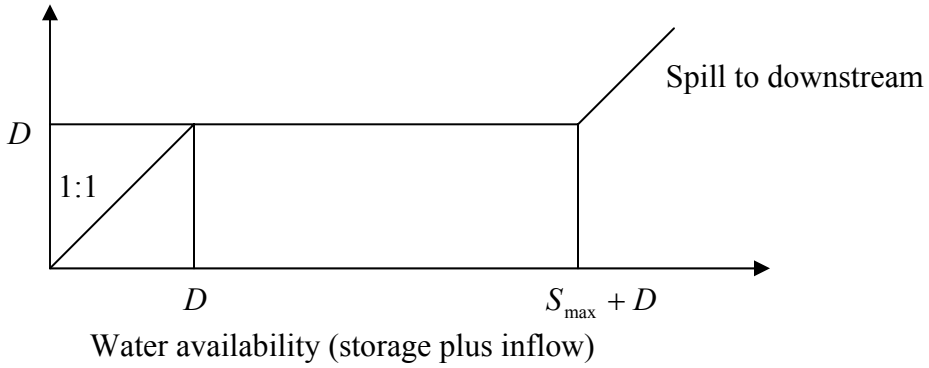

Figure 6. 4 Standard operation policy for Gilgel Abay reservoir

6.6.4 Evaporation and Seepage from reservoir

Because lake evaporation cannot be measured directly, it should be determined indirectly by one or more of several methods, such as water balance, energy balance, Penman–Monteith's formula, pan evaporation technique and so on.

For the present study, the Penman–Monteith method was selected to determine the monthly evaporation rates.

Open water evaporation was calculated by using the FAO CROPWAT Version 4.3 program which uses the Penman-Monteith method and then applies an aridity correction factor. The CROPWAT program was developed to estimate potential evapotranspiration (PET) or ETo which is also defined as reference evapotranspiration (FAO, 1998). According to FAO Irrigation and Drainage Paper 56, page 114, the conversion of ETo to evaporation of open water, with depth higher than 5 m, clear of turbidity, in temperate climate, would be varied between 0.65 and

1.25. The lower values "correspond to the period when the water body is gaining thermal energy", and the higher to the period "during the fall and the winter when heat is released from the water body". For Ethiopia, the aridity correction factor was estimated to be 1.2(source-Feasibility study of lake tan sub-basin dam project).

Since, Bahir-Dar and Dangila are closest to the dam site area; they were selected to represent the Gilgel Abay reservoir evaporation rates. The open water evaporation for future time period is found by multiplying the evapo-transpiration found in table 6.5 and table 6.6 by aridity correction factor of 1.2. The monthly seepage from the Gilgel Abay reservoir was estimated as 25% of monthly evaporation.

Table 6. 9 Current (1996-2005) mean monthly evaporation and rainfall (mm) for Gilgle Abay reservoir

Parameter	Jan	Feb	Mar	Apr	May	Jun	Jul	Aug	Sep	Oct	Nov	Dec
Evaporation	127.5	134.0	151.4	159.8	148.8	117.3	104.5	117.2	124.2	126.8	122.0	114.6
Rainfall	5.6	5.8	26.4	47.3	151	292	411.1	418.7	296.5	138	45.3	13.3

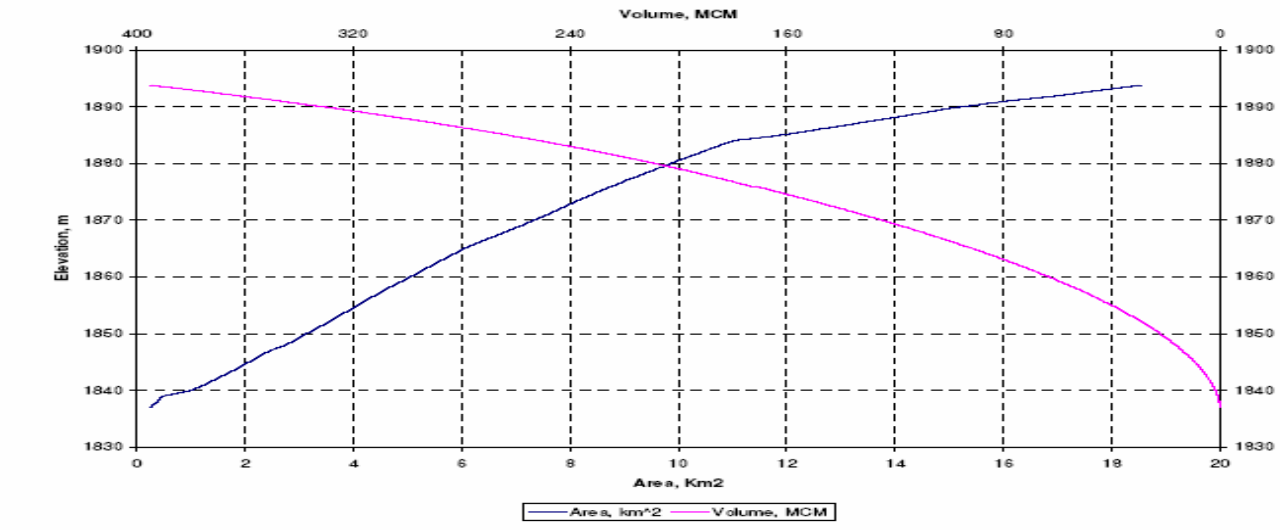

Figure 6. 5 Gilgel Abay Reservoir elevation-area-volume relationship

6.7 HBV-Model Calibration

The process of model caliberation is done either manually or by computer-based automatic procedures. In manually calibration, a trial and error parameter adjustment is made. The goodness-of-fit of calibrated model is basically based on good water balance and a good over all agreement of the shape of the hydrograph by comparing the simulated and observed hydrographs. For an experienced hydrologist it is possible to obtain a very good and hydrologically sound model using manual calibration (Wale A. 2008).In automatic calibration, parameters adjusted automatically according to a specified search scheme and numerical measures of the goodness-of-fit. As compared to manual calibration, automatic calibration is fast, and the confidence of the model simulation can be explicitly stated.

IHMS HBV model parameters can be grouped into volume controlling (FC, LP and Beta) that influence the total volume and shape controlling parameters (K_4, Perc, KHQ, HQ and Alfa) that distribute the calculated discharge in time and inflaming the shape of hydrograph. The parameter maxbas which control the smoothness of the hydrograph also calibrated for this study. HQ is the high flow level at which the recession rate KHQ is assumed to hold, normally the parameter HQ is not calibrated, it is calculated from the mean of observed discharge over the whole period and the mean of annual peak flows**.**

$$HQ = \frac{\sqrt{(MQ * MHQ)}}{A} * 86.4 \qquad \text{(mm/day)} \qquad \text{.....} 6.5$$

Where: MQ: the mean of observed discharge over the whole period, MHQ: is the mean of annual peak flow and A: area of catchment in Km^2.

For this specific study HQ is calculated and is found with a value of 7**.**52 mm/day.

The quick flow is calibrated by KHQ and Alfa. KHQ result in higher peaks and more dynamic response in hydrograph. Alfa is used in order to fit the higher peaks in to the hydrograph, the

higher the Alfa the higher the peaks and the quicker the recession (IHMS, 2006). Base flow is adjusted with PERC and K_4.the level of the base flow is adjusted with PERC as a lower value of PERC result in low base flow. K_4 describes the recession of base flow. The following table shows recommended start values and range of parameters for new basin/ sub-basin to be calibrated.

Table 6 .10 Model parameters and their range values (IHMS, 2006)

Parameters	Starting Values	Approximate Interval	Comment
FC	Use a value for the region	100 – 1500	Maximum soil moisture storage [mm]
Lp	1	<=1	Limit for potential evaporation
Beta	1	1 - 4	Exponent in the equation for discharge from the zone of soil water
K_4	0.01	0.001 – 0.1	Recession coefficient for lower response box
PERC	0.5	0.01 - 6	Percolation from upper to the lower response box [mm]
KHQ	0.09	0.005 – 0.2	Recession coefficient for upper response box
Alfa	0.9	0.5 – 1.1	Measure of non-linearity to the response of upper reservoir

For this study a 10 year daily data from 1996-2005 is used for model calibration and validation. Before starting the calibration, 1 year of daily data is used as warming period and then six year daily data is used for model calibration and the rest is used for model validation. The model calibration is done manually by trial and error method. The approach of calibration have two steps, first the model will be calibrated by volume controlling parameters FC, LP and Beta, that is followed by calibration of shape governing parameters KHQ and Alfa for the quick flow and K_4 and PERC for the base flow.

6.8 Hypothetical Scenario

Hypothetical scenario is applied by increasing and decreasing the precipitation in plausible amount and increasing the temperature from the baseline temperature, for the purpose of examining the reservoir performance for different climatic scenario. The following table shows the incremental scenario adopted by this study for sensitivity analysis of the reservoir.

Table 6. 11 Adopted incremental scenario

Scenarios	S1	S2	S3	S4	S5	S6	S7	S8	S9	S10
Temp. (oC)	+2	+2	+2	+2	+2	+4	+4	+4	+4	+4
Pcp. %	-20%	-10%	0	+10%	+20%	-20%	-10%	0	+10%	+20%

7. Result and discussion

7.1 Climate Projection

7.1.1 Correlation of predictor with predictand

As discussed in the previous section downscaling is carried out for precipitation, maximum and minimum temperature. The selected predictors (see table 6.2) show a good correlation with their respective predictand in all months. Precipitation shows stronger correlation with nceppr500 and ncepp_zh from the month of April to October and necpp_v also exhibits a better correlation for the month January and December. The maximum temperature shows remarkably very good correlations for all months with the selected predictors. It shows high correlation with nceptem for the month January, February, March, June and July. The correlations of observed minimum temperature with the selected predictor result in great correlation with ncepp500 for all months except for the month November.

7.1.2 Calibration and Validation

Calibration of SDSM model is carried out for 20 year of daily data, i.e. for a period of 1961-1980, and the validation takes the rest of 10 year daily data i.e. from the 1981-1990. The maximum and minimum temperature reveals very good regression equations than precipitation this is because of the conditional nature of precipitation table 7.1 shows R^2 value for the observed and downscaled climate variables. One of the other criteria to measure the capability of the predictor, its ability to replicate the historical (observed) data for the baseline period (1961-1990).

Lower R^2 value for precipitation is exhibited because of its complex nature and high special variability. Consequently, its difficulty to capture this variable by the course resolution GCMs .

Table 7. 1 R^2 value between downscaled and observed data for baseline period

	R^2		
	Maximum Temperature	Minimum Temperature	Precipitation
Calibration	0.62	0.55	0.38
Validation	0.60	0.53	0.31

7.1.3 Maximum Temperature

The downscaled monthly average maximum temperature reveals good quality relations with the observed temperature for the baseline period of both in A2a and B2a emission scenarios.

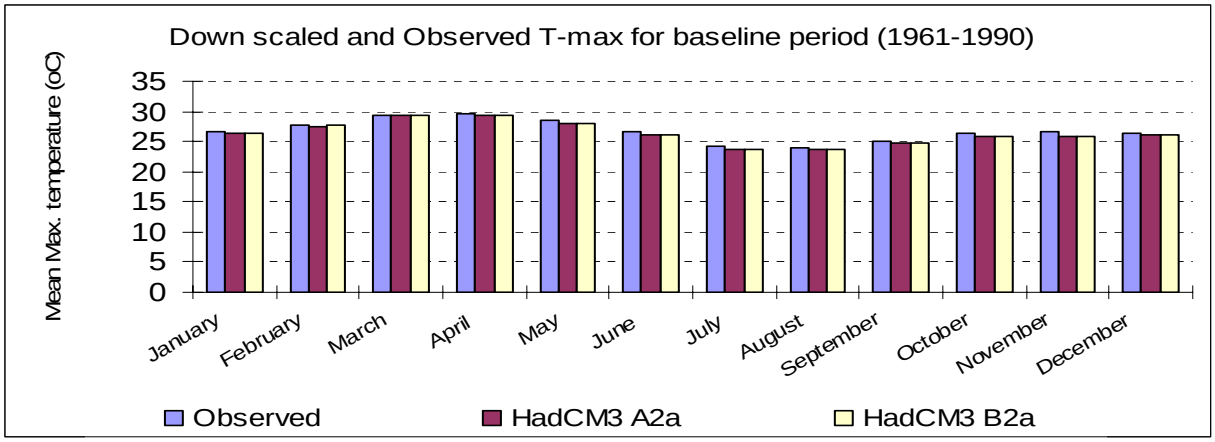

Figure 7. 1 Downscaled and Observed mean monthly maximum temperature (1961-1990)

The monthly absolute model error of the downscaled maximum temperature for the baseline period shows almost similar result for both A2a and B2a emission scenarios. Though the magnitude is small, the model underestimates the maximum temperature for both A2a and B2a emission scenario. The maximum and minimum monthly absolute model error is found on the month of November and March respectively. On average the monthly absolute model error for both the A2a and B2a emission scenario is found to be - 0.37^{o}C.

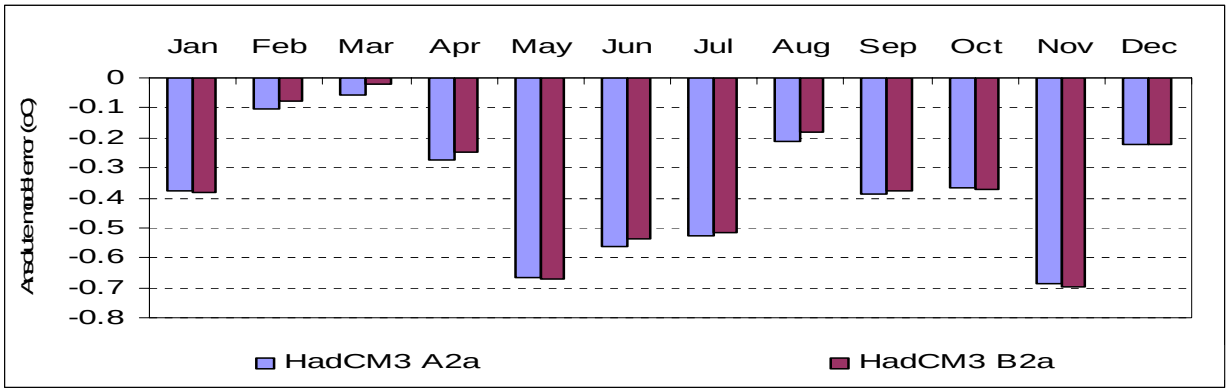

Figure 7. 2 Absolute model error for each month of downscaled maximum temperature (1961-1990)

7.1.4 Minimum temperature

Like that of the maximum temperature the downscaled minimum temperature also shows a reasonably good agreement with the observed minimum temperature for all months both under A2a and B2a emission scenarios.

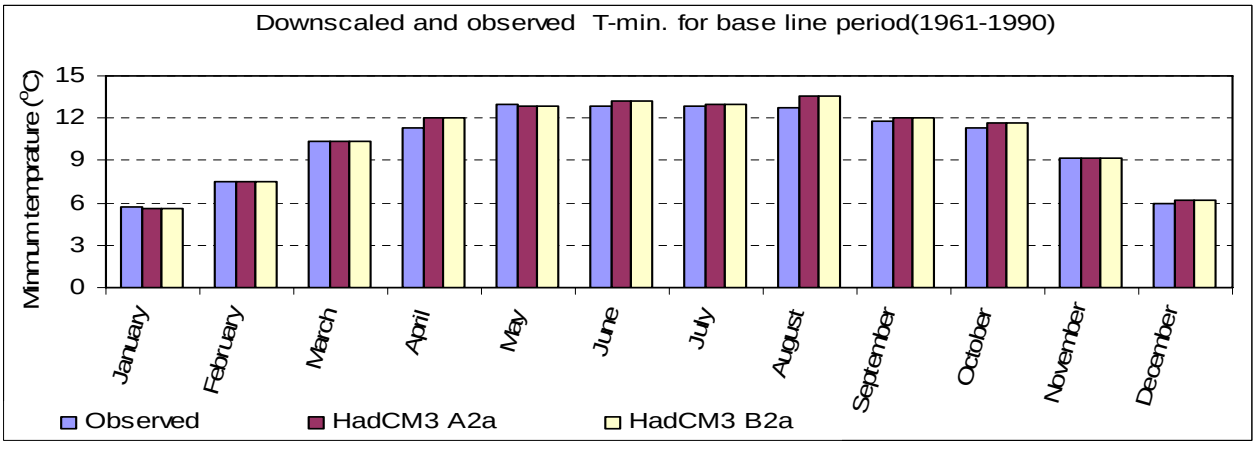

Figure 7. 3 Downscaled and observed mean monthly minimum temperature (1961-1990)

Unlike of the maximum temperature, the absolute model error of the downscaled minimum temperature does not show underestimating of the observed value for the whole baseline period.

On contrary it was identified that the model overestimates the minimum temperature by small amount for most of the months, relative to the actually observed value. It was also found that, during the month of February and November the model error is negligible and on average, the absolute model error is found to be 0.21^{o}C in both scenarios.

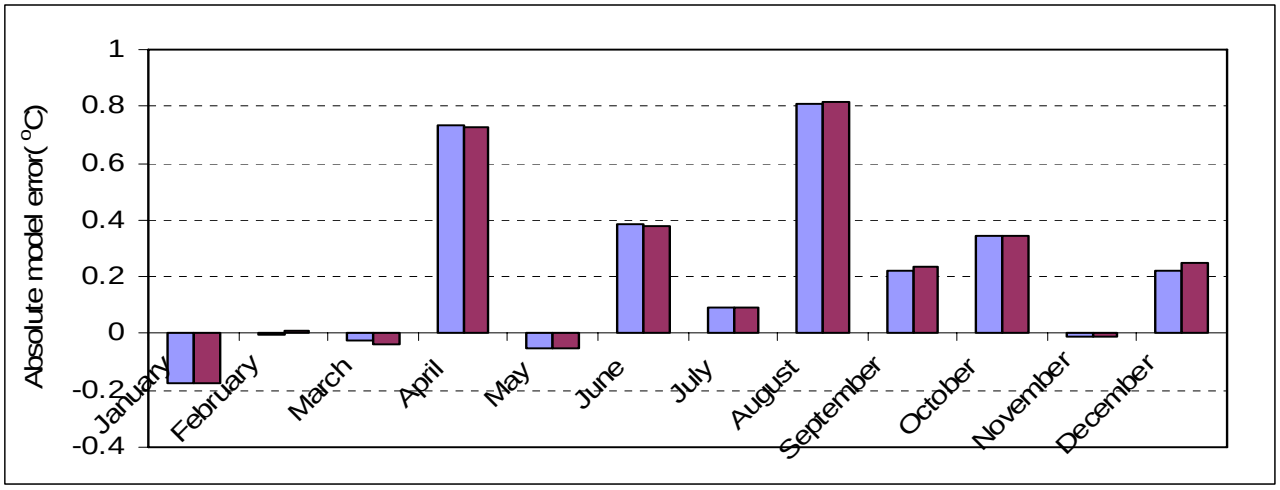

Figure 7. 4 Absolute model error for minimum temperature (1961-1990)

7.1.5 Precipitation

Relative to the minimum and maximum temperature the precipitation could not able to replicate the historical (observed) data. This is due to complicated nature of precipitation processes and its distribution in space and time. Climate model simulation of precipitation has improved over time but is still a problematic (Bates et al., 2008). Thorpe (2005) also added that rainfall predictions have a larger degree of uncertainty than those for temperature. This is because rainfall is highly variable in space and so the relatively coarse spatial resolution of the current generation of climate models is not adequate to fully capture that variability.

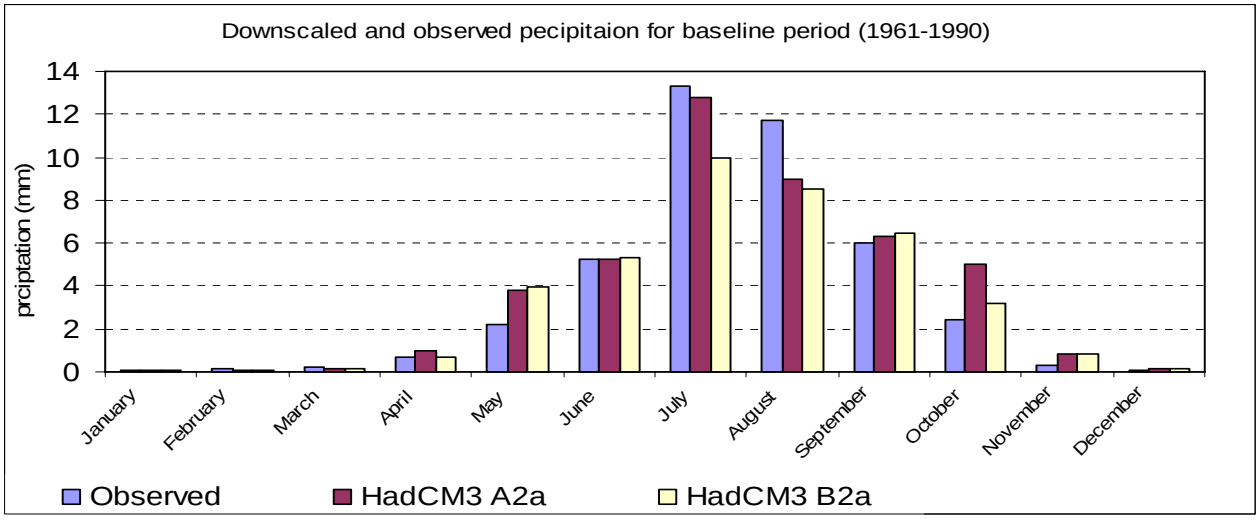

Figure 7. 5 Downscaled and observed mean monthly precipitation (1961-1990)

The downscaled precipitation shows an average absolute model error of 0.17 mm and 0.24 mm for A2a and B2a emission scenarios respectively.

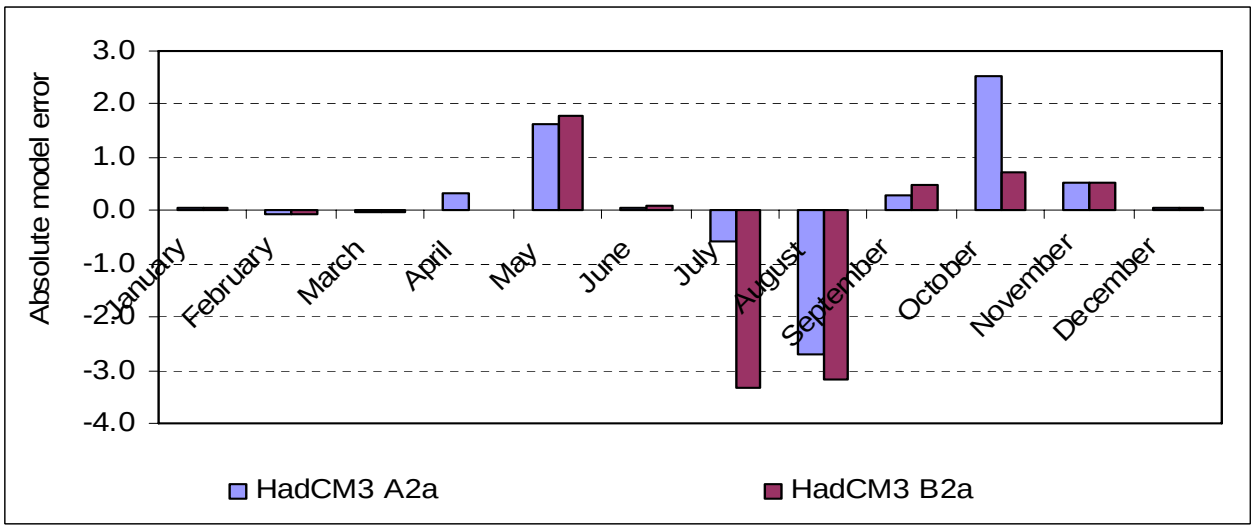

Figure 7. 6 Absolute model error for the downscaled precipitation (1961-1990)

7.1.6 Projected future climate variables (Scenario generation)

After the calibration and validation of SDSM model carried out, the daily future climate variables are projected for the next century using the HadCM3 Global Circulation Model. The projection generates 20 ensembles of daily climate variables, which are equally plausible hence; these ensembles are averaged out in order to consider the characteristics of all those 20 ensembles.

7.1.6.1 Maximum temperature

The projected maximum temperature shows an increase trend for all time horizons (figure 7.7). Comparatively, A2a which is the high emission scenario prevail higher change in maximum temperature trend at the end of the next century than the B2a (low emission) scenario. And relatively, a larger absolute monthly difference from the baseline temperature is found at the month of June; both emission scenario. As shown in figure 7.8 the change is observed for all the three time horizons (2020s, 2050s and 2080s).

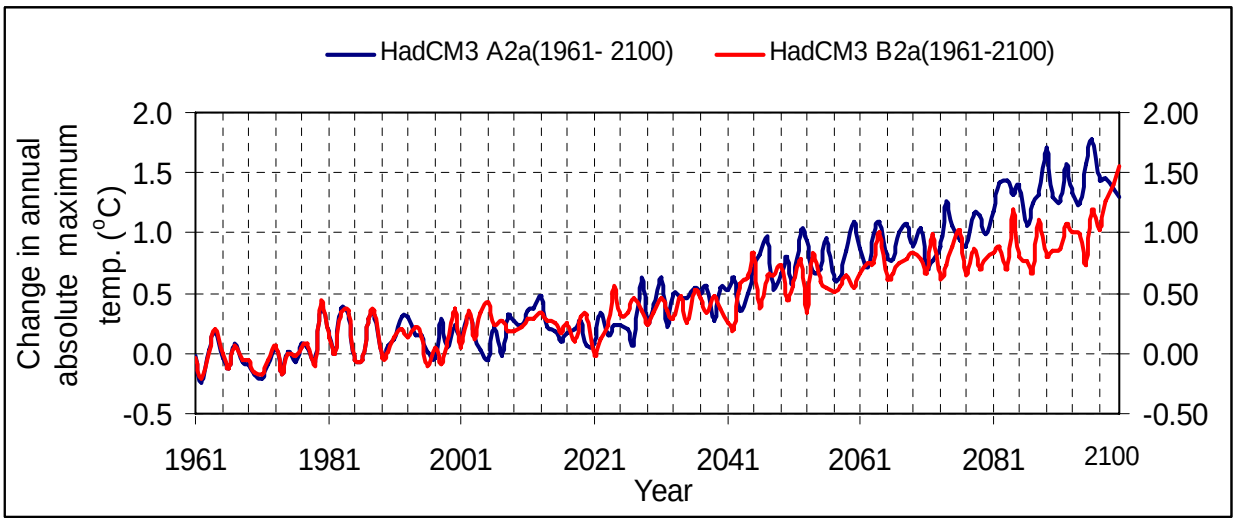

Figure 7. 7 Trend of absolute maximum temperature change for next century (1961-2100)

The mean annual changes also confirm the average increasing trend of maximum temperature.

Table 7. 2 Absolute change in mean annual maximum temperature in ^{o}C at different time horizons

Scenario	2020s	2050s	2080s
HadCM3 A2a	+ 0.341	+0.839	+1.407
HadCM3 B2a	+0.356	+0.670	+1.002

The following figure describes the mean monthly absolute change in maximum temperature

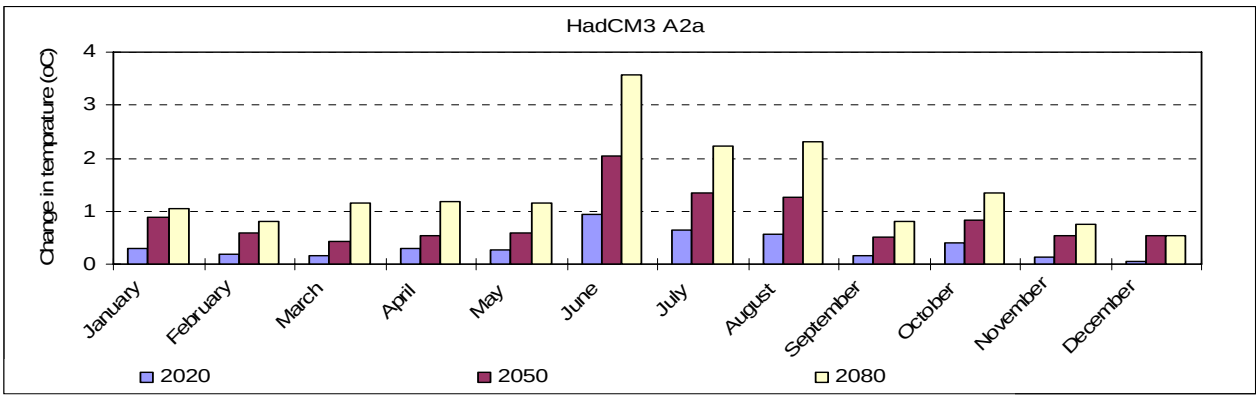

(a)

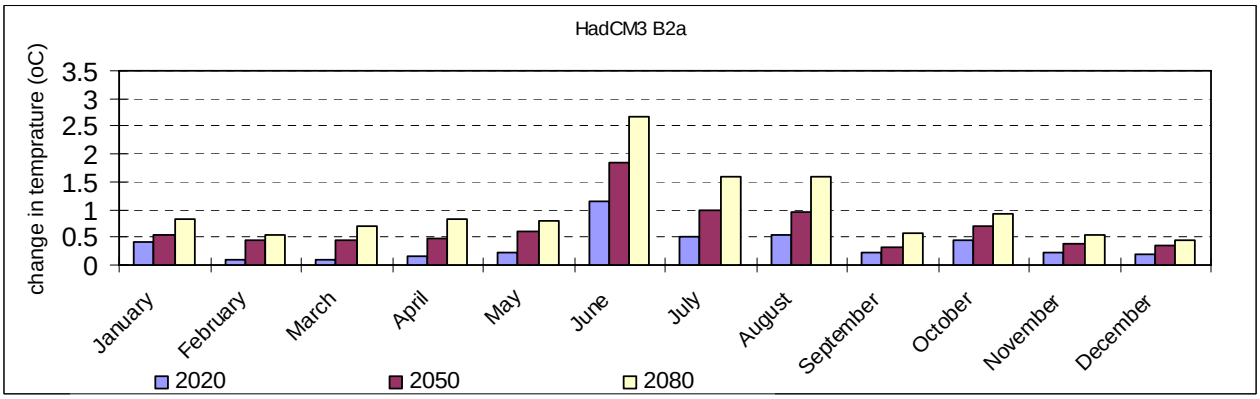

(b)

Figure 7. 8 Mean monthly absolute change in Maximum temperature (a) for A2a and (b) for B2a scenarios

7.1.6.2 Minimum Temperature

The generated minimum temperature shows an increasing trend in the next century. In this case both the A2a and B2a emission scenario generate the future minimum temperature in similar manner.

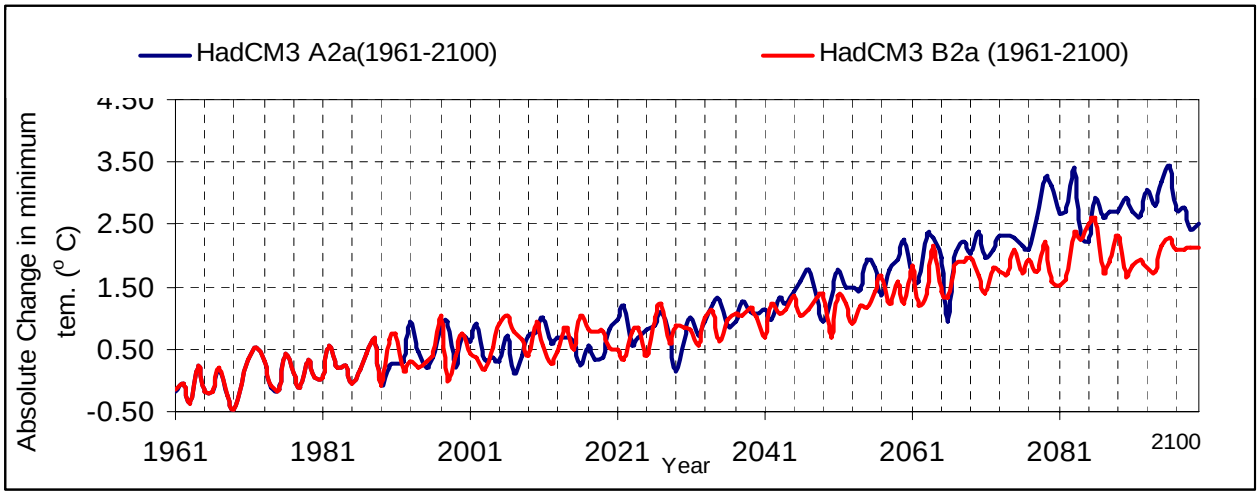

Figure 7. 9 trend of minimum temperature in the next century

As explained in the previous section the temperature trend for the historical period shows a higher rate increase for minimum temperature than maximum temperature. As per the downscaled result this behavior will expected continue in the next century.

Table 7. 3 Mean annual absolute change in minimum temperature

Scenario	2020s	2050s	2080s
HadCM3 A2a	+0.714	+1.468	+2.549
HadCM3 B2a	+0.687	+1.174	+1.819

Generally, the observed changes in temperature are with in the limits of the latest projection of IPCC (2007), i.e. the global temperatures will expected to rise by 0.6 – 1.4^{o}C.

7.1.6.3 Precipitation

Unlike the maximum and minimum temperature the projected precipitation does not show an increase trend. The precipitation experiences a mean annul increase amount by 0.82%, 0.85% and 1.6% for A2a scenario at 2020s, 2050s and 2080 respectively. But, the precipitation exhibits a mean annual decrease in amount by 0.5% and 1.0% for B2a scenario at 2020s and 2050s and increase by 0.54% in 2080s. Generally, for both A2a and B2a scenario the precipitation shows an increasing trend for the months January to April and for October to November, and a decreasing trend from May-September.

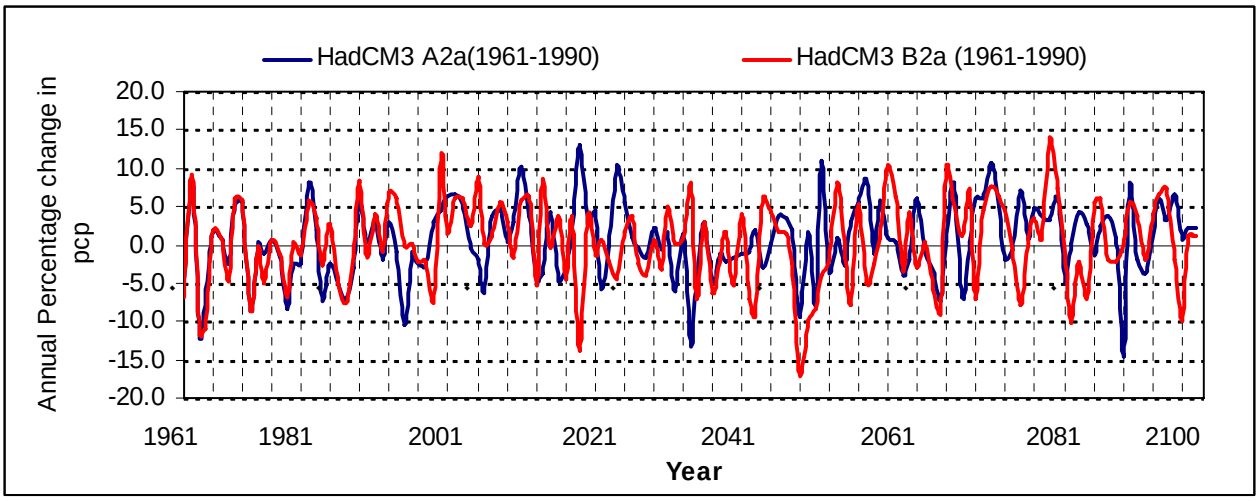

Figure 7. 10 the downscaled trend of precipitation for the next century

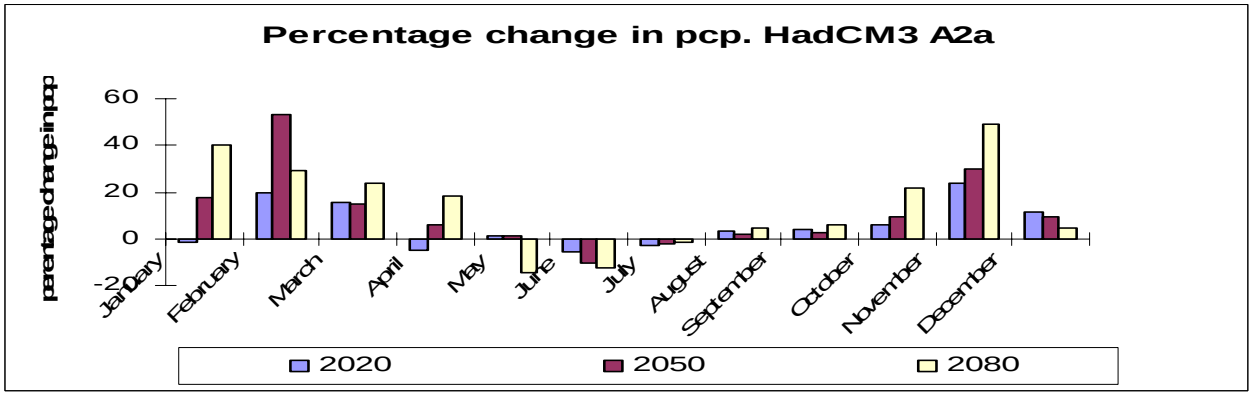

Figure 7. 11 Percentage change in mean monthly precipitation at different time horizon under A2a emission scenario

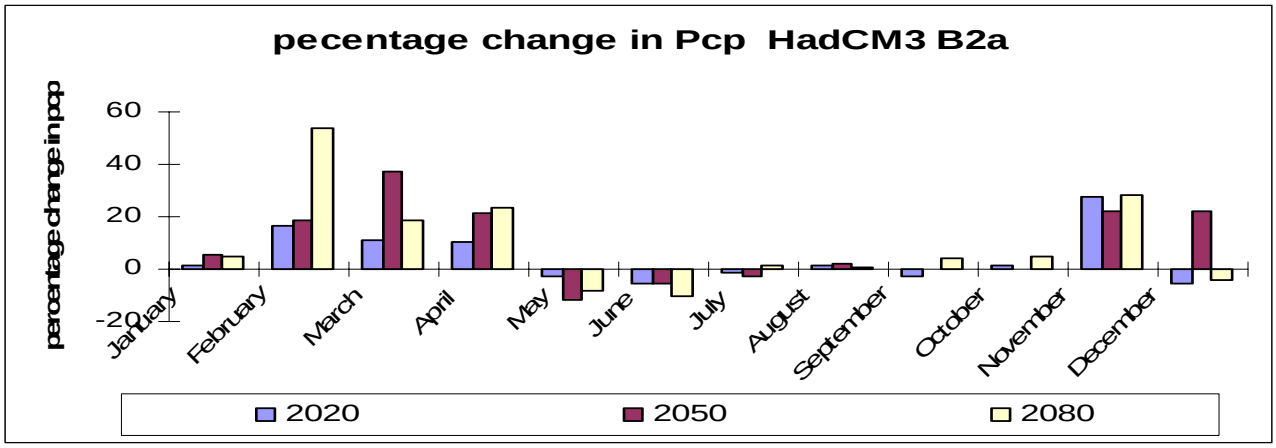

Figure 7. 12 Percentage change in mean monthly precipitation at different time horizon under B2a emission scenario

When comparing the historical climatic variables (see section 3.7) and generated future climate trends, it is generally observed that the future trends of maximum and minimum temperature follows the same increasing behaviors or trends as that of the previously observed condition and in the case of the precipitation, the future condition exhibits a fluctuating trend i.e. it does not reveals a systematic increase or decreasing trend while the historically observed trend show a decreasing trend in small rate around northern half of Ethiopia as it described in section 3.7, this is due to complicate nature of precipitation processes and its distribution in space and time.

7.1.6.4 Evaporation from the reservoir

As explained in section 6.4.3.1, the open water evaporation is calculated by multiplying the respective potential evaporation by the aridity correction factor of 1.2. The average annual open water evaporation shows increases in amount by 2.1% in 2020s; by 6% in 2050s and 22% increase is projected in 2080s under the A2a emission scenario. In the case B2a scenario the evaporation is expected to increase by 6.2 % in 2020s and by 6.4% in 2050s and 20% increase in change is expected by 2080s under B2a scenarios.

The rate of monthly open water evaporation is found to increase relatively at higher rate during the month May to September in 2020s and during the months of July-October in 2050s and during July-December for 2080s under A2a scenario.

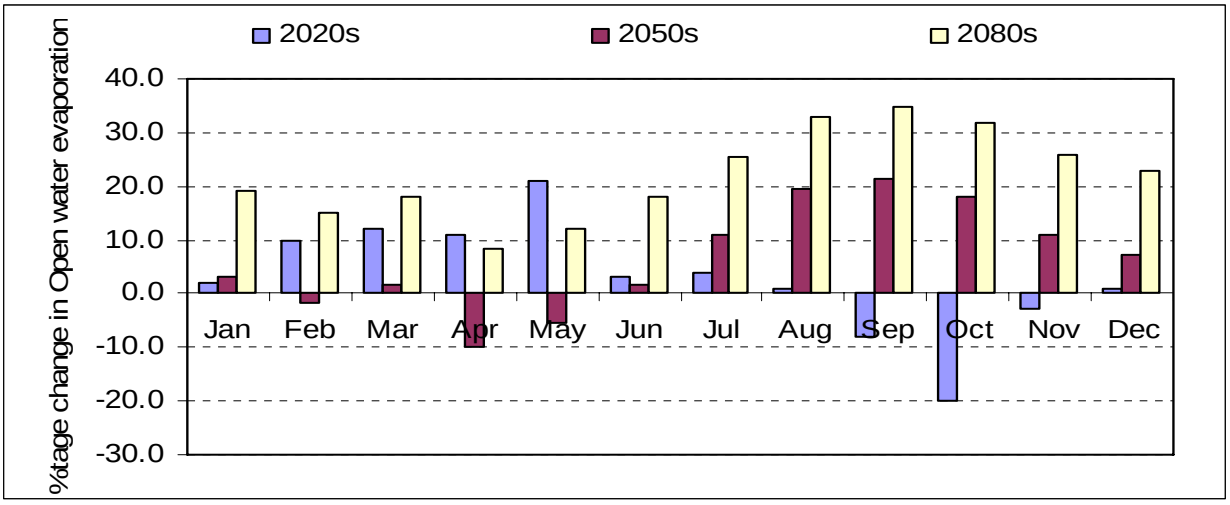

(a)

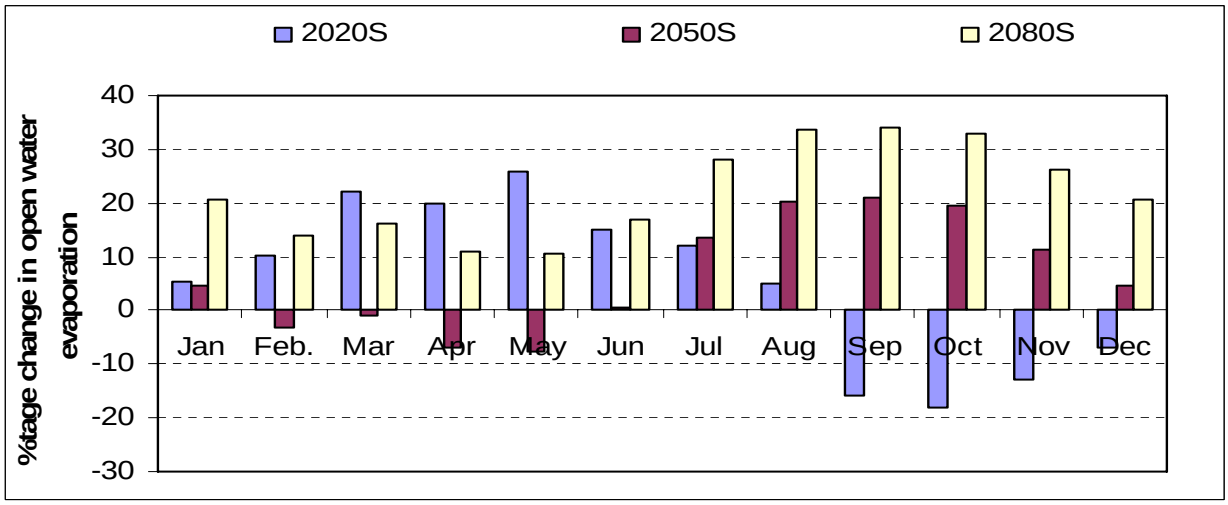

(b)

Figure 7. 13 Projected monthly percentage change in open water evaporation under (a) A2a emission (b) B2a emission scenario

7.2 Hydrologic Model

7.2.1 Calibration and validation

The HBV-model is calibrated and validate for the observed period of ten year (1996-2005) and the best-fit parameters sets are selected. Calibration aimed at the water balance and over all shape agreement of the observed discharge using RV_E (relative volume error) and R^2 (Nash and Sutcliffe coefficient). In simulation of the runoff the observed period is divided in to three zones, the first is for warm up the model (1996) and the second is to calibrate (1997-2002) and the last is calibration (2003-2005).The calibration and validation is carried out for both daily and monthly time steps. It is observed that the model has a very good capability to simulate the observed flow for both low flow and high flow period with $RV_E < 5\%$ and $R^2 > 0.8$ (see figure 7.14).

Table 7. 4 Calibrated model parameters for Gilgle Abay catchment with their recommended range of values

Parameters	α	β	FC	KHQ	K_4	Lp	Perc
Range	0.5 -1.1	1 - 4	100 -1500	0.005-0.2	0.001-0.1	<=1	0.01-6
Calibrated value	0.5	1	140.5	0.094	0.054	0.98	0.02

-Alfa (α) is a measure of non-linearity of the upper reservoir to transfer excess water from the soil zone as quick flow, it is used in equation $Q=K.UZ^{(1+alfa).}$

-Beta (β) is the exponent in the equation for discharge from the zone of soil water.

-FC is the maximum soil moisture storage capacity in the model [mm] which is related to soil properties.

-KHQ is the recession coefficient for the upper response box when the discharge is HQ.

-K4 is the recession coefficient for lower response box, describes the recession of the base flow.

-Perc describes the percolation from the upper to lower response box [mm/day].

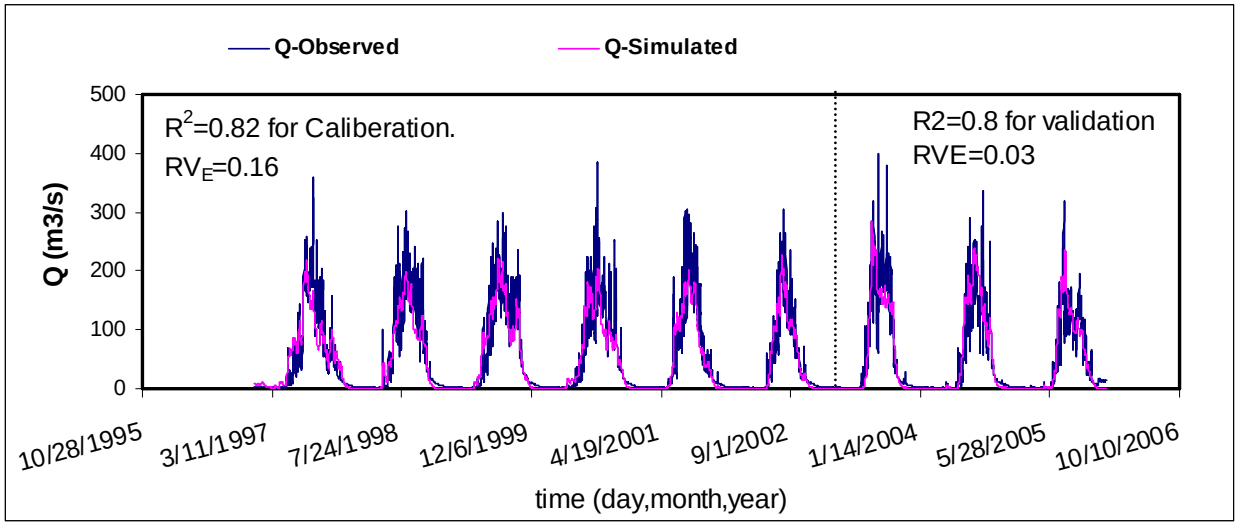

(a)

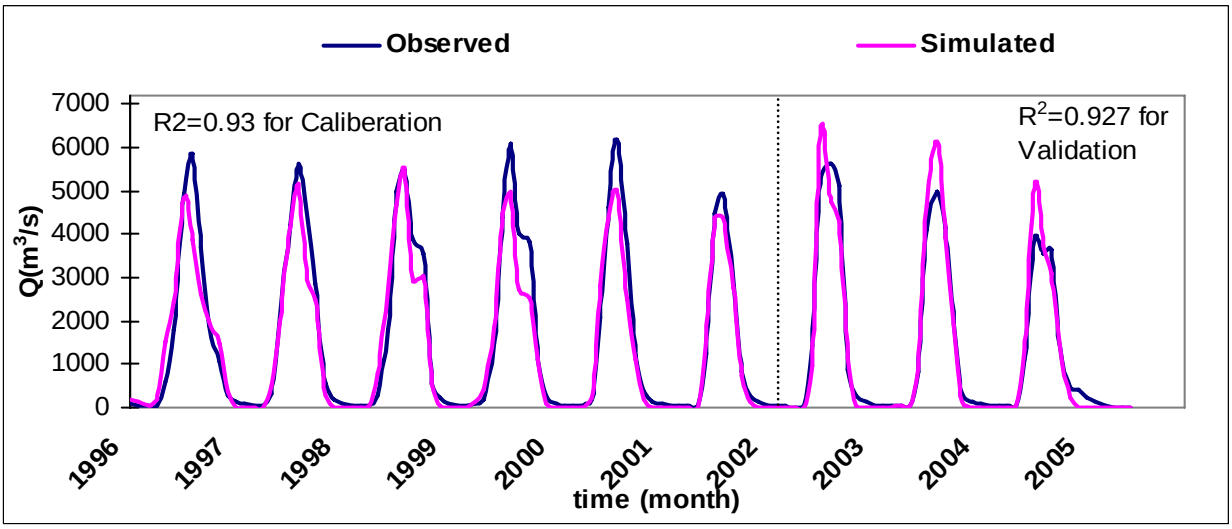

(b)

Figure 7. 14 Simulated and observed hydrograph for calibration and validation period (a) daily time scale (b) monthly time scale

7.3 Reservoir inflow volume

The inflow volume to the Gilgel Abay reservoir is generated in by using the downscaled climate variable as an input to the HBV-hydrological model. For comparison purpose the generated inflow is compared with the current (1996-2005) mean monthly flow.

Relative to the current condition, the simulated future inflow shows an average annual decrease in volume by 3.73% in 2020s under A2a scenario. And in 2050s it is expected that the average annual volume of inflow will increased by 9.14% where the average annual absolute change in temperature reveals an increase amount by 1.15 ^{o}C and the precipitation shows an increase in 0.851%, while in 2080s the projection reveals the inflow will decrease by 1.65% under A2a emission scenario.

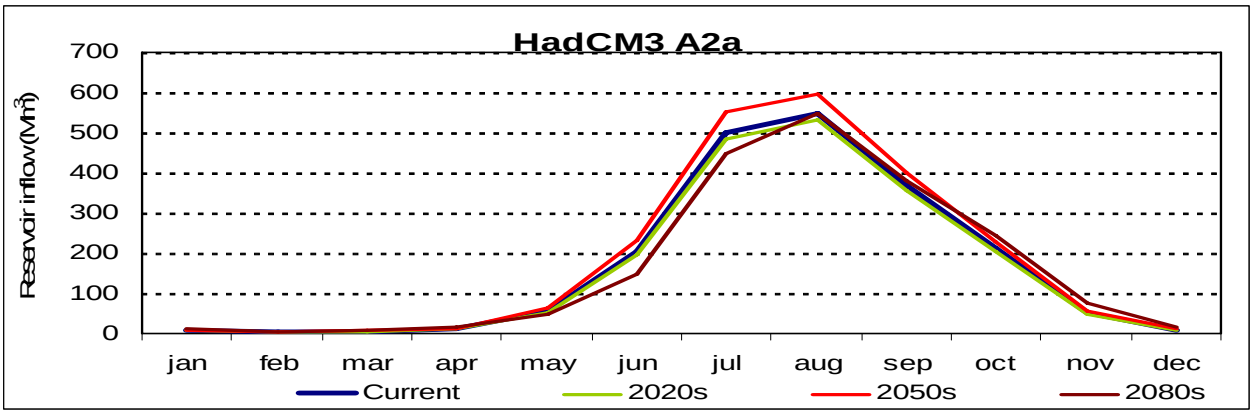

Figure 7. 15 Reservoir inflow (Mm^3) at different time horizons under A2a emission scenario.

In the case of B2a scenario, the inflow exhibits an average annual decreasing trend, for all the three time horizons. The inflow to Gilgel Abay reservoir projected to decrease by 2% in 2020s which exhibits an average annual absolute temperature increase by 0.520 ^{o}C and the precipitation decreased by 0.5% in the same time horizon, while in 2050s the inflow volume decreases by 3% where the absolute annual average increased by 0.92 ^{o}C and the precipitation decreased by 1%.

At the end of the next century (i.e. in 2080s) the inflow volume to the reservoir is expected to decrease by 2.33 %.

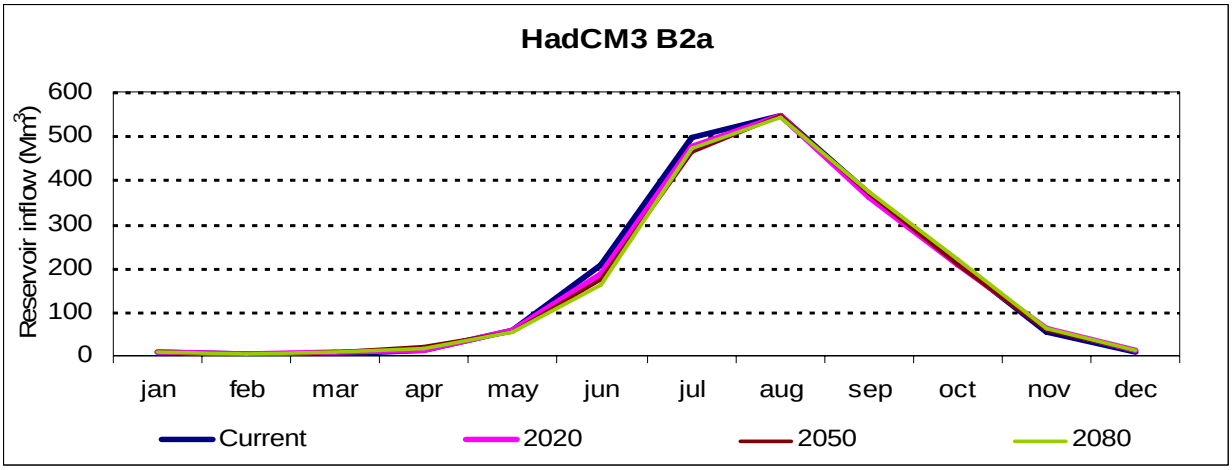

Figure 7. 16 Reservoir inflow (Mm^3) at different time horizons under B2a emission scenario

Generally, for both A2a and B2a scenarios the changes in the reservoir inflow are observed during the in June to November, whereas, in the month of January-May (dry- period) the change is not much significant.

7.3.1 Change in Reservoir Inflow for Hypothetical Scenario

Hypothetical or incremental scenario is applied for this specific study in order to analyze the sensitivity of the reservoir in terms of its performance indices i.e. reliability, resilience and vulnerability. For this study ten hypothetical scenarios are carried out and the inflow to the reservoir is generated for each of the ten hypothetical scenarios.

The reservoir inflow volume change for each of the hypothetical scenario is summarized in the following table

Table 7. 5 Change in reservoir inflow at different hypothetical scenario

Scenarios	S1	S2	S3	S4	S5	S6	S7	S8	S9	S10
Temp.(oC)	+2	+2	+2	+2	+2	+4	+4	+4	+4	+4
Pcp. (%)	-20	-10	0	+10	+20	-20	-10	0	+10	+20
Change in Reservoir inflow (%)	-42.7	-20.4	-3.4	+9.1	+19.1	-48.6	-25	-7.4	6.1	16.7

The hypothetical or incremental scenario with its monthly inflow is described in the figure below. As that of the inflow generated from the downscaled climate variable, the incremental scenario also explain that the inflow volume change in dry period is not significant.

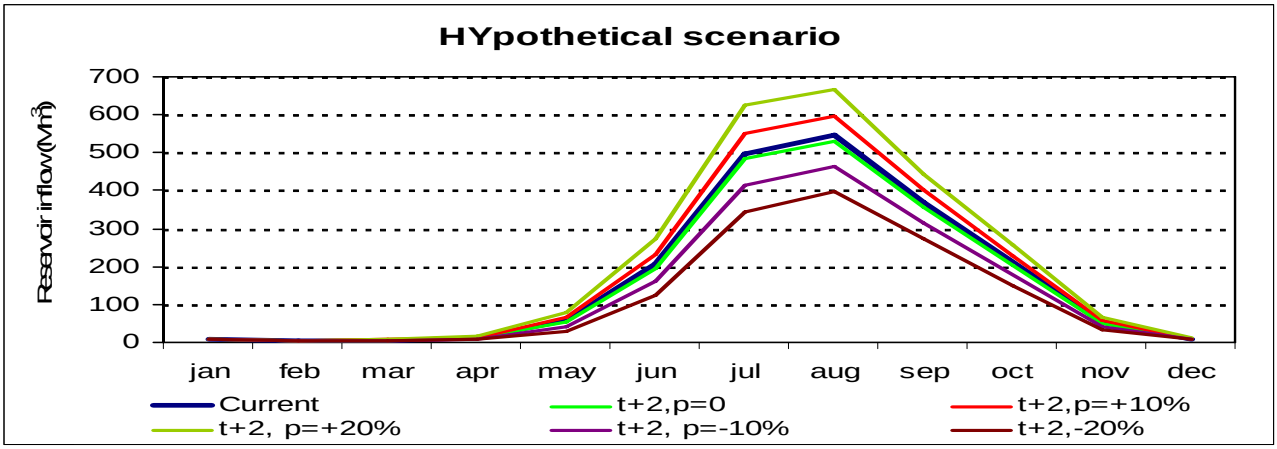

Figure 7. 17 Reservoir inflows (Mm^3) at $+2^oC$ increase in temperature and different percentage change in precipitation

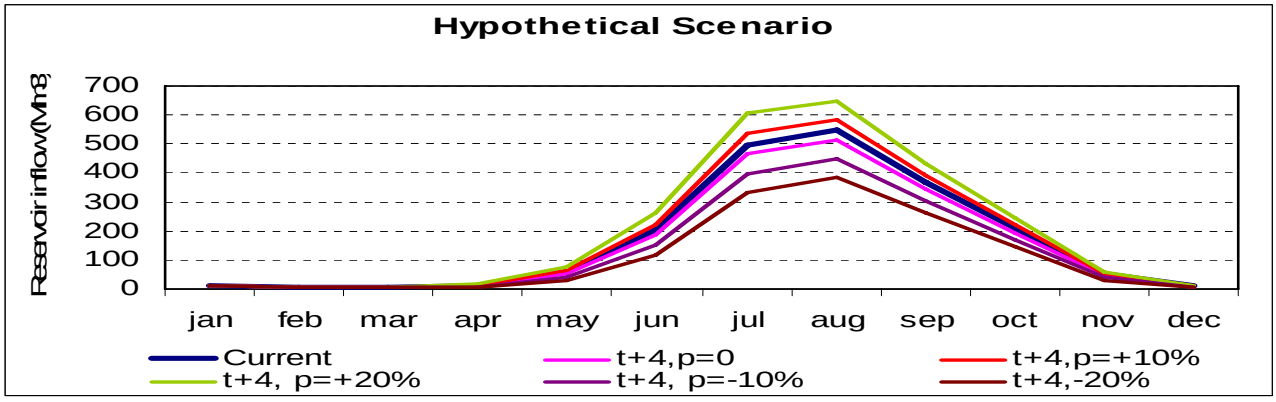

Figure 7. 18 Reservoir inflow (Mm^3) at $+4^oC$ increase in temperature and different percentage change in precipitation

7.5 Evaluating of the performance indices of reservoir

After generating the reservoir inflow, the Gilgel Abay reservoir is examined by using five performance indices under the standard operation policy of the reservoir. Both current and future generation (including the hypothetically generated) inflow are considered during quantifying the performance indices. For the sake of comparative purpose the indices also examined with out the reservoir existing condition.

7.5.1 Reliability of Gilgel Abay reservoir

7.5.1.1 Time based reliability (R_t)

The averaged time-based reliability of the Gilgle Abay reservoir reveals a value of above 80% for both A2a and B2a scenarios under all the three time horizons, a value of 100% time based reliability can be explained as, the reservoir can meet the target demand for all its simulation period. Actually, slight increase in the time based reliability is observed, when the reservoir simulation is done by starting the reservoir with its full supply level than starting from the reservoir empty condition. On average this time based reliability decreases to 54 % for no

reservoir conditions from 80% of reservoir existing condition. The probability density function for the time based reliability under all scenarios (including the hypothetical) also reveals the same condition.

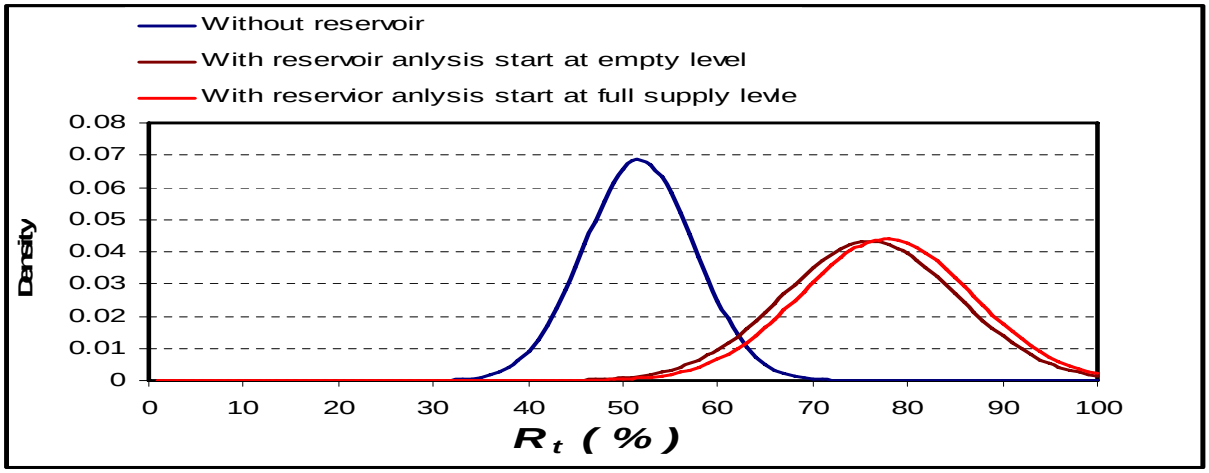

Figure 7. 19 Probability density function for time based reliability at different scenario

7.5.1.2 Volumetric Reliability (R_v)

The volumetric reliability describes the total volume water supplied to the reservoir or demand site i.e. the value of volumetric reliability index indicts that, how much the supplied volume of water can meet the required volume of demand. A 100 % of volumetric reliability index of reservoir tells that there is no shortage for the reservoir to meet the demanded from the volume (amount) point of view.

The result of the analysis for the study area reveals that the annual average volumetric reliability is above 80% for no reservoir conditions and above 93 % for reservoir existing condition. The result value of above 80% tells there exist very good potential at the site to meet the demand in-terms of volume. For the case of the proposed Gilgel Abay reservoir the value 93% indicts that the reservoir has high ability to meet the total volume required by targeted demand. The

probability density function for the volumetric reliability, using different climate scenario is shown below.

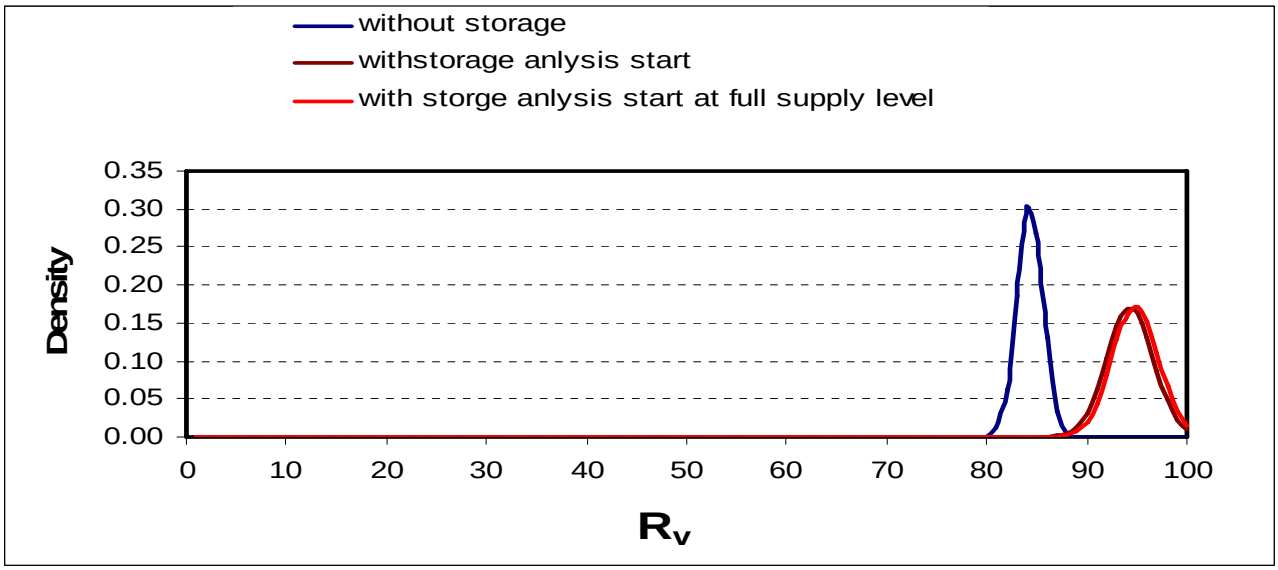

Figure 7. 20 Probability density function for volumetric reliability under different climate scenario

7.5.2 Resilience of Gilgel Abay Reservoir

The Gilgel Abay reservoir resilience which is the indication of how quickly the reservoir system recovers its self from failing to meet the targeted demand to full satisfy the required demand exhibits a percentage value of above 60%, for all the climate scenarios. This value indicates that the Gilgel Abay reservoir has a satisfactory speed of recovery, to meet the demand once the failure to meet the target demand is occurred. A value of 100% resilience indicates the reservoir system will recover it self from failure to meet the target demand with in very short period of time. This resilience value of statistics shows a decreasing amount for no reservoir condition, i.e. on average of all scenarios, the resilience goes down to 18 % for no reservoir exiting condition from 60 % of reservoir condition. The probability density function that shows the falling range of the resilience for most of simulated period is shown in the figure below.

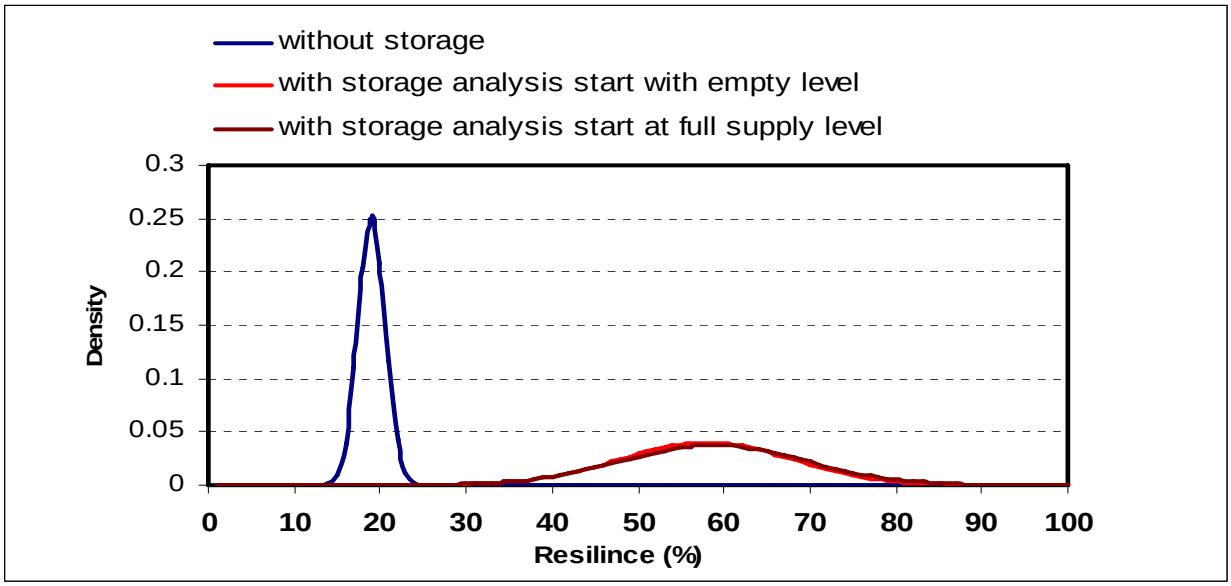

Figure 7. 21 Probability density function for resilience index under different climate scenario

7.5.3 Vulnerability of Gilgel Abay Reservoir

7.5.3.1 Vulnerability by volume (η')

The vulnerability which indicates the average of maximum volumes of shortages in the reservoir reveals that for most of the future scenarios the shortage is found with in the ranges of 27Mm3-30Mm$^{3.}$ Comparing A2a and B2a scenario the maximum shortage is occurred in B2a scenario at 2020s and 2050s where the precipitation exhibits average annual decrease (see section 7.1.6.3)

Relatively, the with reservoir condition has lower volumetric vulnerability than for no reservoir condition, for example on average for all scenario, it was observed that the volumetric vulnerability is increased from 29 Mm^3 for reservoir condition to 55Mm^3 for no reservoir

condition i.e. the implementation of the reservoir will secure 26 Mm^3 volume of water from shortage.

7.5.3.2 Dimensionless Vulnerability (η)

Because vulnerability by volume averaged out the maximum volumetric shortage it some time generate anomaly (see, section 4.5.3) hence, the dimensionless vulnerability is used to remove the problem. The average dimensionless vulnerability of the Gligel Abay reservoir is goes up to 48 % for no reservoir condition and it will reach up to 27 % for reservoir condition. A 100 % of dimensionless vulnerability reflects that the reservoir face a shortage of flow to meet the demand in all simulation period.

7.6 Sensitivity of Reservoir

Generally, in sensitivity analysis of the reservoir, it was observed that the reservoir reliability and resilience are most sensitive to the change in precipitation than change temperature (see. Table 7.6 to 7.8). For example, on average, when the precipitation is decreased by 20 % with out the changing in temperature, the reliability also decreased by 30% to 35%. This result can further be explained as when the precipitation is decreasing with out the change in the temperature, the Gilge Abay reservoir partially losses its capability of meeting the target demand. Like wise the resilience of Gilgel Abay reservoir will decrease by 35%-45%, with the decrease in 20% precipitation and no change in temperature. This can also be explained as, the decrease in resilience percentage shows in the less speed of the reservoir to meet the demand and this reveals in the less water availability in the reservoir consequently, the time required to fill the Gilgel Abay reservoir will be more after, once the reservoir is reached to the minimum level. Whereas the vulnerability doesn't show a change of more than 3 % for the same conditions. Hence, the Gilgel Abay reservoir vulnerability does not show remarkable change with the change in climate precipitation and temperature.

7.7 Reservoir Water level

The range of average annual maximum and minimum reservoir water level is simulated for each scenario according to the generated future inflow volume and the available storage-elevation-area relation ship of the Gilgel Abay reservoir (see. table 7.6 to 7.8).

Results of the performance indices and reservoir water level for with and without reservoir condition under all climate scenario (i.e. for hypothetical and HadCM3 Scenario) are summarized in the following tables.

Table 7. 6 Performance indices for no reservoir existing conditions

Without Storage						
Scenario		Rt (%)	Rv (%)	Resilence (%)	η (Mm3)	η'(%)
Current		54.17	84.72	18.18	52.09	47.99
	2020	53.33	84.53	17.86	52.15	48.04
HadCM3 A2a	2050	55.00	84.87	18.52	52.09	47.99
	2080	56.67	85.33	19.23	51.95	47.85
	2020	54.17	85.03	18.18	52.03	47.93
HadCM3 B2a	2050	54.17	85.16	18.18	51.97	47.88
	2080	54.17	85.10	18.18	52.03	47.93
Hypothetical Scenario	t+2,p=0	53.33	84.53	17.86	52.15	48.04
	t+2,p=+10%	55.00	84.87	18.52	52.09	47.99
	t+2, p=+20%	55.83	85.20	18.87	52.00	47.91
	t+2, p=-10%	48.33	83.94	19.35	52.21	48.10
	t+2,-20%	40.00	81.64	22.22	52.24	48.12
	t+4,p=0	52.50	84.35	17.54	52.18	48.07
	t+4,p=+10%	55.00	84.71	18.52	52.15	48.04
	t+4, p=+20%	55.00	85.03	18.52	52.09	47.99
	t+4, p=-10%	46.67	83.48	20.31	52.21	48.10
	t+4,-20%	35.83	80.64	23.38	52.24	48.12

Table 7. 7 Performance indices for the reservoir under different scenarios with the analysis start at reservoir empty level

With Storage								
Analysis start at empty reservoir level								
Scenario		Rt (%)	Rv (%)	Resilence (%)	η (Mm3)	η'(%)	Max .Reservoir Water level m m.a.s.l	Min. Reservoir Water level m m.a.s.l
Current		80.00	95.07	62.50	30.09	27.72	1891.80	1854.44
	2020	79.17	94.60	60.00	31.12	28.67	1891.80	1852.98
HadCM3 A2a	2050	80.83	95.79	65.22	29.06	26.77	1891.80	1856.23
	2080	81.67	95.98	63.64	28.63	26.37	1891.80	1858.23
	2020	79.17	95.11	60.00	30.74	28.32	1891.80	1855.29
HadCM3 B2a	2050	80.00	95.29	62.50	30.52	28.11	1891.80	1855.89
	2080	80.00	95.51	62.50	29.87	27.52	1891.80	1856.30
Hypothetical Scenario	t+2,p=0	79.17	94.62	60.00	31.10	28.65	1891.80	1852.98
	t+2,p=+10%	80.83	95.81	65.22	28.98	26.69	1891.80	1856.23
	t+2, p=+20%	83.33	96.53	70.00	27.74	25.56	1891.80	1858.23
	t+2, p=-10%	73.33	93.03	50.00	31.93	29.41	1891.80	1846.93
	t+2,-20%	56.67	89.62	38.46	31.93	29.41	1891.80	1840.50
	t+4,p=0	77.50	94.15	59.26	31.60	29.12	1891.80	1851.63
	t+4,p=+10%	80.00	95.42	62.50	29.87	27.52	1891.80	1854.89
	t+4, p=+20%	81.67	96.32	63.64	27.84	25.65	1891.80	1857.74
	t+4, p=-10%	69.17	92.33	45.95	31.93	29.41	1891.80	1844.49
	t+4,-20%	50.00	88.07	33.33	31.93	29.41	1891.80	1840.50

Table 7. 8 Performance indices for the reservoir under different scenarios with the analysis start at reservoir full supply level

With Storage								
Analysis start at full supply level								
Scenario		Rt (%)	Rv (%)	Resilence (%)	η (Mm3)	η'(%)	Max. Reservoir Water level (m) m.a.s.l	Min .Reservoir Water level (m)m.a.s.l
Current		81.67	95.59	63.64	30.09	27.72	1891.80	1857.34
	2020	80.83	95.13	60.87	31.12	28.67	1891.80	1855.88
HadCM3 A2a	2050	82.50	96.29	66.67	29.06	26.77	1891.80	1859.01
	2080	83.33	96.44	65.00	28.63	26.37	1891.80	1861.43
	2020	80.83	95.60	60.87	30.74	28.32	1891.80	1858.07
HadCM3 B2a	2050	81.67	95.69	63.64	30.52	28.11	1891.80	1858.67
	2080	81.67	95.98	63.64	29.87	27.52	1891.80	1859.08
Hypothetical Scenario	t+2,p=0	80.83	95.14	60.87	31.10	28.65	1891.80	1855.88
	t+2,p=+10%	82.50	96.31	66.67	28.98	26.69	1891.80	1859.01
	t+2, p=+20%	85.00	97.01	72.22	27.74	25.56	1891.80	1861.43
	t+2, p=-10%	75.00	93.58	50.00	31.93	29.41	1891.80	1849.38
	t+2,-20%	58.33	90.19	38.00	31.93	29.41	1891.80	1841.55
	t+4,p=0	79.17	94.68	60.00	31.60	29.12	1891.80	1854.53
	t+4,p=+10%	81.67	95.93	63.64	29.87	27.52	1891.80	1857.67
	t+4, p=+20%	83.33	96.80	65.00	27.84	25.65	1891.80	1860.52
	t+4, p=-10%	70.83	92.88	45.71	31.93	29.41	1891.80	1846.53
	t+4,-20%	52.50	88.65	33.33	31.93	29.41	1891.80	1841.55

In addition to the previous explanations, from the above tables one can observe that, the resilience index falls with in the range of 17 to 23 % under all climate scenario, for the case of "without storage" condition, this reflects that, if the Gilgel Abay reservoir does not implemented then the runoff by itself need very long period of time to satisfy the targeted demand in other word it means that the runoff (i.e. without the implementation of reservoir) meets the targeted demand only during rainy seasons(June to September).

The other important point observed from the above tables is that, when comparing A2a and B2a scenario for reservoir existing condition, the maximum draw down in water level is exhibited during 2020s under A2a scenario where the projected inflow is minimum (i.e. decreased by 3.73 % compared to the present condition) and the evaporation from the open water surface of reservoir during this period is also expected to rise by 2.1%.

7.8 Uncertainties related to study

There may exist various sources of uncertainties related to this study staring from the quality of the data, uncertainty related to model assumptions it self and uncertainties arise from the level of understanding the atmospheric chemistry. The uncertainties related to the climate models are described in section.3.2. The climate change impact on the Gilgel Abay reservoir is evaluated only by considering the change in precipitation, maximum and minimum. However, in real situation other climatic variables, land use and sediment inflow to the reservoir will also change. Such and other similar characteristics will certainly reduce the reliability of the result.

8. Conclusion and Recommendation

8.1 Conclusion

In this study the Gilgel Abay reservoir performance under the climate change is quantified by using the reliability, resilience and vulnerability indices (RRV-criteria). The reservoir inflow to the dam site is estimated by transferring the runoff from the gauging station by using the area ratio method. Based on the study the following conclusions are drawn;

1. The result of climate projection reveals that the SDSM model has very good ability to replicate the historical maximum and minimum temperature for the observed period; but less for the observed precipitation with the simulated precipitation due to its conditional nature and high variability in space.

2. Generally the projected maximum and minimum temperature shows an increasing trend for the next century, but the precipitation doesn't show significant difference from the current condition. All the projected maximum and minimum temperature are with in the limits of the expected projection carried by the latest IPCC, 2007.

3. The projected precipitation reveals an annual increase for all the three time horizons (i.e. 2020s, 2050s and 2080s) in A2a emission scenario, but for the case B2a emission scenario on average, annual decreasing is observed during 2020s and 2050s while in 2080s the precipitation shows increasing trend. The reason for getting different results for A2a and B2a scenario is that each of them considers the future aspect of climate system indifferent ways.

4. The evaporation from the open water generally shows an increasing trend i.e. it exhibits an average annual increase of 22 % for A2a emission scenario and 20 % increase for B2a

emission scenario at the end of the next century. This causes its own impact on the reservoir water balance by changing the reservoir volume.

5. The HBV model which is calibrated and validated in daily time step, simulate the observed discharge in reasonably well manner with the model performance criteria of Nash and Sutcliffe value R^2=0.82 for calibration and R^2= 0.8 for validation. Hence, it is concluded that the HBV is an acceptable hydrological model for this study, in order generate the inflow and simulate the reservoir at future climatic condition.

6. The generated inflow to the reservoir in 2020s shows an average annual decrease in volume by 3.73%, in 2050s the inflow volume is expected to increase by 9.14%, while in 2080s the volume will expected to increase by 1.65% under A2a emission scenario. The B2a emission scenario projects that the average annual inflow volume will decrease for all the three time horizons by 2%, 3% and 2.3% in 2020s, 2050s and 2080s respectively.

7. It was generally observed that the reliability index of the Gilgel Abay reservoir for all climate scenarios (including the hypothetical scenario) reveals above 80%, hence it is concluded that the Gilgel Abay reservoir has high capability to meet the required target demand in the next century.

8. The Gilgel Abay reservoir has a index of greater than 60 % for all climate scenarios as result of this it was concluded that the reservoir has satisfactory rate to recover itself from failure to meet the demand to satisfying the target draft.

9. The sensitivity analysis indicates that Gilgel Abay reservoir is more sensitive to precipitation than temperature change. Compared to current (1996-2005) condition, the decrease in precipitation by 20% may lead the reservoir to loss its capability to meet the targeted demand by 50%.

10. In general from performance indices of the Gilgel Abay reservoir, the decision makers, concerned persons or any reservoir water users can be assured that the reservoir has very good potential to irrigate the required area under future climatic condition with the consideration of described research limitations.

11. Finally, from points of view of water availability and meeting development demands, one can conclude that the implementations of Gilgel Abay reservoir will make the surrounding environment to be more secured under climate change. Accordingly, this will lead the overall economy of the country to move further one step self food production.

8.2 Recommendation

Generally from this specific study the following two main pointes are strongly recommended;

1. In order to assure the development of water resource and agricultural efficiency of poor countries like Ethiopia as well as the region of Africa, further studies which incorporate the impact of climate change with land use and land cover change, plus sediment inflow to the reservoirs should be undertaken by using more than one and more finer resolution of Global Circulation Models (GCMs). These studies should also investigate the adaptation options for the impact of climate change consequences.

2. To make the evaluation of climate change impact more complete, it is appreciable to use other physically based regional downscaling methods with the addition of other performance indices, such as Drought Risk Index (DRI) and Sustainability Index.

References:

Abeyou wale .*Hydrological balance of Lake Tana, Upper Blue Nile Basin*, Ethiopia, a Msc thesis, International Institute for Geo-information science and Earth observation, Netherlands.

Amin S. et al,2007 *How to Quantify Sustainable Development*: A Risk-Based Approach to Water Quality Management

Bates, B.C., Z.W. Kundzewicz, S. Wu and J.P. Palutikof, Eds., 2008: *Climate Change and Water*. Technical Paper of the Intergovernmental Panel on Climate Change, IPCC Secretariat, Geneva, 210 pp.

Bergkamp, G., Orlando, B., and Burton, I. (2003) Change: *Adaptation of Water Management to Climate Chang*e. International Union for Conservation of Nature and Natural Resources, Gland & Cambridge.

Bergstrom, S. (1992) *The HBV model - its structure and applications*, SMHI Hydrology, RH No.4, Norrköping, 35 pp.

Beven, K.J. (2000). *Rainfall-runoff modelling*. The Primer. Wiley, 360 p.

Bimrew, 2008. *Evaluation of Impact of Climate Change on Water Resource Availability in the Catchments of Blue Nile Basin,* (MSc thesis, Arba-Minch University, 2008, Amu)

Box, G.P. and G.M. Jenkins 1976. Time-Series Analysis, Forecasting and Conirol. Holden-Day, San Francisco

Calder, I. R. (2005) Blue Revolution: *Integrated Land and Water Resource Management*, Earthscan, London.

Colin Hayes (2007) *A Review of Climate Change and its Potential Impacts on Water Resources in the UK*. England.

Conway.D (1999): *The Climate and Hydrology of the Upper Blue Nile River*, School of Development Studies, University of East Anglia, Norwich NR4 7U,The Geographical Journal, Vol. 166, No. 1, March 2000, pp. 49-62

Conway. D (2000).*A water balance model of the Upper Blue Nile in Ethiopia* ,Hydrological Sciences Journal des Sciences Hydrologiques, 42(2)

Frederick, K. D. 2002.Introduction in: *Water resource and climate change*, Fredrick, K.D.(ed.) Northampton MA: Edward Elgar Publishing. 514 pp

Gates WL, Boyle JS, Covey C, Dease CG, Doutriaux CM, Drach RS, Florino M, Gleckler P, Hnilo JJ, Marlais SM, Phillips TJ, Potter GL, Santer BD, Sperber KS, Taylor KE, Williams DN (1999) *An overview of the results of the Atmospheric Model Intercomparison Project* (AMIP I). Bull Am Meteorol Soc 80

Gordon, N.D., T. A. McMahon and B.L. Finlayson (1992), *Stream hydrology*, John Wiley & Sons Ltd, Chichester, New York, Brisbane, Toronto, Singapore.

Goswami, M., K.M. O'Connor, K.P. Bhattarai and A.Y. Shamseldin (2005), *Assessing the performance of eight real-time updating models and procedures for the Brosna River*, Hydrology and the Earth System Sciences. 9 (4): 394-411

Hadley Centre for Climate Change and Prediction. (HCCCP, 2005a) *Climate Change and the Greenhouse Effec*t: A Briefing from the Hadley Centre. Hadley Centre for Climate Change and Prediction, Exeter.

Hadley Centre for Climate Change and Prediction. (HCCCP 2004a) *Uncertainty, Risk and Dangerous Climate Change*. Hadley Centre for Climate Change and Prediction, Exeter

Haan, C.T., Johnson, H.P., Brakensiek, D.L. (1982). *Hydrologic modeling of small watersheds*. ASAE, 533 p.

Hashimoto, T., Stedinger, J.R., Loucks, D.P., 1982. *Reliability, resiliency and vulnerability crireria for water resource system performance evaluation. WaterResources* Research 18 (1), 14–20.

Intergovernmental Panel on Climate Change. (2007a) Working Group I: The Physical Basis of Climate Change. Accessed on 8 May 2007 from http://ipccwg1. ucar.edu/wg1/wg1-report.html.

Intergovernmental Panel on Climate Change. (2001a) Climate Change 2001: *The Scientific Basis*. Intergovernmental Panel on Climate Change.

IPCC-TGICA, 2007: *General Guidelines on the Use of Scenario Data for Climate Impact and Adaptation Assessment*. Version 2. Prepared by T.R. Carter on behalf of the Intergovernmental Panel on Climate Change, Task Group on Data and Scenario Support for Impact and Climate Assessment, 66 pp.

IPCC Technical Summary, 2001. Climate Change 2001: *The Scientific Basis. Technical Summary of the Working Group I Report* [Houghton, J.T., Y. Ding, D.J. Griggs, M. Noguer, P.J. van der Linden, X. Dai, K. Maskell, and C.A. Johnson (eds.)]. Cambridge University Press, Cambridge, United Kingdom and New York, NY, USA, 94pp.

Juraj M, 2003, Hydrological model selection for CFCAS project, *Assessment of water Resource Risk and Vulnerability to change in climate condition,* University of Western Ontario.

Kebede, S., Y. Travi, T. Alemayehu, T. Ayenew (2006), *Water balance of Lake Tana and its sensitivity to fluctuations in rainfall, Blue Nile Basin*, Ethiopia, Journal of Hydrology, 316: 233-247.

Lambert, S.J. and Boer, G.J., 2001. CMIP1 *evaluation and intercomparison of coupled climate models*. *Clim. Dynam*., 17, 83–106

Lindström, G., Johansson, B., Persson, M., Gardelin, M., Bergström, S. (1997).*Development and test of the distributed HBV-96 hydrological model*. Journal of Hydrology 201, pp.272-288.

Loucks, D.P., 1997. *Quantifying trends in system sustainability.* Hydrological Sciences Journal 42 (4), 513–530.

LOUCKS, D.P.; INGER, J.R ASTEDND HAITH, D.A. 1981. *Water resource systems planning and analysis*. Englewood Cliffs, N.J., Prentice Hall.

Research report , RR-126 Ungtae Kim et.al, *Climate change Impact on Hydrology and Water resource of the Upper Blue Nile River,* IWMI, Colombo, Sir Lanka.

Robert Keirle & Colin Hayes, 2007 *A Review of Climate Change and its Potential Impacts on Water Resources in the UK,* Official Publication of the European Water Association (EWA), UK.

SHMI (2003). Homepage of the Original HBV-Model.; http://www.smhi.se/foretag/m/hbv_demo/html/welcome.html.

Sutcliffe, J. V., and Y. P. Parks (1999); *The Hydrology of the Nile*, IAHS Special Publication no. 5, pp 127-141.

Tarekegn. D & Tadege .A (2005); *Assessing the impact of climate change on the water resource of Lake Tana sub –basin using WATBAL model*, Ethiopia

Thomas A.et al. 2004, *Understanding performance measures of reservoirs* Journal of Hydrology 324 (2006) 359–382

Thorpe A.J., 2005, Climate Change Predictions: *A challenging scientific problem*. Institute of physics, [online]4 Apr., available at: http://www.iop.org/activity/policy/Publications/file_4147 .pdf [accessed 4 April 2009]

Tsegaye.E., 2006 *Regionalization of potential Evapotranspiration prediction for Blue Nile (Abbay) river basin, Ethiopia*, Msc Thesis, Arba-Minch University, Ethiopia.

USAID, 2007. A Guidance Manual for Development Planning: *Adapting to Climate Variability and Challenge* United states, August 2007

Wilby, Robert L., and Christian W. Dawson, August 2007. Using SDSM Version 4.1 SDSM 4.2.2 – *A decision support tool for the assessment of regional climate change impacts*, User Manual, Leics., LE11 3TU, UK

World Meteorological Organization/WMO 1966. Climatic Change. J.M. Mitchell (Editor). WMO No. 195. TP. 100. WMO, Geneva.

Wurbs, R.A.; Muttiah, R. S.; Felden, F.2005.*Incorporation of climate change in water availability modeling*. Journal of Hydrologic Engineering 10(5):375-385

Yevjevich, V. and R.I. Jeng 1969. Properties of Non-Homogeneous Hydrologic Time Series. Hydrology Paper 32. Colorado State University Press, Fort Collins

Annexes

Appendix A: List of Acronyms

Alfa	Parameter defining the non linearity of the quick runoff reservoir in the HBV model
Bata	Parameter in soil moisture routine in the HBV model
CCCM	Climate and Carbon Cycle Model Group
CFCAS	Canadian Foundation for Climatic and Atmospheric Sciences
DEM	Digital elevation model
FAO	Food and Agricultural Organizations
FC	Parameter defining the maximum soil moisture storage in HBV model
GCM/s	Global circulation Model/s
HadCM3	Hadley Center for Climate Prediction
HBV	Hydrologiska Byrans Vattenbalansavdelning (Hydrological Bureau Water balance Section)
Hq	Parameter representing the high flow rate in the HBV model.
IHMS	Integrated Hydrological Modeling System
IPCC	Inter Governmental Panel on Climate Change
ITCZ	Inter Tropical Convergent Zone
KHQ	Parameter representing a recession coefficient at a corresponding reservoir volume in HBV model
MoWR	Ministry of water resource
NMSA	Ethiopian National Metrological Service Agency
NCEP	National Center for Environmental Prediction
PERC	Percolation from upper to lower reservoir box [mm/day]
r^2	Correlation Coefficient
R^2	Nash and Sutcliffe coefficient
RR	Research Report
RV_E	Relative volume error.
SHMI	Swedish Metrological and Hydrological Institute.
SRTM	Shuttle Radar Topography Mission

SDSM Statistical Down Scaling Method

SRES Special Report on Emission Scenario

UKMo United Kingdom Metrological office

USAID United States Agency for International Development

WMO World Metrological Organization

Appendix B: Definitions of some important words

- Storyline: a narrative description of a scenario (or a family of scenarios), highlighting the main scenario characteristics and dynamics, and the relationships between key driving forces.
- Emission Scenario: projections of a potential future, based on a clear logic and a quantified storyline.
- Scenario family: one or more scenarios that have the same demographic, politico-societal, economic and technological storyline.

Appendix C: Available Predictors

No	Predictor variable	Predictor description	No	Predictor variable	Predictor description
1	mslpaf	mean sea level pressure	14	p5zhaf	500 hpa divergence
2	p_faf	surface air flow strength	15	p8_faf	850 hpa airflow strength
3	p_uaf	surface zonal velocity	16	p8_uaf	850 hpa zonal velocity
4	p_vaf	surface meridional velocity	17	p8_vaf	850 hpa meridional velocity
5	p_zaf	surface vorticity	18	p8_zaf	850 hpa vorticity
6	p_thaf	surface wind direction	19	p850af	850 hpa geopotential height
7	p_zhaf	Surface divergence	20	p8thaf	850 hpa wind direction
8	p5_faf	500 hpa airflow strength	21	p8zhaf	850 hpa divergence
9	p5_uaf	500 hpa zonal velocity	22	p500af	Relative humidity at 500 hpa
10	p5_vaf	500 hpa meridional velocity	23	p850af	Relative humidity at 850 hpa
11	p5_zaf	500 hpa vorticity	24	rhumaf	Near surface relative humidity
12	p500af	500 hpa geopotential height	25	shumaf	Surface specific humidity
13	p5thaf	500 hpa wind direction	26	tempaf	Mean temperature at 2 m

Appendix D: Available flow station used for analysis

	SUB						INSTA.	AREA	REGIONAL	
CATCHM.	CATCHM.	STN. No.	RIV/LAKE	SITE	LAT.	LON.	DATE	Km^2	OFFICE	GOVERN.
ABBAY	LAKE TANA	111002	GELGEL A.	Nr. MARAWI	11d22'n	37d02'e	27-3-59	1664	BHD	AMHARA
ABBAY	LAKE TANA	111003	KOGA	@ MERAWI	11d22'n	37d03'e	27-3-59	244	BHD	AMHARA

Appendix E: List of station name, location and available metrological variables

S.No.	Station Name	Latitude (degree)	Longitudes (degree)	Rainfall	Max. Temp	Min. Temp	Relative humidity	Wind Speed	Sunshine hours
1	Sekela	*11*	*37.22*	√					
2	Gundil	*10.95*	*37.07*	√	√	√			
3	Dangila	*11.12*	*36.83*	√	√	√	√	√	√
4	Abay shelko	*11.38*	*36.87*	√	√	√			
5	Kidamja	*11*	*36.80*	√	√	√			
6	Bahir-dar	*11.6*	*37.42*	√	√	√	√	√	√
7	Adet	*11.27*	*27.47*	√	√	√	√	√	√
8	Enjabran	*10.97*	*36.90*	√					